# METHOD DEVELOPMENT FOR ELEMENTAL ANALYSIS OF SOILS AND ENVIRONMENTAL SEDIMENTS USING X-RAY FLUORESCENCE

**THESIS RESEARCH**

BY

SAMWEL MOKAYA ONDIEKI

Submitted in partial fulfilment of the requirements

for the degree of

**Master of Science**

**in**

**Chemistry**

**YOUNGSTOWN STATE UNIVERSITY**

**May, 2023**

# Method Development for Elemental Analysis of Soils and Environmental Sediments Using X-Ray Fluorescence

**Samwel Mokaya Ondieki**

I hereby release this thesis to the public. I understand that this **thesis** will be made available from the OhioLINK ETD Center and the Maag Library Circulation Desk for public access. I also authorize the University or other individuals to make copies of this thesis as needed for scholarly research.

Signature:_____

Samwel Mokaya Ondieki, Student Date

Approvals:

_____

Dr. Josef Blair Simeonsson, Thesis Advisor Date

_____

Dr. Ganesaratnam K Balendiran, Professor. Committee Member Date

_____

Dr. Clovis Linkous, Professor Committee Member Date

_____

Dr. Salvatore A. Sanders, PhD, Dean, College of Graduate Studies Date

# ABSTRACT

X-Ray Fluorescence (XRF) spectroscopy is a good analytical method for determination of both trace and major elements in different samples, it has the important advantages of allowing direct analysis of soils and sediments and is also non-destructive.

The major aim of this study was to develop an XRF method for the determination of total metal concentrations in soils and sediments. Limit of detection and limit of quantitation were used as the figures of merit to evaluate the method. Standard Reference materials: **NIST-2586, NIST-2587, NIST-1645** and **NIST-1645** were used for calibration. Different calibration methods were explored. background corrected peak height to Background corrected **Compto**n peak height **ratio** had the highest correlation coefficient (0.99) for **Fe, Cu, Mn, Zn, Al, Cr, Ca** and **Pb.**

The method was applied to measure 120 sediment samples that were collected from the yellow creek watershed Poland, Ohio. The results of the **XRF** method were compared with those obtained by **ICP-MS. Al, Mn, Zn, Fe** and **Cu** had good agreement.

A **sequential extraction** approach was developed for characterizing the availability of metals in the water from the sediments. **Ca** and **Mn** were found to be easily extracted under weakly acidic conditions.

# ACKNOWLEDGEMENT

My sincere gratitude to Dr. Simeonsson For his great support in advising, supervising, and overseeing this project this far. A special thank you to Department of Biological and Chemical Sciences, Youngstown State University for an opportunity to pursue my masters from this great institution. Much appreciation to all my analytical chemistry group members for their support and encouragement.

# TABLE OF CONTENTS

# LIST OF FIGURES

# LIST OF TABLES

# APPENDIX

# 1. INTRODUCTION

## 1.1 XRF in elemental analysis

The main objective of this research project was to develop a method of elemental analysis in sediments and soils using X-ray Fluorescence (XRF) to determine the major and trace elements in sediments from the Yellow Creek watershed in Poland, Ohio and measure their concentrations. It was also of interest to conduct a comparison of elemental analysis using inductively coupled mass spectroscopy (ICP MS). Standard Reference Materials (SRMs) obtained from the National Institute of Standards and Technology (NIST) were used for calibration.

X-ray fluorescence (XRF) is an analytical method that can be used in the elemental analysis of various types of samples, including environmental and aerosol samples. (Stosnach, 2006). Soil is an important natural resource that supports food production and recycles key nutrients in the environment. The analysis of soil samples is necessary to evaluate soil quality and its impact on human nutrition and economic development in many countries (Towett et al., 2013). Sediments can be indicators of water quality and can also be used to assess water contamination, including by toxic trace elements. The analysis of sediments can indicate the presence of potentially harmful metals and lead to the identification of their sources. (Sinem Atgin et al., 2000)

Portable XRF spectrometers have been developed for use in the field. By taking advantage of smaller and improved parts such as the X-ray tube and detectors, XRF has improved significantly in recent years. As a result, XRF is fast, cost-cheaper and non-destructive alternative to expensive and time-consuming analytical methods such as ICP-MS. (Rouillon & Taylor, 2016)

Trace elements can be useful for determining the sources of pollution at a specific location as the chemical composition of waste discharges varies significantly depending on the source. For example, facilities producing alloy and ceramic factories may be high in Cd, while Cr and Zn may be contributed by discharges from tanneries. Textile, metal, and glass manufacturers are known to produce waste that is high in Cu, while Pb is often high in waste discharges from battery recycling factories, and Hg is often emitted in paper production. (Sinem Atgin et al., 2000)

Although XRF does not have the high sensitivity that several other methods may have, such as ICP atomic emission and ICP mass spectrometry methods, XRF does have the important advantages of allowing direct analysis of soils and sediments and is also non-destructive, which

allows faster measurements and the potential for using the method to identify samples that may be unsafe due to high levels of contamination.

The main objectives of this project were to develop an XRF method for the determination of total metal concentrations in soil and sediment samples, to develop a sequential extraction approach for characterizing the availability of metals in the samples, and to compare the results of the XRF method with those obtained by ICP-MS.

## 1.2 Principle of XRF

### 1.2.1 X-ray

X-ray radiation is characterized by its high energy photons whose wavelength range from 10-0.01 nm. X-ray radiation was first discovered and named by William Röntgen (1845-1923) in 1895, in which X means unknown. Rontgen was awarded the Nobel prize for this discovery.[i] Owing to the very high photon energies, X-ray has the ability to penetrate many materials. This ability is found in X-ray elemental analysis methods such as XRF spectroscopy which can be used to quantify elements in bulk materials, minerals, consumer products and environmental samples.

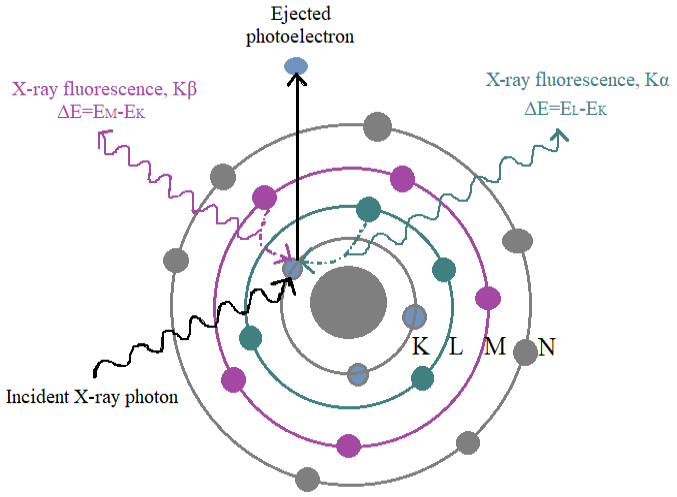


**Figure 1:** X-ray fluorescence (Kα, Kβ) following the ejection of an electron from K orbital by an incident X-ray photon. ( https://xrf-spectroscopy.com)

Fluorescence is the emission of light that occurs when materials absorb or are excited by an external radiation source. In XRF, an X-ray tube is used to generate a primary X-ray, which is the

first step in the XRF process. When an atom absorbs a photon from the X-ray source, an inner shell electron can be excited and removed from the atom and fluorescence is emitted when an electron from a higher energy orbital fills the vacancy left by the electron that was removed. The photon energy of the XRF radiation is unique to each atom and can be used to identify which atoms are present in the sample. Since the intensity of the XRF emission depends on the number of atoms, measurements of the XRF intensity can be used for quantitative analysis.

Many atoms may be present in a given sample, resulting in the emission of X-rays of various energies. The X-ray fluorescence detector collects these fluorescence photons and produces electrical pulses in the detector that are proportional to the photon energy of the incoming radiation. A multi-channel analyzer is used to process and record the signals so that they can be transformed into an XRF spectrum. (Oyedotun,2018). The y-axis shows the XRF intensity in counts per second, while the x-axis shows the XRF photon energy.

The X-Ray fluorescence spectrometer used in this research is an S2 Ranger (Bruker). Its **X-Ray source** contains a Pd anode, Max. power 50 W, max. voltage 50 kV, max. current 2 mA. X-Ray radiation from the source (Primary X-Ray) is produced by a high energy beam of electrons accelerated towards a target metal. The resulting X-Rays are used to produce XRF from the sample materials. The photon energies of the X ray source radiation depend on the voltage applied to the electrons in the source. The intensity of resulting photons depends on the current pass through the tube. The X ray photons coming from of the source can be filtered by certain metals such as Al, Cu, or no filters to select appropriate energy ranges for certain elements of interest.

## 1.2.2 Scattering

### Compton Scattering

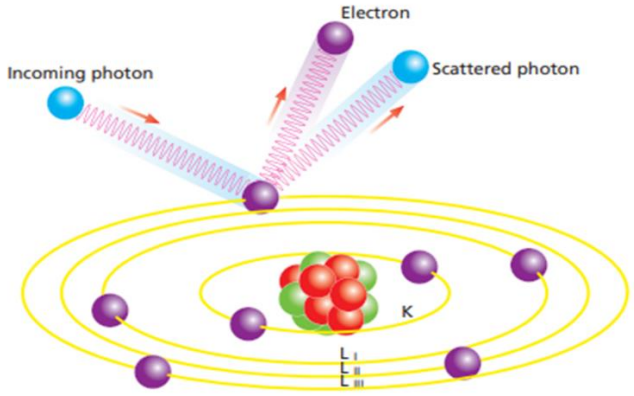


**Figure 2**: Diagram illustrating Compton scattering.

(https://www.chem.purdue.edu/xray/docs/Theory of XRF.pdf)

Compton (inelastic scattering): part of the incoming X-ray is scattered by electrons of the samples instead of producing characteristic radiation. The photons hit the electrons and bounce away and lose a fraction of its energy, the amount of energy lost related to the sample matrix.

## Rayleigh scattering

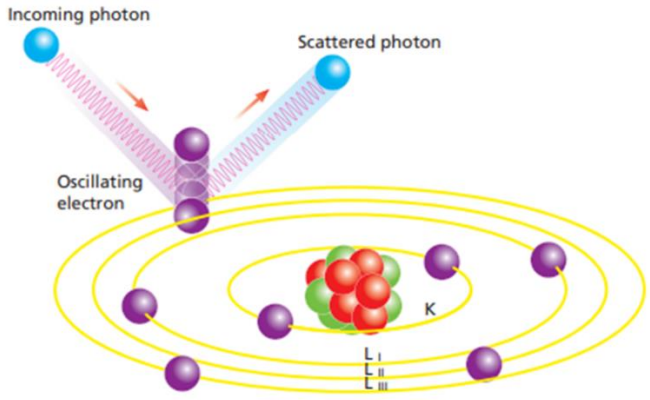


**Figure 3**: Diagram illustrating Rayleigh scattering (Theory of XRF-Analytica)

(https://www.chem.purdue.edu/xray/docs/Theory of XRF.pdf)

Rayleigh (elastic): photons collide with strongly bound electrons. The electrons absorb the energy and start oscillation (but not escape from the orbital like Compton), then electrons emit radiation at the same frequency.

***Table 1:*** *Filters and their corresponding transmitted energies in the Bruker S2 Ranger X-ray fluorescence spectrometer.*

| **Range 1** | **Range 2** | **Range 3** | **Range 4** |
|---|---|---|---|
| Filter = "Cu 250µm" | Filter = "Al 500µm" | Filter = "None" | Filter = "None" |
| KV = 50<br>mA = 1 | KV = 40<br>mA = 0.714 | KV = 20<br>mA = 0.301 | KV = 10<br>mA = 1.186 |
| 250µm, 500µm are filters' thickness.<br>Voltage is the energy range of the photons. The higher the voltage is, the more energy the photons have.<br>Current is proportional to the number of electrons interacting with the X-ray target. The higher the current is, the more photons will be sent to the samples. | | | |

XRF from a sample depends on the wavelength or energy of the photons. Photons are detected by energy dispersive detectors. Fluorescent photons are plotted terms of intensity (in counts per second) versus KeV of the photons.

Shown below is photo of the S2 Ranger XRF instrument used in these studies. The instrument contains the X ray source, the sample tray, sample measurement space, the energy dispersive detector and the multichannel analyzer.

## 1.3 X-Ray fluorescence spectrometry (XRF)

**Figure 4**. YSU XRF spectrometer

In general, two types of detectors in XRF are wavelength dispersive detector (WDXRF) and energy dispersive detector (EDD) (EDXRF).

In the wavelength dispersive approach (WDXRF), the fluorescence X-rays are processed by the monochromator to select the appropriate wavelength corresponds to the wavelength (photon energy) of the element of interest. This approach usually provides high selectivity and high sensitivity for a given element. (Chen et al., 2008)

In the energy dispersive approach (EDXRF), several elements can be measured simultaneously as different X ray wavelengths produce different pulse heights in the detector, which can be evaluated separately by the detection system. However, the spectral resolution in EDXRF is not as high as it is WDXRF, which can lead to worse performance. (Chen et al., 2008).

Shown below is a figure of the energy dispersive detector used in the S2 Ranger XRF instrument used in these studies.

**Figure 5**: The YSU XRF- ED-solid state Silicon Detector. (YSU instrumentation Bruker S2-Ranger file)

When X ray fluorescence photons from the sample material strike the detector, the detector produces an electrical pulse where the height of the pulse is proportional to the incoming photon energy. The pulses are amplified and then counted by the multichannel analyzer (**MCA**). The number of pulses of a certain height that are counted during a measurement is proportional to the intensity of the X ray fluorescence at the corresponding photon energy. An X ray fluorescence spectrum indicating the energy (**keV**) and Intensity (**Cps)** is produced.

The analytical advantages of XRF are that it is nondestructive, requires minimal or no sample preparation, and can detect elements from the ppm to % range in solid, liquid and powder samples.

## 1.4 Metal quantification in a sample.

In most cases a calibration curve is generated using external standard reference materials, this has a drawback in that the matrix effect of the sample is not taken care of as the standard reference materials and the sample may have different matrix effects. To correct for matrix effect the scattering peaks i.e. Compton and Rayleigh are used. This is because they are both affected by the same matrix as the characteristic peaks. This will greatly improve the accuracy of the metal quantitation. (Carvalho et al.,2020)

## 1.5 Figures of merit for XRF measurements.

Linearity: The concentration of the analyte and the signals produced by the XRF have a linear relationship. A correlation coefficient of 0.99 is the acceptable for calibration in an analytical method. At least five standard solutions are required to be measured in order to build a calibration curve. The curve should be as linear as possible. (Furukawa et al,2017)

Accuracy/specificity: Accuracy can be assessed using recovery. A higher recovery indicated a good method for quantifying a sample. This can be done by adding a known concentration of an element into the sample and watch out for the recovery. It is also possible to do it using a known analytical method to compare the analyte concentrations. (Furukawa et al,2017)

Quantification limit: By increasing the standard deviation of at least six replicate measurements of a blank by ten, one can estimate the limit of quantitation. The acceptable standards: The analytical process must be able to determine the analyte reliably and precisely at a level equal to 50% of the specification. (Furukawa et al, 2017)

## 1.6 Internal calibration by using Compton and Rayleigh peaks to make calibration curves.

Rayleigh and Compton peaks for uranium quantitation in different matrices has been investigated. EDXRF was used to analyze samples that were given as pressed pellets and fusion beads. The calibration map was created using the ratio of the intensity between that of Uranium peaks and the scattered peaks. Without adding any internal standards to the samples, the established methodology was successfully used to determine U in a number of samples (Kumar and Dhara,2022)

ICP-MS is a method frequently employed to determine metal concentrations in samples. However, sample treatment is the major source of uncertainty. The question of how well analyte recovery may be achieved by altering the leaching/extraction technique has been hotly contested in the literature for many years (Congiu et al,2013).

There isn't much research that compare XRF and ICP data reported in the literature. The ICP measurements are dependent on the digestion process, which is frequently imprecise. Harmonizing the data from various analytical approaches is important but can also be a significant challenge. (Congiu et al, 2013)

In this project a comparison between the XRF and ICP concentration of the different metals in sediments and soils is reported.

# 2. EXPERIMENTAL

## 2.1 Instrumentation

The X-Ray fluorescence spectrometer used in this research is S2 Ranger (Bruker). Its X-Ray source contains a Pd anode, Maximum power of 50 W, maximum voltage of 50 kV, maximum current of 2 mA. It uses a silicon detector (WL=0.3176725).

As mentioned earlier, the S2 ranger does the measurement using four ranges with each range having different energy, power and voltage as shown in the table below.

***Table 2**: XRF ranges with their respective current and voltage.(Instrument set up values displayed after the XRF takes a sample measurement).*

| Range 1 | Range 2 | Range 3 | Range 4 |
|---|---|---|---|
| Filter = "Cu 250µm" | Filter = "Al 500µm" | Filter = "None" | Filter = "None" |
| KV = 50<br>mA = 1 | KV = 40<br>mA = 0.714 | KV = 20<br>mA = 0.301 | KV = 10<br>mA = 1.186 |

Voltage is the energy range of the photons emitted by the source. The higher the voltage, the greater the energy the photons may have.

Current is proportional to the number of electrons interacting with the X-ray target. The higher the current is, the more photons will be produced in the source and higher intensity used for sample measurements.

## 2.2 Standard Reference Materials (SRMs)

The standard reference materials used were sourced from the National Institute of Standards and Technology (NIST). A total of four standard refence materials were used:

**NIST-SRM 2586- Trace elements in soil containing trace elements.**

**NIST-SRM 2587-Trace elements in soil containing Lead from paint.**

**NIST-SRM 1645-A river sediment**

**NIST-SRM 8704- Trace elements in Buffalo River Sediment.**


**Figure 6**: Image of the NIST SRMs.

### *2.2.1 Certified Percentage of elements in the NIST Standard refence materials.*

***Table 3:*** *Certified Percentage of elements in the NIST Standard refence materials.*

| Elements | **NIST-SRM** 2586 | **NIST-SRM** 2587 | **NIST-SRM** 1645 | **NIST-SRM** 8704 |
|---|---|---|---|---|
| **Co** | 0.0035 | 0.0014 | x | 0.0014 |
| **Sr** | 0.0841 | 0.0126 | x | 0.0130 |
| **Mn** | 0.1000 | 0.0651 | 0.0785 | 0.0544 |
| **Zn** | 0.0352 | 0.0336 | 0.1720 | 0.0408 |
| **Ga** | 0.0014 | 0.0013 | x | x |
| **Pb** | 0.0401 | 0.3242 | 0.0714 | 0.0150 |
| **Ca** | 2.2180 | 0.9270 | 2.9000 | 2.6410 |
| **Fe** | 5.1610 | 2.8130 | 3.9700 | 3.9700 |
| **Cu** | 0.0810 | 0.0160 | 0.0109 | 0.0099 |
| **Mg** | 1.7070 | 0.6690 | 0.7400 | 1.2000 |
| **Al** | 6.6520 | 5.8600 | 2.2600 | 6.1000 |
| **Si** | 29.1500 | 33.1300 | x | x |
| **P** | 0.1001 | 0.0970 | 0.0510 | x |
| **K** | 0.9760 | 1.5830 | 1.2600 | 2.0010 |
| **Ti** | 0.6050 | 0.3920 | x | 0.4570 |
| **Cr** | 0.0301 | 0.0092 | 2.9600 | 0.0122 |

### *2.2.2 Preparation and measurement of samples*

Using an analytical balance, 5 grams of the sample or reference material was weighed. A plastic spatula was used in transferring the sample to minimize metal contamination of the samples. The weighed sample was then transferred into the already prepared sample cup. Each sample was placed in the 35mm sample cups using the 3.6 mm mylar covers. The measurement of the standards was performed for calibration of the instrument response for each element of interest.

## 2.3 Dilution procedure for $CaCO_3$ for internal calibration

5 g of sample mixture was used in varying percentage as shown in the table below:

***Table 4**: sample mixture percentages for **$CaCO_3$ dilution***

| **Sample mixture** | **Sediment sample %** | **$CaCO_3$ %** |
|---|---|---|
| A | 100 | 0 |
| B | 50 | 50 |
| C | 25 | 75 |
| D | 12.5 | 87.5 |
| E | 6.25 | 93.75 |
| F | 0 | 100 |

## 2.4 Sediment Sampling

### *2.4.1 Sampling site and procedure*

The sediment samples were collected from the Yellow Creek watershed, in Poland, Ohio. To avoid sample contamination the sample collection was done from downstream to upstream i.e., from Poland Riverside Cemetery to Poland Library and finally in the Poland Municipal Forest. Each sampling site was divided into 4 sub-sites which are about one meter apart. In flowing water, the sediments tend to accumulate behind the stable body such as rocks and logs, so samples were often collected at or near those locations.

- Cemetery, located between a road and cemetery

- Library, located behind The Municipal Poland Library in Poland. adjacent to a large parking lot and under a road bridge which is busy.

- Woods, located within the Poland Municipal Forest. This site has a lot of vegetation, a shallow stream with a normal current.

Samplings were carried out in four different seasons, at least 5 times per season (Fall 2021, Spring 2022, Summer 2022, and Winter 2022). At each position, an amount of approximately 100 g of wet sediment was taken in the middle and at the bottom of the creek. Sample containers were polyethylene vials that are produced for low metal background measurement applications by ICP-MS. Sediments were dried at 105$^{o}$C for 24 hours and then sieved through a non-metal membrane (size 1mm) to get remove larger solids including gravel.

### *2.4.2 Laboratory Preparation of sediment samples for X-RF measurement.*

The wet sediments were placed separately in glass pans to be dried.

- Drying: The collected wet samples were placed in separate glass pans/plates and dried in an oven at 100$^{o}$ C overnight/for 12 hrs.
- Grinding: A mortar and pestle were used to grind the samples into a fine powder
- Sieving: The ground sample was sieved using a plastic sieve 1mm to remove larger pieces of gravel and organic debris.
- Weighing: 5 g of each sample was weighed into the sample cup using an analytical balance.
- The samples were transferred into open-ended sample cups using 3.6 mm Chemplex Mylar X-ray film.
- The samples were labeled as:

  Poland wood samples **(W1, W2, W3, and W4)**

  Poland Library samples **(L1, L2, L3, L4)**

  Cemetery area samples **(C1, C2, C3, C4)**

  To reduce measurement variations and uncertainties, all samples were subjected to the same preparation procedure and particle size during grinding.

### *2.4.3 BCR Three step sequential extraction procedure. (*Raulet et al. 1999*).*

A total of 12 samples each weighing 5 g were used. The dried sediment samples were ground, sieved and weighed and treated with a series of chemical selective solutions. Between each solution treatment, the samples were centrifuged, and the residue dried and measured.

**Step 1**

200 mL of 0.11 M $CH_3COOH$ (Acetic acid) was added to the sediment in a 200 mL-centrifuge tube then shaken overnight using a shaker. To separate the extract from the residue, the sample was centrifuged at 3000 g for 20 minutes. To wash the residue 20 mL of distilled water was added and shaken for 15minutes and centrifuged for 20 minutes at 3000 g. The supernatant was decanted. The residue was placed on glass evaporating dishes and dried at $100^0$C in an oven. The residue was then placed in a sample cup for XRF measurement. This was labelled as Sequential extraction step 1(SEQ 1) measurement.

**Step 2**

200 mL of 0.5 M $NH_2OH.HCl$ (hydroxylammonium chloride) was added to the residue from step 1 in 200 mL centrifuge plastic tubes, stoppered and shaken by a shaker overnight. The centrifuge tubes with the sediment mixture were centrifuged at 3000 g for 20 minutes, then decanted to collect the residue. The residue was washed with DI water, shaken for 15 minutes, centrifuged at 3000 g for 20 minutes. The supernatant was decanted, the residue was then dried in an oven at $100^0$C. After drying completely, the residue was placed in sample cups and measured by XRF. The residue was labelled Sequential extraction 2 (SEQ 2) measurement.

**Step 3**

The residue from step 2 was transferred to a beaker. 50 mL of 8.8 M $H_2O_2$ was added to the beaker. It was digested at room temperature for 1hour then at $85^o$C for an hour in a water bath until the volume in the beaker was less than 3 mL. Another 10 mL of 8.8 M $H_2O_2$ was added to the same beaker and heated in a water bath at $85^0$c until the volume reduced to 2 mL. Then 5 mL of 1 M $CH_3COONH_4$ (ammonium acetate) was added to the residue in the beaker at pH 2 in a 200 mL centrifuge tubes and shaken overnight. The extract was separated from the residue by centrifuging at 3000 g for 20 minutes. The residue was washed with DI water, shaken for 15 minutes, centrifuged at 3000 g for 20 minutes. The supernatant was decanted, the residue was then dried in

an oven at $100^0$C. After drying completely, the residue was placed in sample cups and measured by XRF. The residue was labelled Sequential extraction 3 (SEQ 3) measurement.

**Total digestion**

50 mL Aqua regia (HCl-$HNO_3$, 3:1 (v/v)) was added to the residue from step 3 in 200 mL centrifuge plastic tubes, stoppered and shaken by a shaker overnight. The extract was separated from the residue by centrifuging at 3000 g for 20 minutes. The residue was washed with DI water, shaken for 15 minutes, centrifuged at 3000 g for 20 minutes. The supernatant was decanted, the residue was then dried in an oven at $100^0$C. After drying completely, the residue was placed in sample cups and XRF measurement was carried out. The residue was labeled as Sequential extraction 4 (SEQ 4) measurement.

### *2.4.4 Definition of Sequential extraction abbreviations:*

**SEQ 0** – XRF measurement of the sediment sample before any extraction.

**SEQ 1**- XRF measurement of the residue after extraction with 200 mL of 0.11 M $CH_3COOH$ (Acetic acid) ;the first step of sequential extraction.

**SEQ 2**-XRF measurement after extraction with 200 mL of 0.5 M $NH_2OH.HCl$ (hydroxylammonium chloride) in the second step of the sequential extraction

**SEQ 3- XRF measurement** of the residue after extraction with 50 mL of 8.8 M $H_2O_2$ and 1 M $CH_3COONH_4$ in the third step of the sequential extraction.

**SEQ 4**- XRF measurement after total extraction using 50 mL Aqua regia (HCl-$HNO_3$, 3:1 (v/v)).

# 3. RESULTS AND DISCUSSION

## 3.1 Identification of element peaks on the XRF spectra

X-Rays are composed of photons whose energies are between 125 KeV to 0.125 KeV. The energy of the emitted fluorescence is directly related to a specific element.

Shown below in Table 5 are the elements that were measured in this work along with their characteristic photon energies.

***Table 5**: Referenced and experimental peak energies on XRF spectra*

| Elements | Range | Referenced KeV | Exp. KeV | Peak range KeV |
|---|---|---|---|---|
| **Pb** | 2 | 10.552/12.614 | 10.55 | 10.35-10.73 |
| **Al** | 4 | 1.487/1.557 | 1.49 | 1.39-1.61 |
| **Ca** | 2 | 3.692/4.013 | 3.69 | 3.51-3.85 |
| **Cr** | 2 | 5.415/5.947 | 5.41 | 5.15-5.71 |
| **Mn** | 2 | 5.899/6.490 | 5.90 | 5.75-6.05 |
| **Fe** | 2 | 6.404/7.058 | 6.41 | 6.21-6.61 |
| **Cu** | 2 | 8.048/8.905 | 8.05 | 7.87-8.37 |
| **Zn** | 2 | 8.639/9.572 | 8.63 | 8.43-8.83 |
| **Mg** | 4 | 1.254/1.302 | 1.29 | 1.17-1.35 |
| **Rh** | 2 | 20.216/22.724 | 20.22 | 19.45-20.73 |

The XRF spectrum obtained shows the intensity of X-rays (in counts per second) as a function of energy (in KeV)

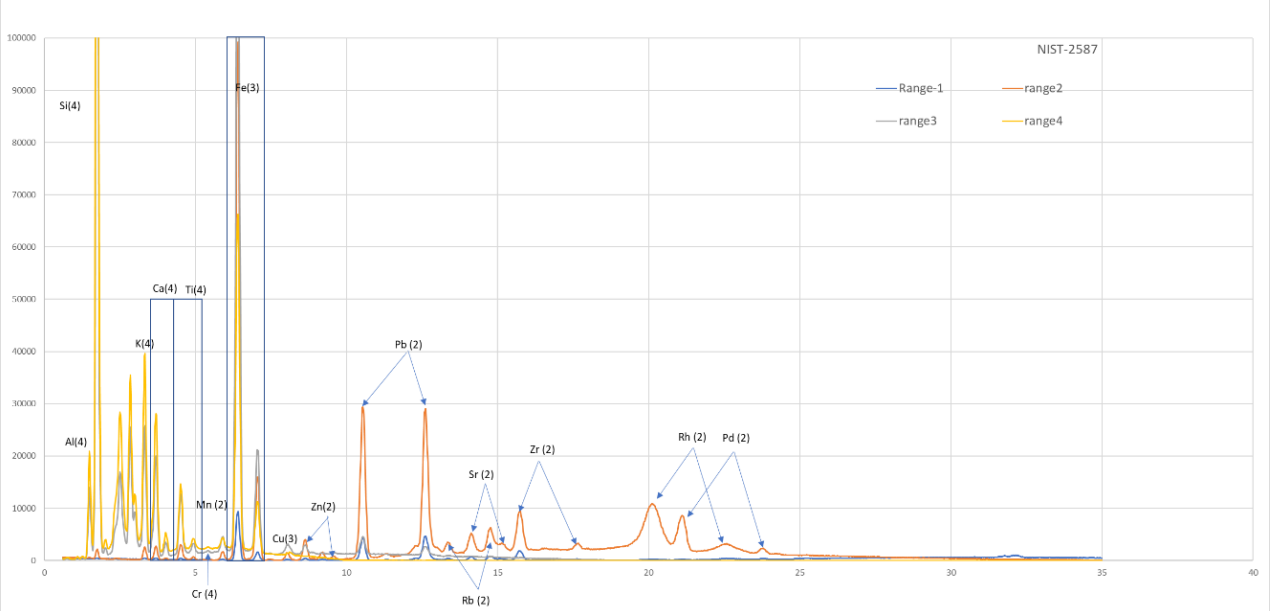


**Figure 7**: XRF spectrum with identified peaks

The peaks observed in XRF spectral data can be used to both identify and quantify metals in a sample. Both peak heights and peak areas be used. The qualitative aspect is to identify each element based on the characteristic XRF photon energy of a peak, while the peak height or amplitude is proportional to the element's concentration. Instead of peak height measurements, peak area measurements can be performed that correspond to the sum of all the intensities within the energy range of the peak.

The corrected peak height or peak area is the peak height/area with the background component of the signal removed. The Compton scattering peak is present in every XRF spectrum and is due to Compton scattering of the X-ray source radiation. In these studies, the Compton scattering peak appears at 21 KeV and is used in the processing the calibration data through calculation of the analyte peak height or area that is adjusted by the Compton peak height or area.

## 3.2. Calibration for element quantitation

### *3.2.1 Internal calibration using sample dilution with Calcium carbonate.*

A series of measurements were performed to evaluate the potential of using a pure compound as an additive that would serve as a dilution agent and contribute to greater uniformity of samples measured by the XRF approach. To reduce variations in the XRF responses due to variations in the sample matrix, samples were diluted with calcium carbonate in fixed ratios and the XRF responses were measured as a function of the concentration/amount of the sample in the mixture.

***Table 6**: Identified Element intensities from Calcium carbonate dilution samples.*

| Elements | Range | Exp. KeV | A | C | D | E | F |
|---|---|---|---|---|---|---|---|
| | | | 100% | 25% | 12.50% | 6.25% | 0% |
| **Mn** (cps) | 2 | 5.899 | 4916 | 371 | 230 | 100 | 47 |
| **Zn** (cps) | 2 | 8.63 | 919 | 151 | 102 | 73 | 52 |
| **Pb (**cps) | 2 | 10.552 | 955 | 382 | 318 | 330 | 276 |
| **Ca** (cps) | 3 | 3.69 | 31034 | 449191 | 452824 | 491247 | 473480 |
| **Fe** (cps) | 3 | 6.41 | 102300 | 4241 | 2311 | 1383 | 365 |
| **Cu** (cps) | 3 | 8.05 | 2066 | 859 | 728 | 781 | 807 |
| **Mg** (cps) | 4 | 1.29 | 1117 | 228 | 237 | 182 | 197 |
| **Al** (cps) | 4 | 1.49 | 33412 | 1911 | 1238 | 811 | 291 |
| **Si** (cps) | 4 | 1.75 | 401365 | 17967 | 9998 | 5512 | 348 |
| **K** (cps) | 4 | 3.31 | 33284 | 3268 | 2309 | 2616 | 1622 |
| **Ti** (cps) | 4 | 4.51 | 9682 | 707 | 617 | 311 | 387 |
| **Cr** (cps) | 4 | 5.41 | 2279 | 626 | 540 | 486 | 422 |

Shown in **Appendix 1** are plots of the XRF responses for several elements as a function of concentration/mixing ratio that indicate a trend where the XRF response increases with the amount of the element of interest, which suggests that the use of calcium carbonate (or another pure compound) to produce more consistent sample matrices has feasibility to normalize the XRF responses.

### *3.2.2 Multielement standard solutions for external calibration*

Multielement standard solutions were prepared at the concentrations of 15.625 ppm, 31.25 ppm, 62.5 ppm, 125 ppm, 250 ppm, 500 ppm, 1000 ppm. Calibration curves were plotted with peak height uncorrected, peak height corrected by Compton and peak area corrected by Compton. The calibration method of peak height corrected by Compton scattering has the highest $R^2$ value where a higher $R^2$ value indicates better correlation and linearity of the data.

***Table 7:*** *XRF 1ntensities of different elements in the multielement solution of varying concentrations*

| Concentrations (ppm) | **15.625** | **31.25** | **62.5** | **125** | **250** | **500** | **1000** |
|---|---|---|---|---|---|---|---|
| Mn (cps) | 1401 | 2742 | 4971 | 9103 | 13300 | 22376 | 30002 |
| Zn (cps) | 6462 | 13502 | 24035 | 45081 | 67052 | 106523 | 135549 |
| Pb (cps) | 11375 | 16526 | 24442 | 39540 | 55823 | 82138 | 100507 |
| Ca (cps) | 33193 | 34595 | 38403 | 42922 | 48988 | 62744 | 77616 |
| Fe (cps) | 44714 | 51049 | 60208 | 77485 | 98628 | 138244 | 175310 |
| Cu (cps) | 63488 | 70103 | 79173 | 95498 | 115939 | 152564 | 186095 |
| Mg (cps) | 5087 | 5330 | 3877 | 4374 | 4999 | 5475 | 6561 |
| Al (cps) | 4907 | 5100 | 3931 | 4259 | 4782 | 5486 | 6563 |
| Cr (cps) | 34404 | 38388 | 46257 | 58221 | 73274 | 103449 | 133223 |
| Co (cps) | 279 | 391 | 438 | 726 | 1193 | 2004 | 3346 |

***Table 8**: Calibration information collected when measured multielement standard solution.*

| | Peak height uncorrected | | Peak height corrected. by Compton | | Peak area corrected. by Compton | |
|---|---|---|---|---|---|---|
| | Y=ax+b | $R^2$ | Y=ax+b | $R^2$ | Y=ax+b | $R^2$ |
| Ca | y = 3.0628x + 1905.5 | 0.9734 | y = 3E-05x + 0.0045 | 0.9897 | y = 6E-06x + 0.0008 | 0.9902 |
| Cr | y = 26.37x + 1402 | 0.9799 | y = 0.0002x + 0.0011 | 0.9982 | y = 5E-05x + 0.0002 | 0.9979 |
| Mn | y = 42.838x + 2089.6 | 0.9777 | y = 0.0004x + 0.0022 | 0.9987 | y = 9E-05x + 0.0005 | 0.998 |
| Fe | y = 62.281x + 3282.3 | 0.9766 | y = 0.0006x + 0.0052 | 0.9981 | y = 0.0001x + 0.0012 | 0.9978 |
| Co | y = 120.54x + 6032.1 | 0.9731 | y = 0.0011x + 0.0097 | 0.9981 | y = 0.0003x + 0.0023 | 0.9979 |
| Cu | y = 152.42x + 8638.4 | 0.9714 | y = 0.0013x + 0.0159 | 0.9978 | y = 5E-05x + 0.0002 | 0.9979 |
| Zn | y = 201.41x + 10732 | 0.9705 | y = 0.0018x + 0.0171 | 0.9978 | y = 0.0005x + 0.0042 | 0.9976 |
| Ga | y = 246.93x + 14605 | 0.9709 | y = 0.0021x + 0.0236 | 0.9979 | y = 0.0006x + 0.0066 | 0.9975 |

As shown in appendix 2, plotting a calibration curve using the multielement solution made it possible to identify more elements and to calibrate with more points in the curves.

As Shown in Appendix 3**,** building a calibration curve using background corrected peak height of the standard reference material to background corrected Compton peak ratio of the different elements, there is a significant improvement in the linearity as indicated by the $R^2$ values for the plots which are 0.99 or higher for all the elements.

### *3.2.3 Building calibration using standard reference material.*

*3.2.3.1 Reference materials*

Certified percentage of elements in NIST-RSMs. Except for Pb and Zn, all other elements' calibration curves were plotted using three of the four reference materials.

***Table 9**: Percentage of elements in NIST-RSMs*

| Elements | RSM2586 (%) | RSM2587 (%) | RSM1645 (%) | RSM8704 (%) |
|---|---|---|---|---|
| **Pb** | 0.0401 | 0.3242 | 0.0714 | 0.0150 |
| **Al** | 6.6520 | 5.8600 | 2.2600 | 6.1000 [a] |
| **Ca** | 2.2180 | 0.9270 | 2.9000[a] | 2.6410 |
| **Cr** | 0.0301 | 0.0092 | 2.9600[a] | 0.0122 |
| **Mn** | 0.1000 | 0.0651 | 0.0785[a] | 0.0544 |
| **Fe** | 5.1610 | 2.8130 | 3.9700[a] | 3.9700 |
| **Cu** | 0.0810[a] | 0.0160 | 0.0109 | 0.0099 |
| **Zn** | 0.0352 | 0.0336 | 0.1720 | 0.0408 |
| **Mg** | 1.7070 [a] | 0.6690 | 0.7400 | 1.2000 |
| [a]: Certified values are outliners and are not included in the calibration curves | | | | |

### 3.2.3.2 Background corrected versus uncorrected peak height.

According to the results shown in Appendix 4, the calibrations based on corrected peak heights provide better linearity compared to uncorrected peak height as seen in the $R^2$ values.

3.2.3.3. Background corrected peak height versus peak area.

Shown in Appendix 5 are calibration curves for different elements for Background corrected peak height versus peak area. Background corrected peak height shows better linearity than background corrected peak area for most elements. This is because for peak area, the peaks are not perfectly symmetrical.

3.2.3.4. Compton corrected versus background corrected peak height.

As shown in appendix 6 the peak height ratio of XRF responses to the Compton scattering provides the best linearity and this approach was chosen for quantification of the sediment samples.

**Choice of Calibration method for metal quantitation**

Calibration was performed using four Standard reference materials (SRMs): NIST 2586- Trace elements in soil containing trace elements. NIST 2587-Trace elements in soil containing Lead from paint. NIST1645-A river sediment NIST8704- Trace elements in Buffalo River Sediment. The four-reference materials matrix was similar to the matrix of the sample sediments.

Four calibration methods were explored in this study to determine which method gave the highest $R^2$ values and best linearity for all of the elements.

**Calibration curve using peak height**: Both uncorrected peak height and background corrected peak height calibration curves gave a correction coefficient less than 0.99 for all the elements of interest.

***Table 10**: Comparison of the correlation coefficient of different methods for all the elements.*

| **Element** | **Correlation coefficient** | | | |
|---|---|---|---|---|
| | **Uncorrected peak height** | **Background corrected peak height** | **Background corrected peak area** | **Background corrected (SRM peak height to Compton peak height ratio)** |
| Mg | $R^2 = 0.8798$ | $R^2 = 0.9708$ | $R^2 = 0.9631$ | |
| Al | $R^2 = 1$ | $R^2 = 0.9998$ | $R^2 = 0.9995$ | |
| Ca | $R^2 = 0.9624$ | $R^2 = 0.9651$ | $R^2 = 0.9475$ | $R^2 = 0.9966$ |
| Cr | $R^2 = 0.961$ | $R^2 = 0.9756$ | $R^2 = 0.9733$ | $R^2 = 0.9904$ |
| Fe | $R^2 = 0.9618$ | $R^2 = 0.9621$ | $R^2 = 0.9638$ | $R^2 = 1$ |
| Zn | $R^2 = 0.9871$ | $R^2 = 0.9696$ | $R^2 = 0.9683$ | $R^2 = 0.9997$ |
| Cu | $R^2 = 0.6861$ | $R^2 = 0.7015$ | $R^2 = 0.6252$ | $R^2 = 0.9986$ |
| Pb | $R^2 = 0.981$ | $R^2 = 0.9829$ | $R^2 = 0.9838$ | $R^2 = 0.9984$ |
| Mn | $R^2 = 0.9334$ | $R^2 = 0.9543$ | $R^2 = 0.9502$ | $R^2 = 0.9778$ |

The $R^2$ values shown above correspond to the square of the correlation coefficient and are an indication of the linearity of the XRF responses to the mass percentage of the element in the sample.

The background corrected peak height ratio of the XRF responses to the Compton scattering provides the best linearity of the three calibration methods considered. It is therefore the method chosen for quantification of the sediment samples.

Background corrected peak height ratio of the XRF response to the Compton scattering provided the lowest limits of detection and limits of quantitation.

## 3. 3 Limit of detection

An important figure of merit used to compare analytical methods is the limit of detection (LOD). According to the IUPAC, the LOD is the smallest amount of analyte that produces a response that is equal to three (3) times the standard deviation of the blank measurements. In this study, the standard deviation of the residuals (from the calibration curve) was used in place of the standard deviation of the blank.

LOD = 3 * standard deviation of the residuals / (m)

Limit of detections were calculated for different calibration methods based on different data processing approaches and compared to metal concentrations in Poland sediments and samples from the sequential extractions.

***Table 11**: Limits of detection (LODs) of different of calibration methods*

| | Background uncorrected peak Height | Background corrected peak Height | Background corrected peak Area | Compton corrected peak Height |
|---|---|---|---|---|
| **Major elements** | **Limit of detection in percentage (%)** | | | |
| Mg (range 4) | 0.4 | 0.2 | 20 | |
| Al (range 4) | 0.01 | 0.1 | 0.2 | |
| Ca (range 2) | 0.8 | 0.7 | 0.9 | 0.2 |
| Fe (range 2) | 1 | 1 | 1 | 0.02 |
| **Trace elements** | **Limit of detection in percentage (%)** | | | |
| Cr (range 2) | 0.01 | 0.008 | 0.008 | 0.005 |
| Mn (range 2) | 0.03 | 0.02 | 0.02 | 0.02 |
| Cu (range 2) | 0.01 | 0.009 | 0.01 | 0.0005 |
| Zn (range 2) | 0.05 | 0.04 | 0.05 | 0.004 |
| Pb (range 2) | 0.07 | 0.07 | 0.06 | 0.02 |

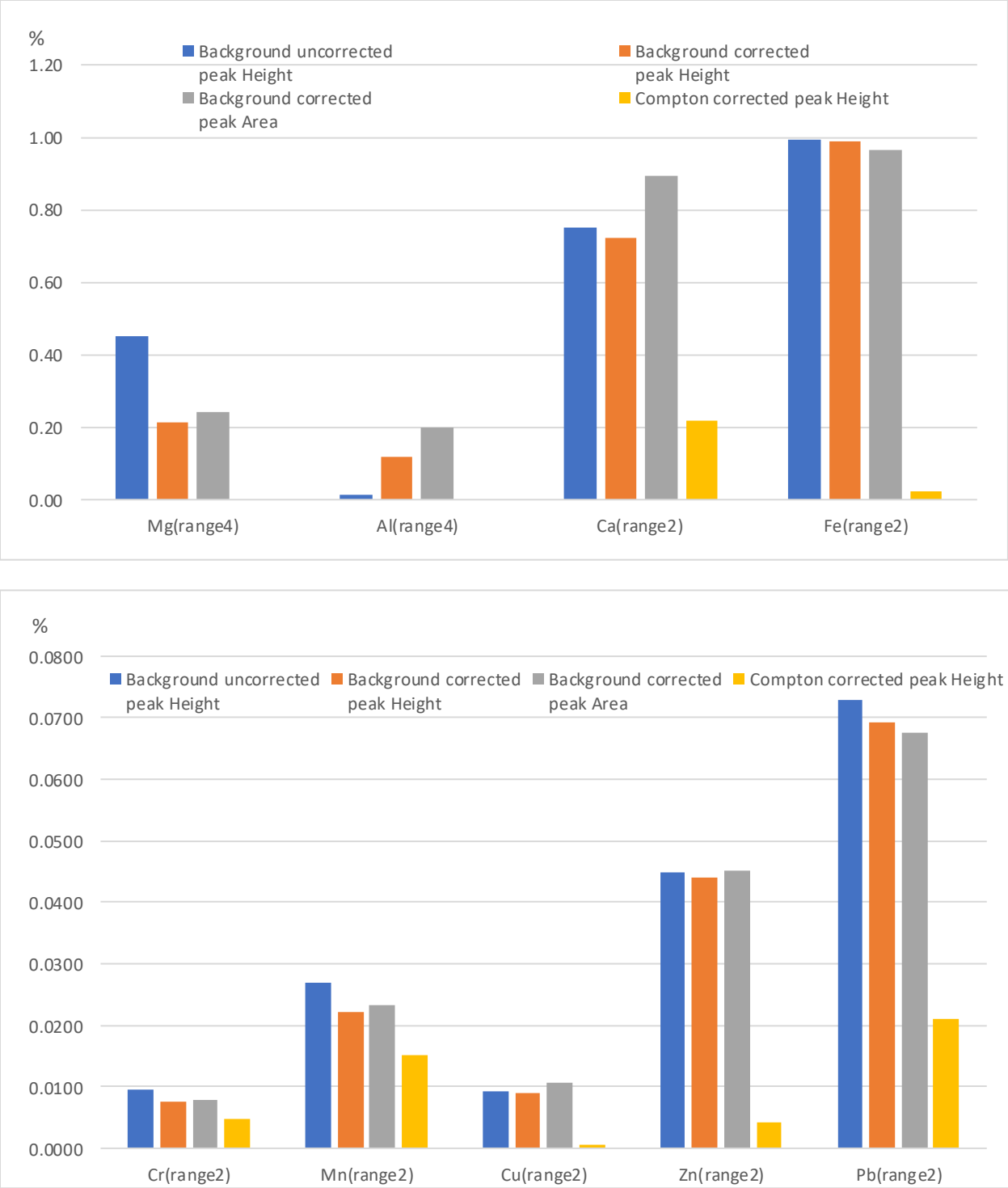


**Figure 8**: Limit of detections of the selected calibration methods and metals' concentrations in samples

## 3.4 Limit of quantitation (LOQs) of different calibration methods

***Table 12**: Limits of quantitation (LOQs) of different of calibration methods*

| | Background uncorrected peak Height | Background corrected peak Height | Background corrected peak Area | Compton corrected peak Height |
|---|---|---|---|---|
| **Major elements** | **Limit of quantitation in percentage (%)** | | | |
| Mg (range 4) | 1.5 | 0.7 | 67.8 | |
| Al (range 4) | 0.05 | 0.4 | 0.7 | |
| Ca (range 2) | 2.5 | 2.4 | 3.0 | 0.7 |
| Fe (range 2) | 3.3 | 3.3 | 3.2 | 0.1 |
| **Trace elements** | **Limit of quantitation in percentage (%)** | | | |
| Cr (range 2) | 0.03 | 0.03 | 0.03 | 0.02 |
| Mn (range 2) | 0.09 | 0.07 | 0.08 | 0.05 |
| Cu (range 2) | 0.031 | 0.030 | 0.036 | 0.002 |
| Zn (range 2) | 0.15 | 0.15 | 0.15 | 0.01 |
| Pb (range 2) | 0.24 | 0.23 | 0.22 | 0.07 |

**Table 13**: Limits of detection of the selected calibration methods and a comparison of the metal concentrations in samples (totals versus residuals)

| Method of calibrations | Elements | LOD (%) | LOQ (%) | Poland samples 1.22.22 (%) | SEQ 4 – last step (%) |
|---|---|---|---|---|---|
| Background corrected peak Height | Mg (range 4) | 0.21 | 0.8 | >0.7 | >0.2 |
| | Al (range 4) | 0.12 | 0.7 | >4 | >3 |
| Compton corrected. peak Height | Ca (range 2) | 0.22 | 3 | >0.6 | >0.1 |
| | Fe (range 2) | 0.02 | 3.2 | >1.5 | >0.3 |
| | Cr (range 2) | 0.0047 | 0.03 | >0.001 | >0.0003 |
| | Mn (range 2) | 0.0152 | 0.08 | >0.05 | >0.0001 |
| | Cu (range 2) | 0.0005 | 0.036 | >0.04 | >0.001 |
| | Zn (range 2) | 0.0042 | 0.15 | >0.04 | >0.001 |
| | Pb (range 2) | 0.0211 | 0.22 | Negative | Negative |

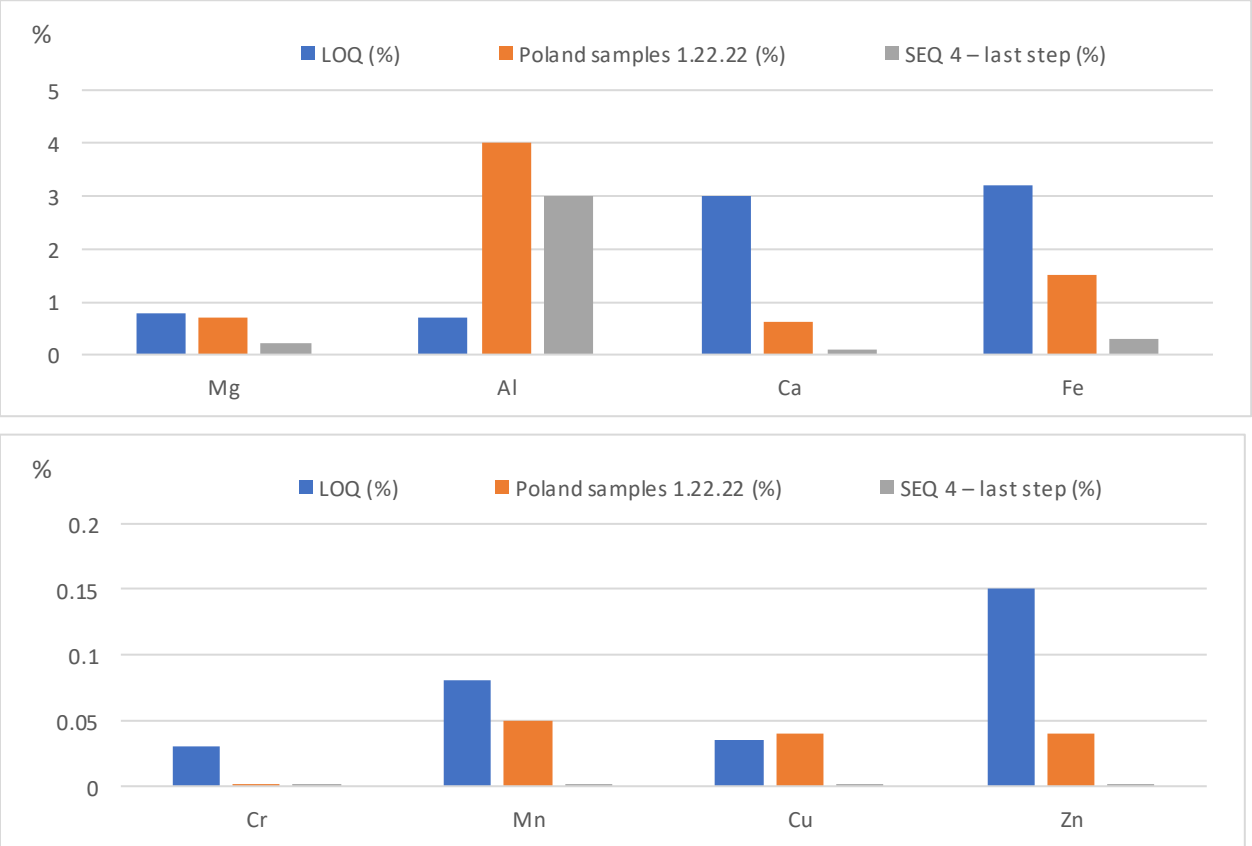


**Figure 9**: Graphical representation of limit of detection and limit of quantitation of different elements

## 3.5 Acetic acid extraction

Three samples each from the three sampling sites were subjected to acetic extraction to determine the bioavailability of elements in the samples when treated with a weak acid. Using the corrected peak height to background corrected Compton peak height ratio, their concentrations were determined before and after extraction. Before extraction the samples were labeled as SEQ O and after extraction with acetic acid they were labeled SEQ 1.

***Table 14**: concentration in percentage of different elements before and after acetic extraction (Key SEQ-0 : Percentage before acetic extraction, SEQ-1: Percentage after acetic acid extraction.*

| | **Wood** | | **Cemetery** | | **Library** | |
|---|---|---|---|---|---|---|
| | **W-SEQ-0** | **W-SEQ-1** | **C-SEQ-0** | **C-SEQ-1** | **L-SEQ-0** | **L-SEQ-1** |
| Mg | 1.37 | 0.95 | 1.35 | 0.78 | 1.02 | 0.88 |
| Al | 8.04 | 7.20 | 6.84 | 6.27 | 5.37 | 5.98 |
| Ca | 0.84 | 0.46 | 1.97 | 0.53 | 0.93 | 0.57 |
| Fe | 1.87 | 1.90 | 2.54 | 2.00 | 1.40 | 1.80 |
| Cr | 0.0038 | 0.0035 | 0.0071 | 0.0054 | 0.0034 | 0.0045 |
| Mn | 0.0837 | 0.0277 | 0.0933 | 0.0344 | 0.0431 | 0.0312 |
| Cu | 0.0025 | 0.0022 | 0.0025 | 0.0025 | 0.0020 | 0.0021 |
| Zn | 0.0067 | 0.0061 | 0.0096 | 0.0062 | 0.0051 | 0.0063 |
| Pb | -0.0043 | -0.0039 | -0.0032 | -0.0045 | -0.0040 | -0.0018 |


**Figure 10:** Graphical representation of element percentage before and after acetic extraction of the different sampling sites. (Wood, Cemetery and Library)

## 3.6 Sequential extraction

In comparison to measuring the total concentrations, a sequential extraction procedure can be used to investigate the environmental availability and mobility of metals in the sediments. These procedures use a series of extractions to characterize which metals are released under different environmental conditions.

Sediment samples from all the sample sites (cemetery, library, and Poland Woods) for one sampling date were characterized using s sequential extraction procedure combined with XRF measurement of the sediment sample following each extraction step.

Shown in the following Table (13) are the results of that procedure combined with the XRF measurements.

As seen in the table, there are values reported for the following steps: SEQ 0, SEQ 1, SEQ 2, SEQ3 and SEQ 4, which correspond to the measured concentrations in the samples before the sequential extraction procedure begins, the concentration in the sample after the first extraction, the concentration in the sample after the second extraction, the concentration in the sample after the third extraction, and the concentration remaining in the sample following the last extraction.

Explanation of abbreviations used in **Table 15** below.

**SEQ 0** – XRF measurement of the sediment sample before any extraction.

**SEQ 1**- XRF measurement of the residue after extraction with 200 ml of 0.11 M $CH_3COOH$ (Acetic acid); the first step of sequential extraction.

**SEQ 2**-XRF measurement after extraction with 200ml of 0.5 M $NH_2OH.HCl$ (hydroxylammonium chloride) in the second step of the sequential extraction.

**SEQ 3- XRF measurement** of the residue after extraction with 50ml of 8.8 M $H_2O_2$ and 1 M $CH_3COONH_4$ in the third step of the sequential extraction.

**SEQ 4**- XRF measurement after total extraction using 50ml Aqua regia ($HCl$-$HNO_3$, 3:1 (v/v)).

W1- Municipal Wood Forest sample sub-site 1, W2- Municipal Wood Forest sample sub-site 2

W3- Municipal Wood Forest sample sub-site 3, W4- Municipal Wood Forest sample sub-site 4

C1-Cemetery sample sub-site 1, C2-Cemetery sample sub-site 2, C3-Cemetery sample sub-site 3

C4-Cemetery sample sub-site 4

L1-Library Sample subsite 1, L2-Library Sample subsite 2, L3-Library Sample subsite 3, L4-Library Sample subsite 4

The concentration of the different elements after each step of sequential extraction are shown in appendix 7 to appendix 11: Appendix 7: Element concentration in SEQ 0, Appendix 8: Element concentration in SEQ 1, Appendix 9**:** Element concentration in SEQ 2, Appendix 10: Element concentration in SEQ 3, Appendix 11: Element concentration in SEQ 4.

To evaluate possible trends in the amounts of the metals and their availability at different sites, the results were combined to determine the average amounts of the metals at each location for each extraction step. The results of those calculations are shown in the following table.

***Table 15****: Average Mg concentrations and standard deviation in each site*

| Mg | SEQ0 | SEQ1 | SEQ2 | SEQ3 | SEQ4 |
|---|---|---|---|---|---|
| Wood | | | | | |
| Average % | 0.59 | 0.46 | 0.35 | 0.34 | 0.27 |
| RSD% | 5.5 | 16.1 | 6.4 | 11.8 | 7.9 |
| Cemetery | | | | | |
| Average % | 0.51 | 0.38 | 0.35 | 0.32 | 0.29 |
| RSD% | 15.8 | 27.0 | 8.7 | 5.3 | 6.5 |
| Library | | | | | |
| Average % | 0.57 | 0.40 | 0.41 | 0.35 | 0.30 |
| RSD% | 6.0 | 7.8 | 8.5 | 12.6 | 6.1 |

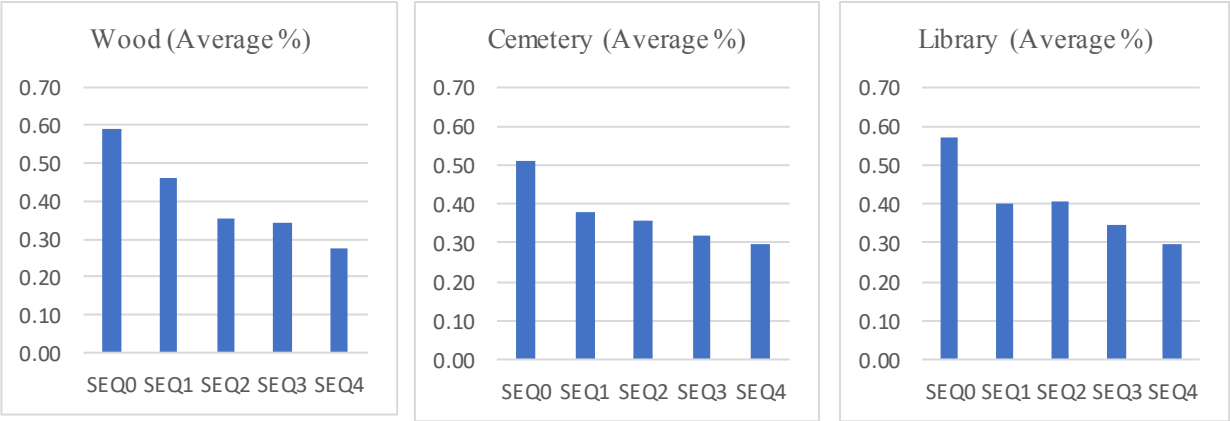


**Figure 11**. Graphical representation of Mg percentage after each extraction step.

***Table 16**: Average Al concentrations and standard deviation in each site*

| Al | SEQ0 | SEQ1 | SEQ2 | SEQ3 | SEQ4 |
|---|---|---|---|---|---|
| Wood | | | | | |
| Average % | 5.34 | 4.50 | 3.82 | 4.15 | 4.19 |
| RSD% | 2.6 | 8.3 | 6.4 | 2.4 | 4.6 |
| Cemetery | | | | | |
| Average % | 4.57 | 3.86 | 3.57 | 3.86 | 4.21 |
| RSD% | 9.2 | 13.8 | 9.0 | 4.6 | 10.4 |
| Library | | | | | |
| Average % | 4.48 | 3.86 | 3.69 | 3.58 | 3.77 |
| RSD% | 3.2 | 3.9 | 6.3 | 5.1 | 2.6 |

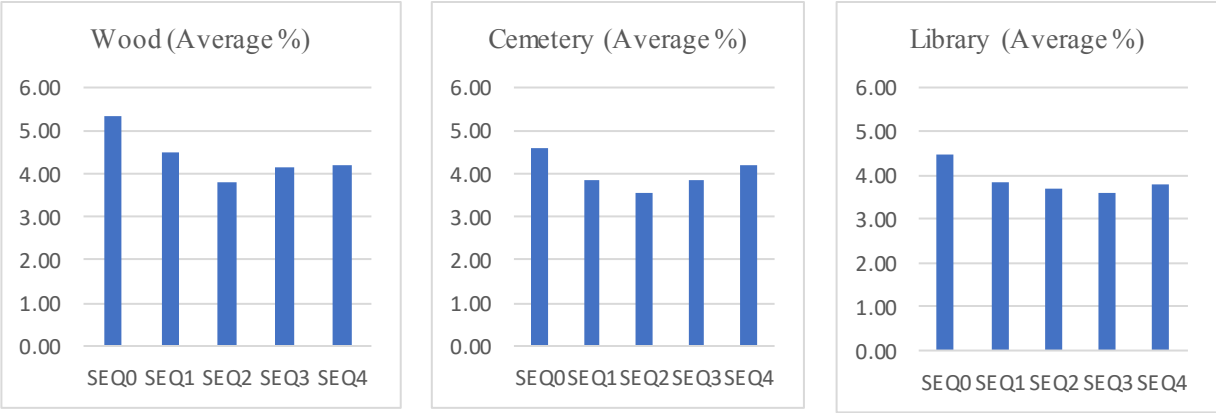


**Figure 12:** Graphical representation of Mg percentage after each extraction step.

***Table 17**: Average Ca concentrations and standard deviation in each site*

| Ca | SEQ0 | SEQ1 | SEQ2 | SEQ3 | SEQ4 |
|---|---|---|---|---|---|
| Wood | | | | | |
| Average % | 0.62 | 0.42 | 0.36 | 0.20 | 0.38 |
| RSD% | 6.1 | 2.2 | 5.4 | 5.1 | 1.8 |
| Cemetery | | | | | |
| Average % | 1.08 | 0.53 | 0.41 | 0.21 | 0.40 |
| RSD% | 24.6 | 24.7 | 10.1 | 11.0 | 6.7 |
| Library | | | | | |
| Average % | 1.37 | 0.58 | 0.51 | 0.33 | 0.50 |
| RSD% | 18.3 | 15.4 | 10.0 | 11.4 | 9.8 |

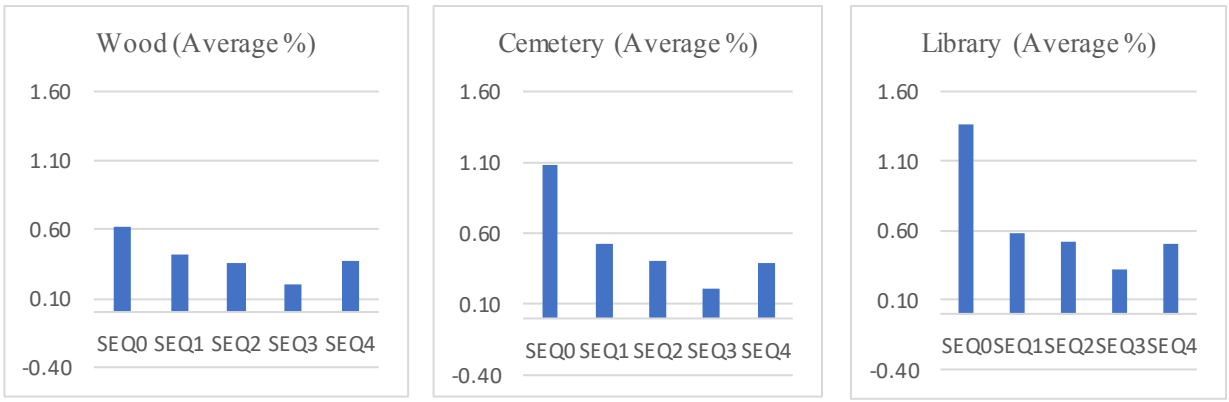


**Figure 13**: Graphical representation of Ca percentage after each extraction step.

***Table 18**: Average Fe concentrations and standard deviation in each site*

| Fe | SEQ0 | SEQ1 | SEQ2 | SEQ3 | SEQ4 |
|---|---|---|---|---|---|
| Wood | | | | | |
| Average % | 1.41 | 1.13 | 1.05 | 0.69 | 0.40 |
| RSD% | 11.0 | 12.1 | 12.7 | 6.8 | 8.7 |
| Cemetery | | | | | |
| Average % | 1.44 | 1.53 | 1.10 | 0.69 | 0.45 |
| RSD% | 9.1 | 47.6 | 10.1 | 7.1 | 15.4 |
| Library | | | | | |
| Average % | 1.80 | 1.70 | 1.57 | 1.28 | 0.70 |
| RSD% | 11.0 | 35.1 | 13.3 | 9.8 | 17.4 |

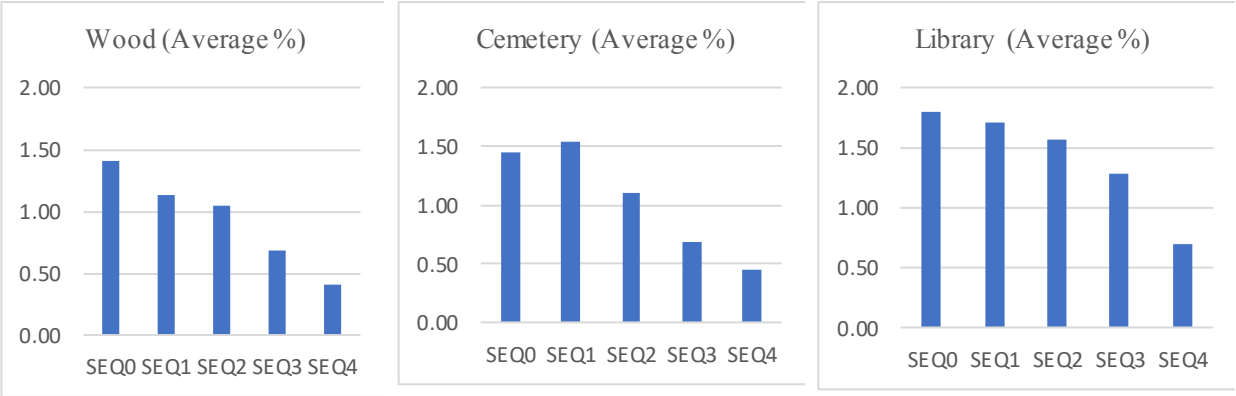


**Figure 14**: Graphical representation of Fe percentage after each extraction step.

***Table19**: Average Cr concentrations and standard deviation in each site*

| Cr | SEQ0 | SEQ1 | SEQ2 | SEQ3 | SEQ4 |
|---|---|---|---|---|---|
| Wood | | | | | |
| Average % | 0.0025 | 0.0033 | 0.0021 | 0.0015 | 0.0004 |
| RSD% | 35.0 | 26.7 | 48.0 | 37.4 | 15.1 |
| Cemetery | | | | | |
| Average % | 0.0023 | 0.0033 | 0.0017 | 0.0017 | 0.0006 |
| RSD% | 23.0 | 53.1 | 89.3 | 11.2 | 136.7 |
| Library | | | | | |
| Average % | 0.0036 | 0.0045 | 0.0039 | 0.0047 | 0.0023 |
| RSD% | 28.8 | 48.7 | 26.2 | 30.1 | 73.9 |

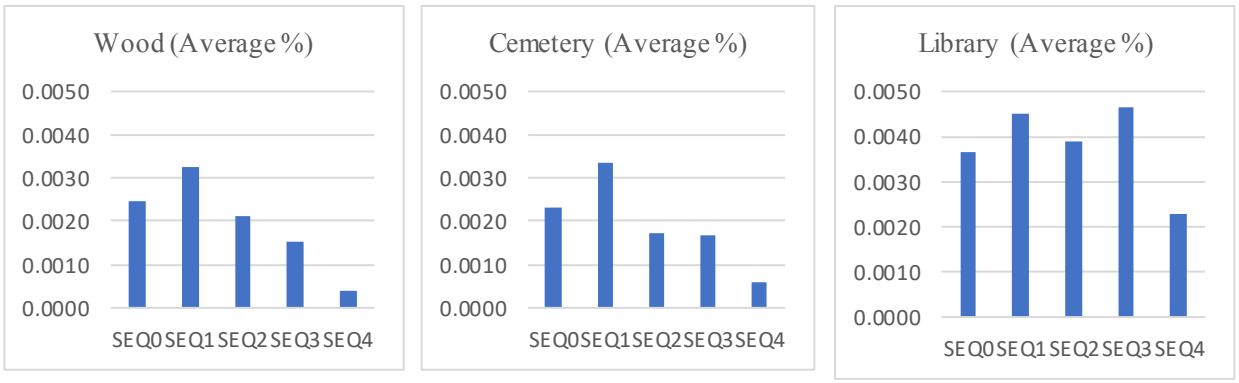


**Figure 15**: Graphical representation of Cr percentage after each extraction step.

***Table 20**: Average Mn concentrations and standard deviation in each site*

| Mn | SEQ0 | SEQ1 | SEQ2 | SEQ3 | SEQ4 |
|---|---|---|---|---|---|
| Wood | | | | | |
| Average % | 0.0983 | 0.0012 | 0.0105 | 0.0033 | -0.0002 |
| RSD% | 30.7 | 64.0 | 16.8 | 45.9 | -220.4 |
| Cemetery | | | | | |
| Average % | 0.1284 | 0.0115 | 0.0130 | 0.0051 | 0.0015 |
| RSD% | 32.3 | 139.0 | 32.3 | 49.0 | 102.1 |
| Library | | | | | |
| Average % | 0.1390 | 0.0150 | 0.0220 | 0.0163 | 0.0088 |
| RSD% | 7.5 | 87.6 | 14.3 | 12.2 | 44.8 |

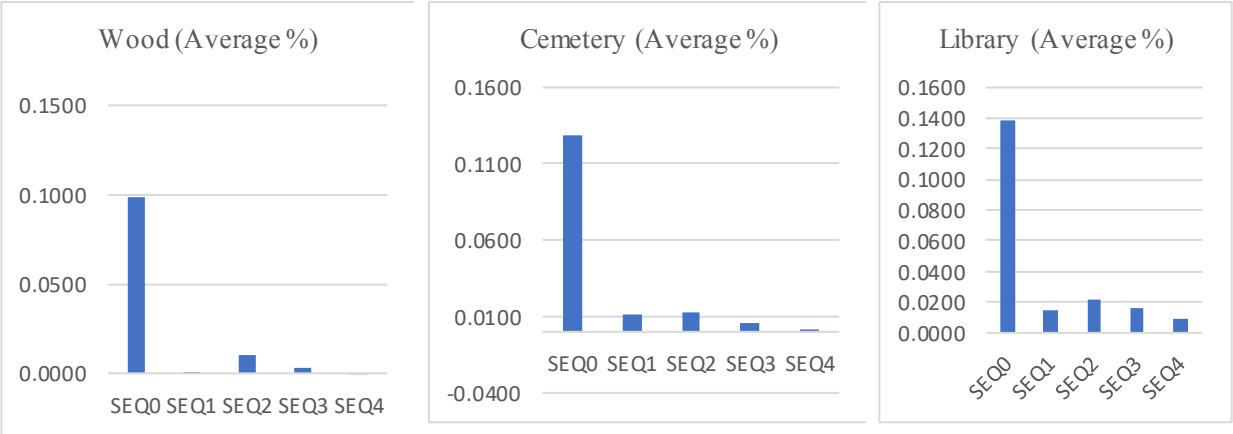


**Figure 16**: Graphical representation of Mn percentage after each extraction step.

***Table 21**: Average Cu concentrations and standard deviation in each site*

| Cu | SEQ0 | SEQ1 | SEQ2 | SEQ3 | SEQ4 |
|---|---|---|---|---|---|
| Wood | | | | | |
| Average % | 0.0033 | 0.0042 | 0.0017 | 0.0029 | 0.0019 |
| RSD% | 3.4 | 4.9 | 11.5 | 2.1 | 6.0 |
| C | | | | | |
| Average % | 0.0033 | 0.0048 | 0.0015 | 0.0030 | 0.0020 |
| RSD% | 1.8 | 23.1 | 16.2 | 3.3 | 2.8 |
| L | | | | | |
| Average % | 0.0036 | 0.0047 | 0.0016 | 0.0030 | 0.0020 |
| RSD% | 6.7 | 24.2 | 1.9 | 3.1 | 3.0 |

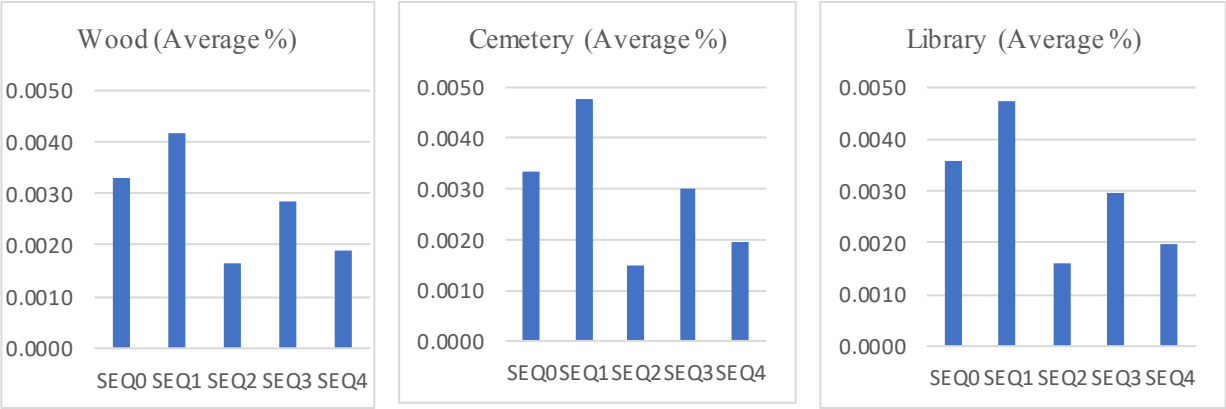


***Table 22**: Average Cu concentrations and standard deviation in each site*

| Zn | SEQ0 | SEQ1 | SEQ2 | SEQ3 | SEQ4 |
|---|---|---|---|---|---|
| Wood | | | | | |
| Average % | 0.0074 | 0.0042 | 0.0032 | 0.0047 | 0.0020 |
| RSD% | 7.2 | 4.9 | 10.7 | 2.5 | 6.7 |
| Cemetery | | | | | |
| Average % | 0.0079 | 0.0048 | 0.0034 | 0.0048 | 0.0022 |
| RSD% | 6.1 | 23.1 | 4.4 | 0.9 | 8.2 |
| Library | | | | | |
| Average % | 0.0080 | 0.0047 | 0.0038 | 0.0053 | 0.0026 |
| RSD% | 3.2 | 24.2 | 16.4 | 5.2 | 5.1 |

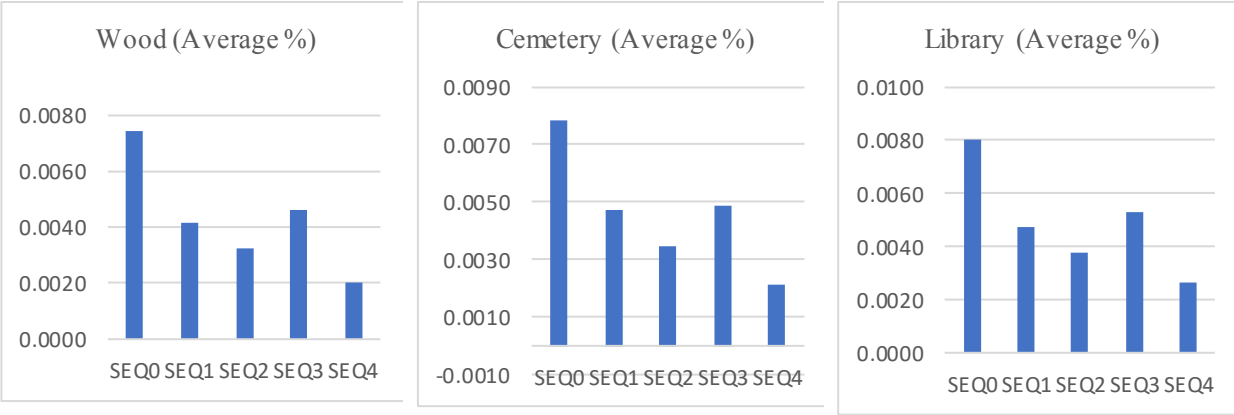


**Figure 18**: Graphical representation of Zn percentage after each extraction step

## 3.7 Discussion on Sequential extraction

The highest percentage of Ca, Mg and Mn was extracted by nitric acid in step one. This indicates that these elements are in the exchangeable or acid-soluble fraction. Therefore, they are easily extracted from the sediments under weakly acidic conditions. The exchangeable fraction is expected to contain weakly adsorbed metals bound on the sediment. These elements can easily be released into the water by ion-exchange processes and co-precipitated with carbonate salts. (Raulet et al. 1999).

A larger percentage of Cu (30%) and Zn (32%) is extracted by 0.5 M $NH_2OH.HCl$, which is a reducing agent. Cu therefore is found in the reducible fraction of elements present in these sediments. Metals that are in the reducible fraction are expected to be associated with Fe and Mn oxides and released by reducing conditions. (Rodgers et al. 2015).

Cr is primarily extracted from the sediments in the last step using aqua regia. It is not released in earlier steps because it is only available under strongly acidic conditions. Most of the trace elements in the residual fraction are expected to be silicate/crystalline-bound and are typically removed by dissolving the sediment residues in concentrated acids and are not expected to normally be available in the environment. (Rodgers et al. 2015).

## 3.8 XRF Measurement of Poland samples.

Shown in Appendix 12 is the Mg concentrations (%) of samples collected in the 10 sampling days.

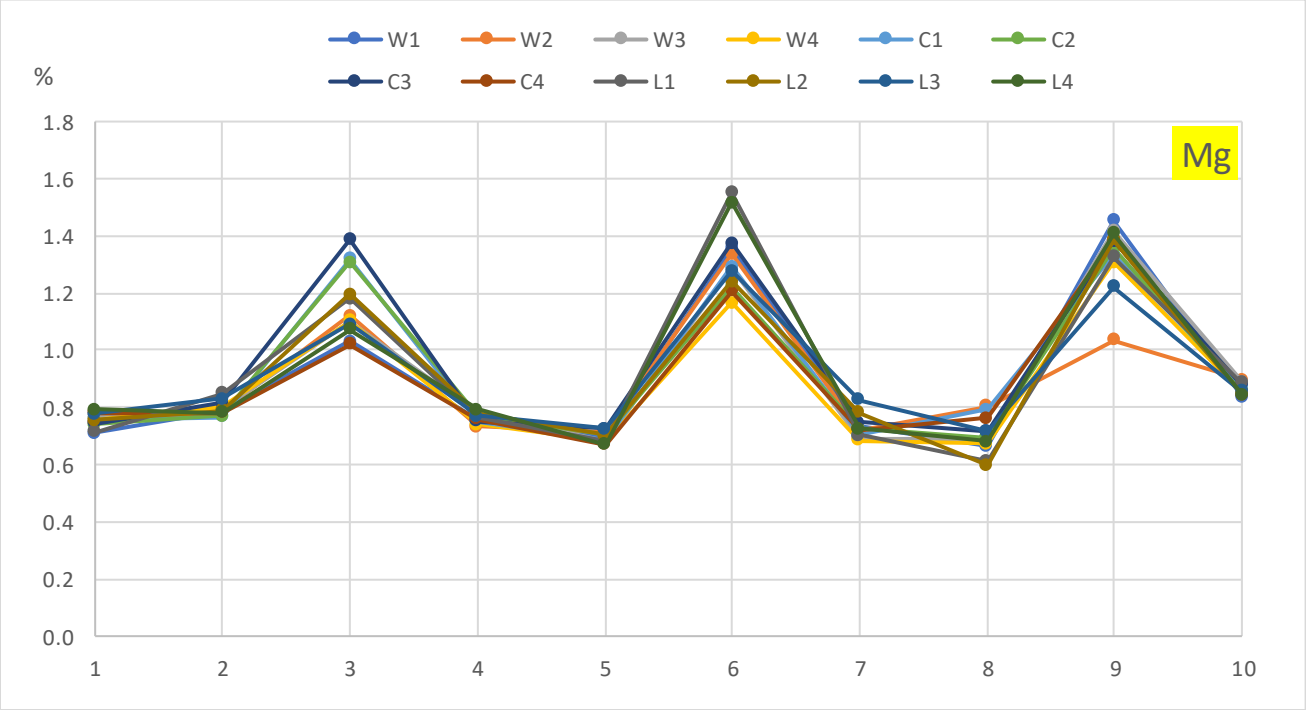


**Figure 19**: Mg concentrations (%) of samples collected 10 sampling days. 1-10.10.21; 2-11.1.21; 3-11.13.21; 4-12.20.21; 5-1.21.22; 6-2.6.22; 7-5.9.22; 8-5.25.22; 9- 7.25.22; 10-8.8.22

The change in concentration of Mg over time shows a good agreement in all the samples. There was high concentration of Mg on sample days 3(11.13.21),6(2.6.22) and 9 (7.25.22), This may be related to high levels of precipitation. The highest concentration of Mg was 1.5% and is considered high by EPA guidelines. Minerals like dolomite ($CaMg(CO_3)2$) and magnetite ($MgCO_3$) are some of the sources of Mg, which is carried away from its sources into the water bodies such as streams and rivers.(Firdiyono et al.2020)

Shown in Appendix 13 is the Al concentrations (%) of samples collected in the 10 sampling days.

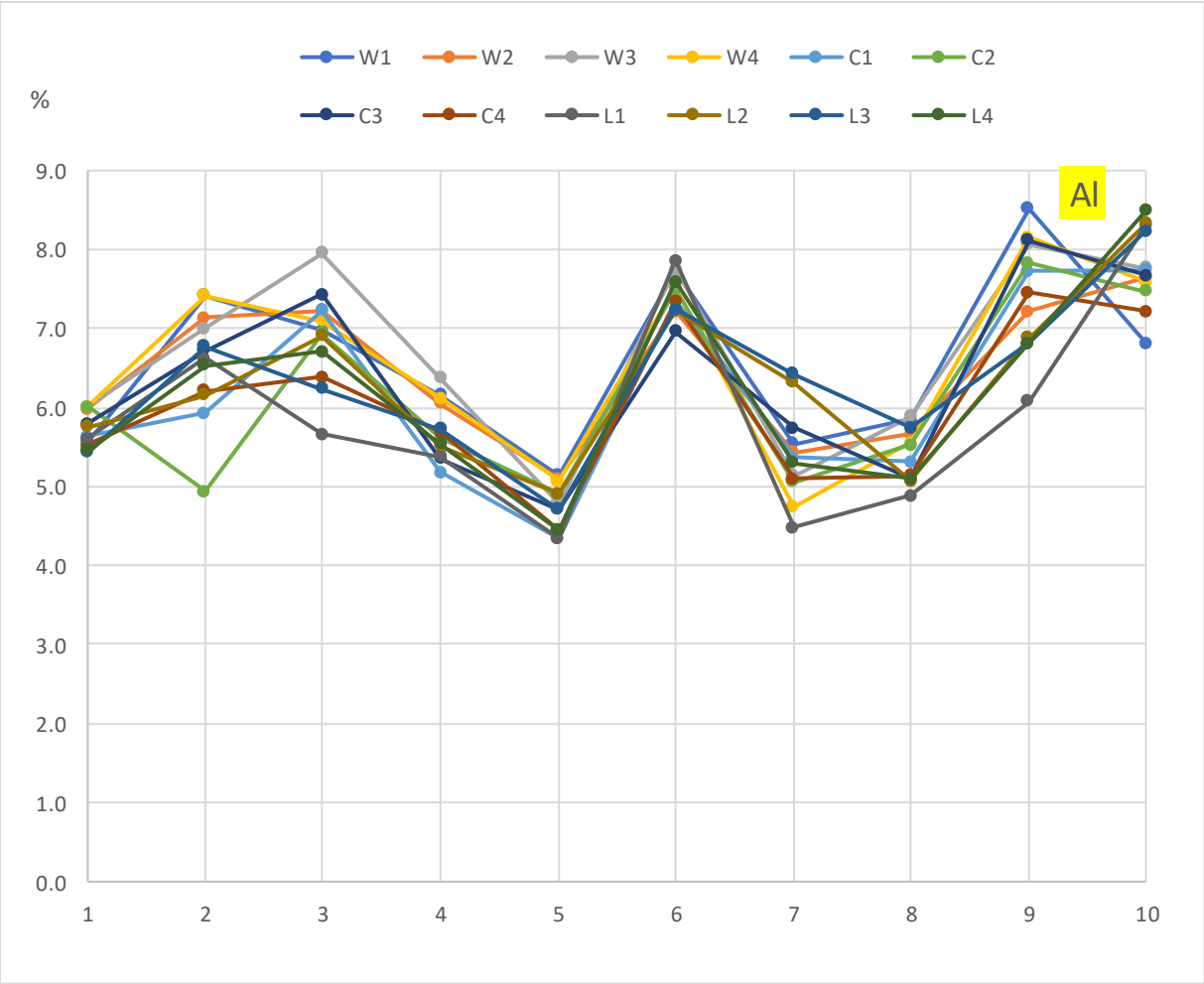


**Figure 20**: Al concentrations (%) of samples collected 10 sampling days. 1-10.10.21; 2-11.1.21; 3-11.13.21; 4-12.20.21; 5-1.21.22; 6-2.6.22; 7-5.9.22; 8-5.25.22; 9- 7.25.22; 10-8.8.22

There was a common trend in the change in concentration of Al for all the samples measured. Samples 6 (2.6.22),9 (7.25.22) and 10 (8.8.22) had the highest concentrations of Al. The highest concentration was 8.5%. Overall, the Cemetery samples had slightly higher concentrations compared to other sites (municipal wood and library). Al is commonly found in natural environments in the form of aluminosilicate in igneous rocks for example. Both natural and human activities are common sources of Al into the environment. Natural processes have a larger impact on the distribution of Al in the environment than anthropogenic sources (Lin et al. 2019).

Shown in Appendix 14 is the Ca concentrations (%) of samples collected in the 10 sampling days.

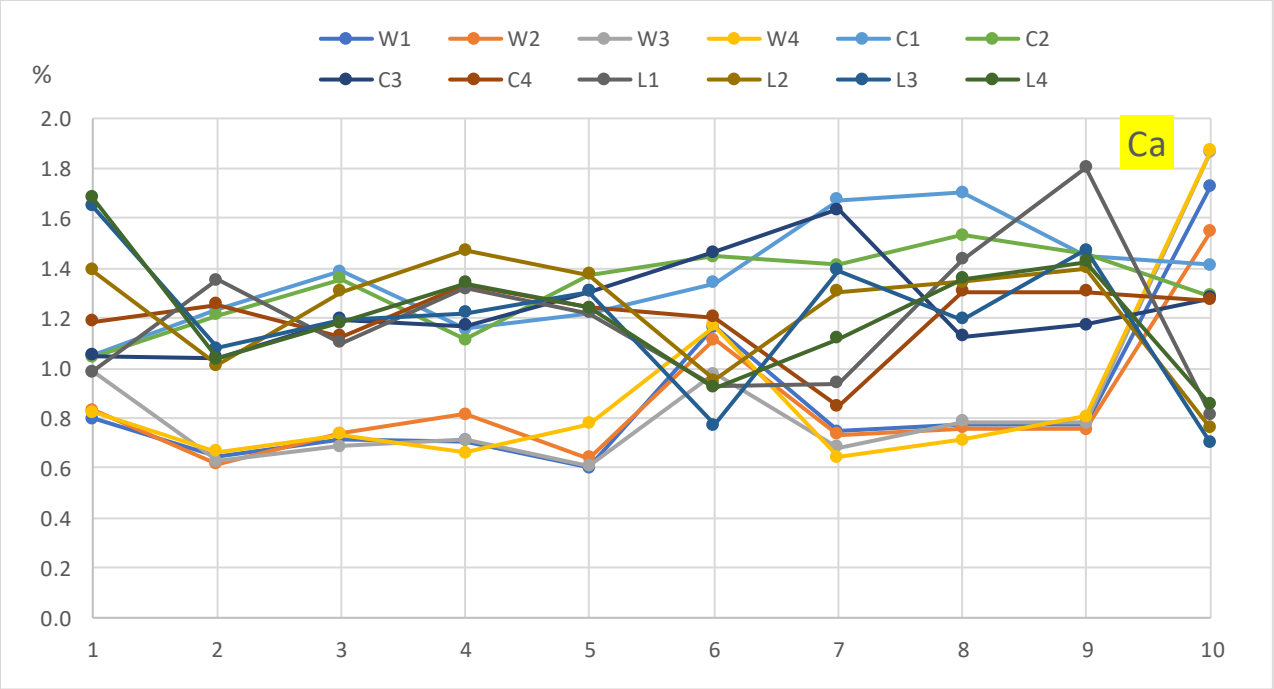


**Figure 21**: Ca concentrations (%) of samples collected 10 sampling days. 1-10.10.21; 2-11.1.21; 3-11.13.21; 4-12.20.21; 5-1.21.22; 6-2.6.22; 7-5.9.22; 8-5.25.22; 9- 7.25.22; 10-8.8.22

There was no specific trend observed in the in changes in concentration of Ca over time. Samples from the municipal wood had the lowest concentration of Ca while the cemetery had the highest. Water naturally contains calcium due to sources such as marble, calcite, dolomite, gypsum, fluorite, and apatite that can be washed into water bodies and settle in sediments. It can also dissolve from limestone. Because Ca exists in water as $Ca^{2+}$ ions, it affects how hard the water is. Several building products, including cement, brick lime, and concrete, also contain calcium.

Shown in Appendix 15 is the Cr concentrations (%) of samples collected in the 10 sampling days.

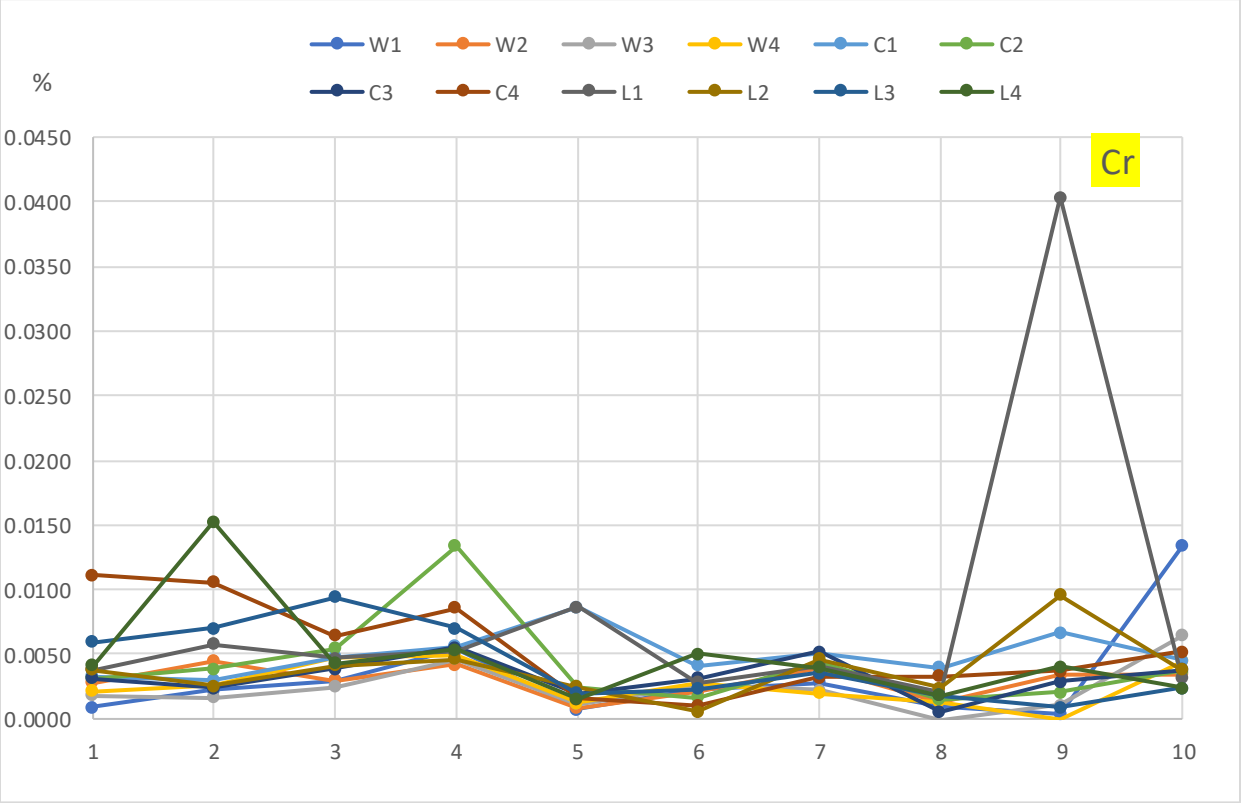


**Figure 22**: Cr concentrations (%) of samples collected 10 sampling days. 1-10.10.21; 2-11.1.21; 3-11.13.21; 4-12.20.21; 5-1.21.22; 6-2.6.22; 7-5.9.22; 8-5.25.22; 9- 7.25.22; 10-8.8.22

Cr is used for the production of steel industry, electroplate metals, tanning, and preserve wood. In addition, Cr can be found in textiles, toner for photocopiers, drilling muds, pigments, dyes, and refractory bricks that are used in high-temperature furnaces. (Atlanta, Ga. Sept 2000). The Cr concentrations observed in the Poland sediment samples are relatively high using the EPA guidelines and could indicate some possible past sources of Cr pollution. The 0.04% Cr observed in the library sample of sample 10 (8.8.2) could be due to contamination during sample preparation.

Shown in Appendix 16 is the Mn concentrations (%) of samples collected in the 10 sampling days.

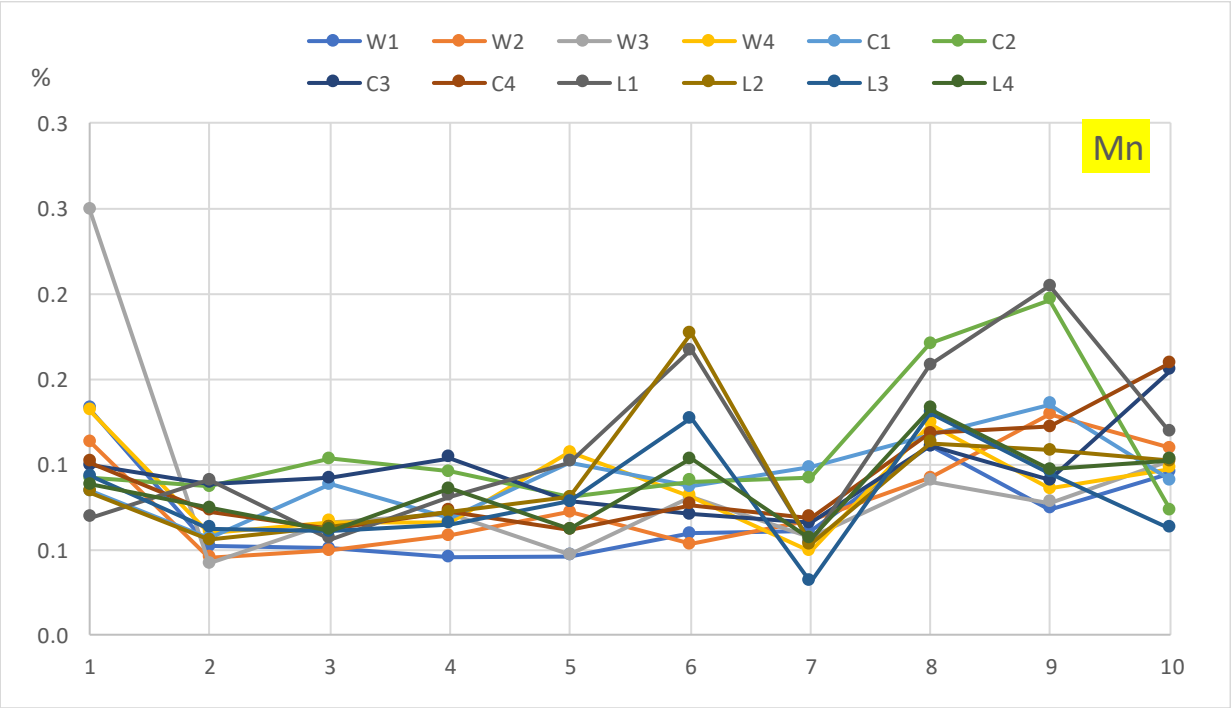


**Figure 23**: Mn concentrations (%) of samples collected 10 sampling days. 1-10.10.21; 2-11.1.21; 3-11.13.21; 4-12.20.21; 5-1.21.22; 6-2.6.22; 7-5.9.22; 8-5.25.22; 9- 7.25.22; 10-8.8.22

Mn occurs naturally in sediments but human activities like industrial wastewater discharge and mining can significantly increases the concentration of Mn in sediments. Our bodies require tiny amounts of manganese since it is an essential mineral. Manganese is also a coenzyme that helps several enzymes that break down lipids, proteins, and carbohydrates (Conly et al.2012). The highest concentration of manganese was 0.2% and is considered high according to EPA guidelines.

Sampling Days 6 (2.6.22) and 9 (7.25.22) appeared to have the highest concentration of Mn. There was good agreement in the concentrations of Mn in all samples except for the Wood site sample of day 1 (10.10.21), which indicated very high Mn percentage. This unusually high value could be due to contamination of the sample during collection and/or sample preparation.

Shown in Appendix 17 is the Fe concentrations (%) of samples collected in the 10 sampling days.

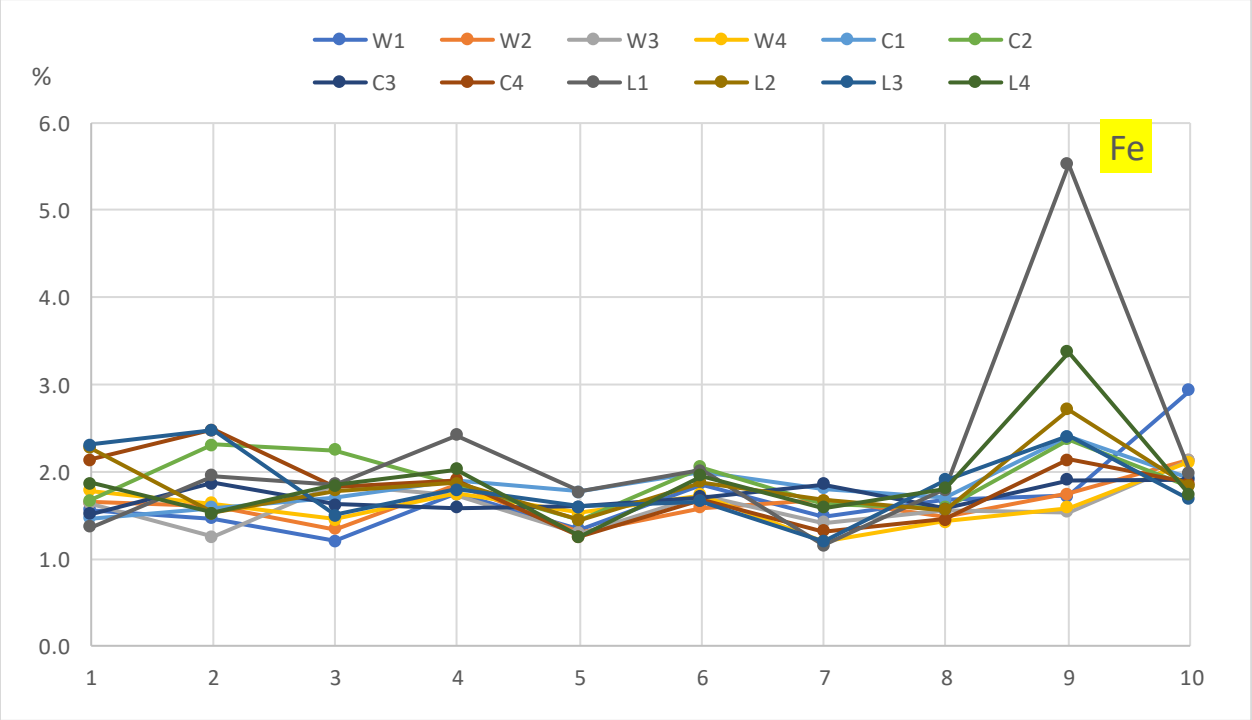


**Figure 24**: Fe concentrations (%) of samples collected 10 sampling days. 1-10.10.21; 2-11.1.21; 3-11.13.21; 4-12.20.21; 5-1.21.22; 6-2.6.22; 7-5.9.22; 8-5.25.22; 9- 7.25.22; 10-8.8.22

Iron is an important element for biological and physiological processes in aquatic life such as chlorophyll pigmentation, photosynthesis, and electron transport. (Schlesinger, 1991)

The highest concentration of Fe in Poland sediments was observed in samples collected on 7.25.22. Samples from the library site had the highest concentration of Fe, which may be due to the location of a stormwater discharge at the library site and also that the library site is next to a parking lot that could act as source of Fe in the sediments. The Poland Woods site had the lowest Fe concentrations.

Shown in Appendix 18 is the Cu concentrations (%) of samples collected in the 10 sampling days.

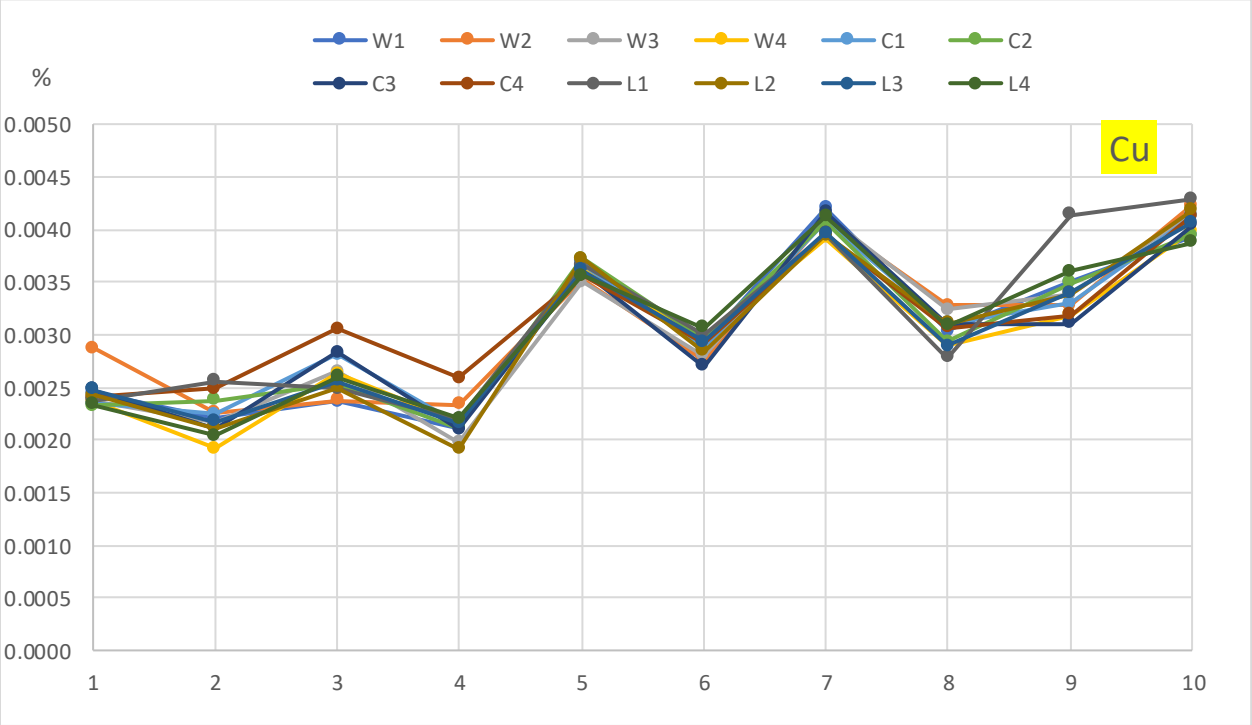


**Figure 25**: Cu concentrations (%) of samples collected 10 sampling days. 1-10.10.21; 2-11.1.21; 3-11.13.21; 4-12.20.21; 5-1.21.22; 6-2.6.22; 7-5.9.22; 8-5.25.22; 9- 7.25.22; 10-8.8.22

Copper (Cu) can be introduced into the environment as a metal or in the form of Cu compounds, such as oxides and sulfides. Copper has many uses as a building material, and in electronic materials and components. The primary sink for Cu in natural waters is sediment. (Sarah & Amal Raj, 2023)

In these studies, there was good agreement in the concentrations of Cu over time in all the samples. It was observed that there was increasing concentration of Cu from sampling day 5 (1.21.22) to 10 (8.8.22). There is a similar distribution of Cu across the sampling sites. The high concentration of Cu on sampling day 5 may be related to a high level of precipitation. Based on the EPA guidelines, the concentration of Cu in the Yellow Creek sediments is moderately high.

**Zinc**

Shown in Appendix 19 is the Zn concentrations (%) of samples collected in the 10 sampling days.

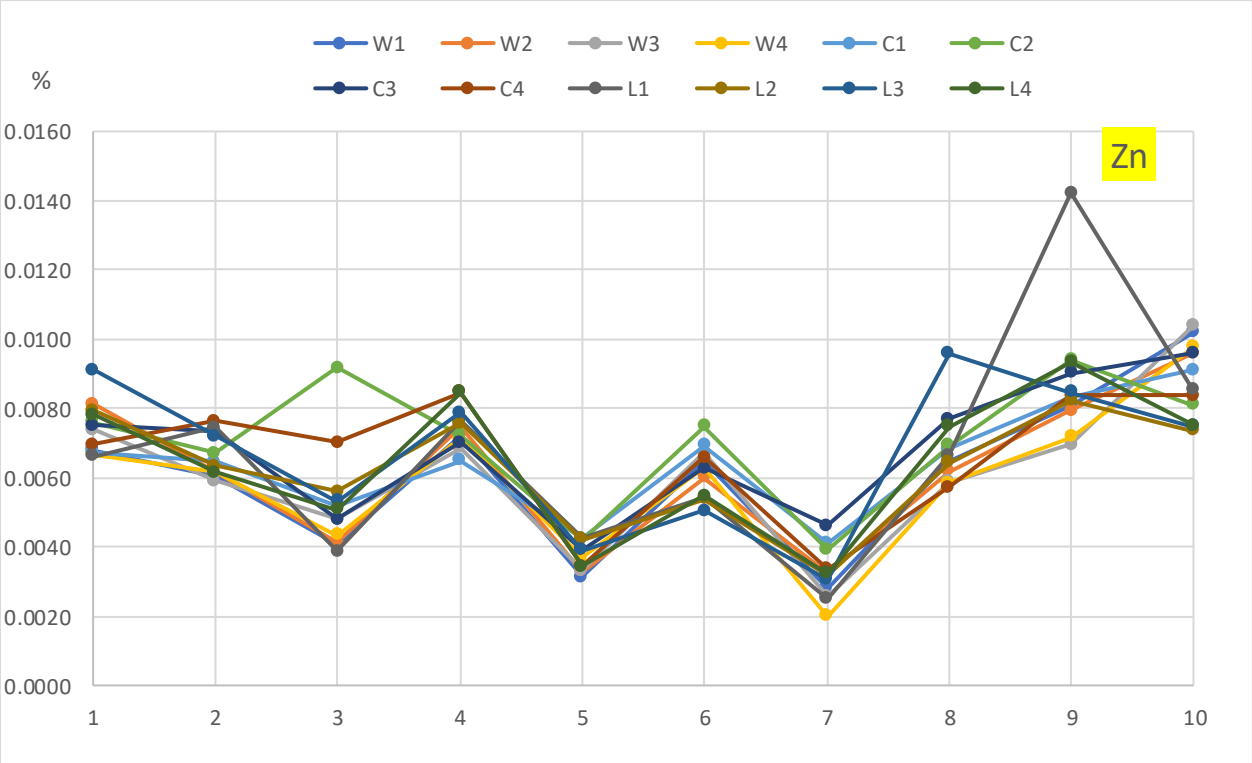


**Figure 26**: Zn concentrations (%) of samples collected 10 sampling days. 1-10.10.21; 2-11.1.21; 3-11.13.21; 4-12.20.21; 5-1.21.22; 6-2.6.22; 7-5.9.22; 8-5.25.22; 9- 7.25.22; 10-8.8.22

The main source of zinc (Zn) in the environment, including natural waters, is human activity, which includes municipal wastewater discharges, coal-burning power plants, metal industrial operations, and atmospheric fallout. Zn can be adsorbed on suspended particles in natural waters and then accumulate in sediments. The use of materials containing Zn, mining and metallurgical processes are also important sources of Zn in the environment. (Dong et al., 2012)

From figure 32, the change in concentration of Zn over time shows the same trend in all the measured samples. The Zn concentrations increase and decrease in a similar way in all of the samples on each sampling day. High sediment concentrations of Zn were observed in sampling

days 4 ,6,9 and 10 and could be due to precipitation leading to increased runoff and mobilization of Zn into Yellow Creek. The highest concentration of Zn in the measured samples was 0.0096% which is high according to the EPA guidelines.

### 3.9 ICP-MS versus XRF results of Poland samples.

Shown in Appendix 20: C1,Appendix 21 C2, Appendix 22 C3,Appendix 23 C3 are metals' concentrations (%) of samples collected at the cemetery sub sites (C1, C2, C3, and C4) measured by XRF and ICP-MS. Sampling dates 11.1.2021, 11.13.2021, 12.20.2021, 1.21.2022 and 2.6.2022.

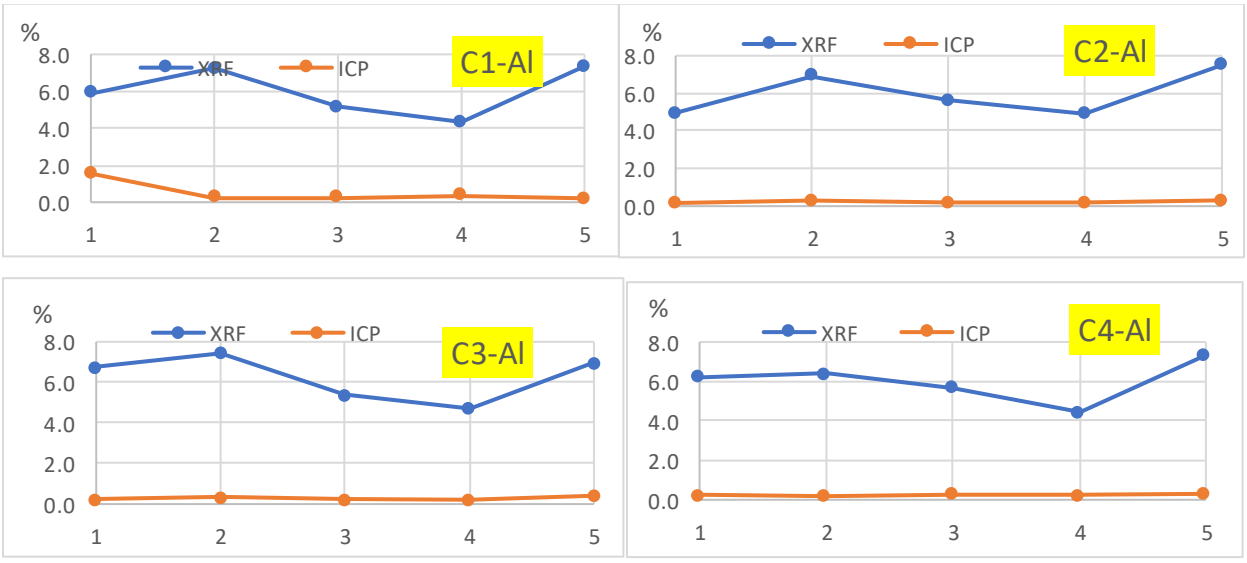


**Figure 27**: Al concentrations of samples collected at the cemetery measured by XRF and ICP-MS. 1-11/01/21; 2-11/13/21; 3-12/20/21; 4-1/22/22; 5-2/6/22.

Al has very low recovery by ICP-MS (27.4 ± 1.5), which may be the reason why the concentration of Al measured by XRF is higher that of ICP-MS. XRF measures total metal concentration in sediments while ICP-MS quantifies the metal concentration extracted by aqua regia. As a result, it may be that XRF is more reliable for quantifying Al in sediments.

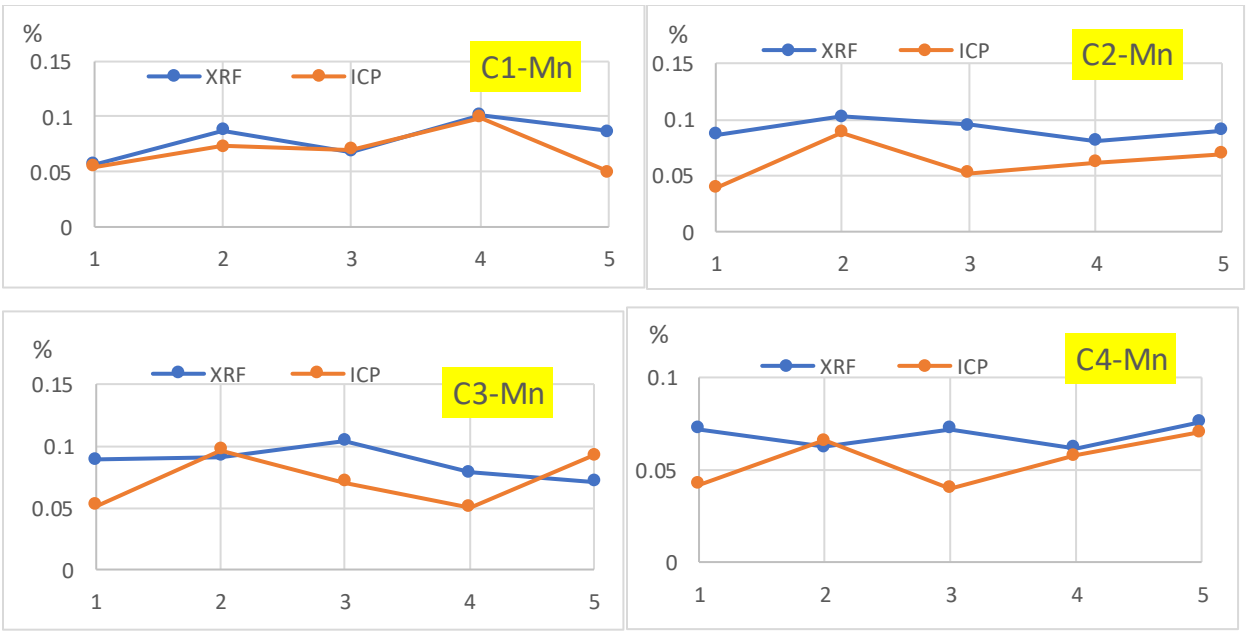


**Figure 28**: Mn concentrations of samples collected at the cemetery measured by XRF and ICP-MS. 1-11/01/21; 2-11/13/21; 3-12/20/21; 4-1/22/22; 5-2/6/22.

There is not much difference in the concentrations of Mn measured by ICP-MS and XRF. This may be because Mn has a high recovery in ICP-MS (107.5 ± 15%) and suggests that ICP-MS and XRF are both equally effective at determining the concentration of Mn in sediments.

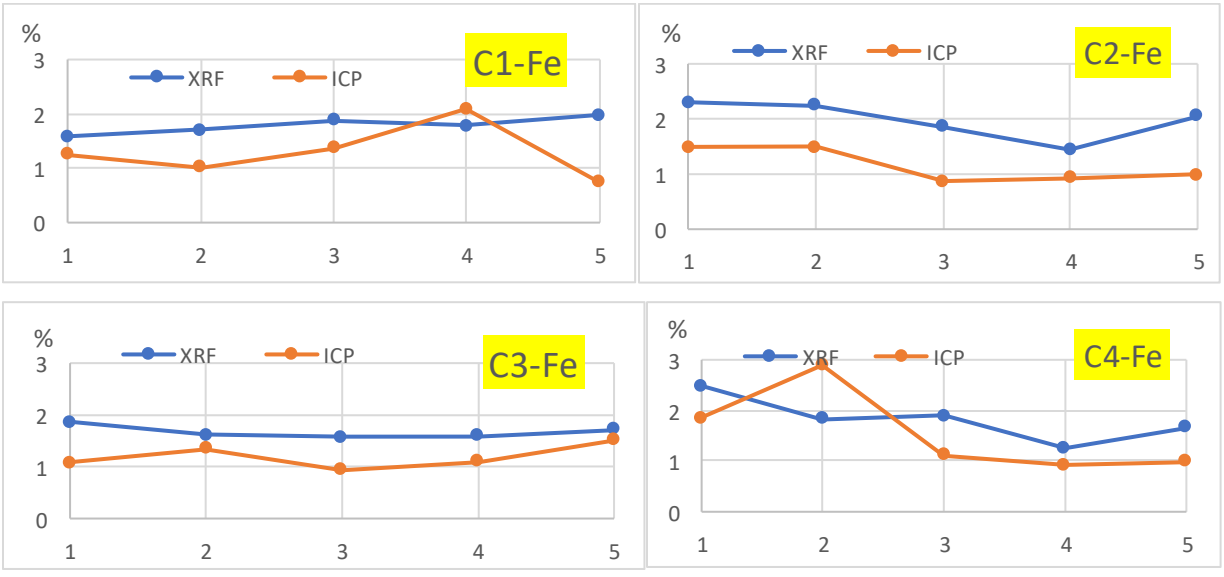


**Figure 29**: Fe concentrations of samples collected at the cemetery measured by XRF and ICP-MS

The sediment concentrations of Fe measured by XRF are higher than in ICP-MS. The recovery of Fe by ICP-MS is 87.4 ± 4.8% which may partially account for the differences. The XRF limit of detection of Fe is 0.1% which compares well to the highest concentration of Fe in the samples of 2.485% and also the lowest concentration of 1.256%. The differences in concentration between ICP-MS and XRF are low, and it suggests that both ICP-MS and XRF can be used to quantify Fe in sediments. Samples L3 2.6.22, L2 1.22.22, C3 12.20.21 and C1 12.20.21 have higher concentrations of Fe measured by ICP-MS that by XRF and may be a result of sample contamination during sample preparation.

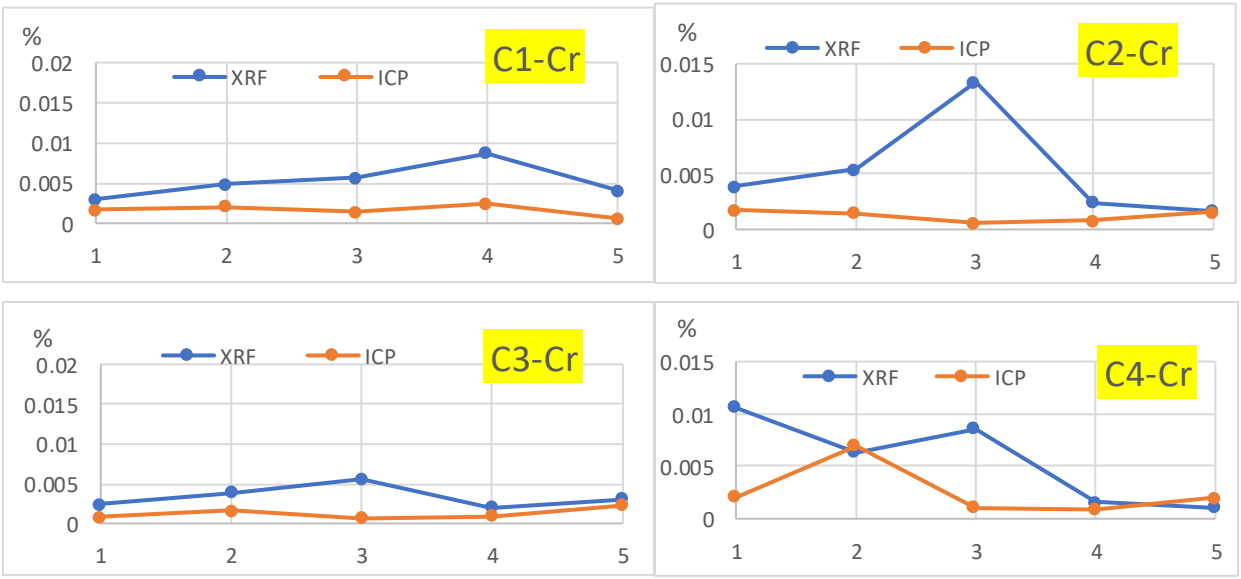


**Figure 30**: Cr concentrations of samples collected at the cemetery measured by XRF and ICP-MS

For chromium (Cr), the concentration measured by XRF is higher than that of ICP-MS. Cr has relatively low recovery by the ICP-MS approach (54.5±4.6%) so it is not unexpected that the XRF results for Cr would be higher. The XRF limit of detection (LOD) for Cr is 0.02%, and the concentrations of Cr appear to be lower than the LOD. This suggests XRF is not effective for measuring Cr in sediments. The high concentration of Cr observed in samples C2 11.13.21, L3.12.20.21 and L3 2.6.22 could be due to locally high concentrations or contamination during sample preparation of the samples.

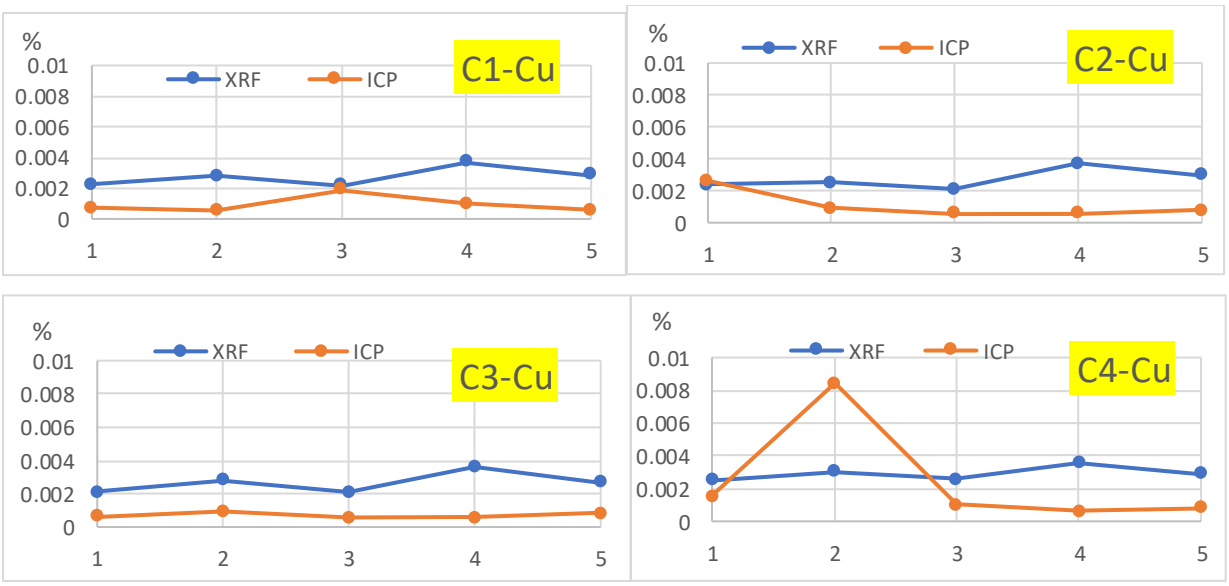


**Figure 31**: Cu concentrations of samples collected at the cemetery measured by XRF and ICP-MS

The concentration of copper (Cu) measured by XRF is generally higher than in ICP-MS. Copper has a good recovery of 82.0 ±15.2% by the ICP-MS approach. The XRF limit of detection for Cu is 0.002% (Table 12) and is lower than the concentrations of Cu in the samples. As a result, XRF and ICP-MS appear to both be effective for measuring Cu in sediments. The higher concentrations of Cu in samples CA 11.13.21 and W1 2.6.22 by ICP-MS may be due to locally high concentrations or sample contamination during sample preparation.

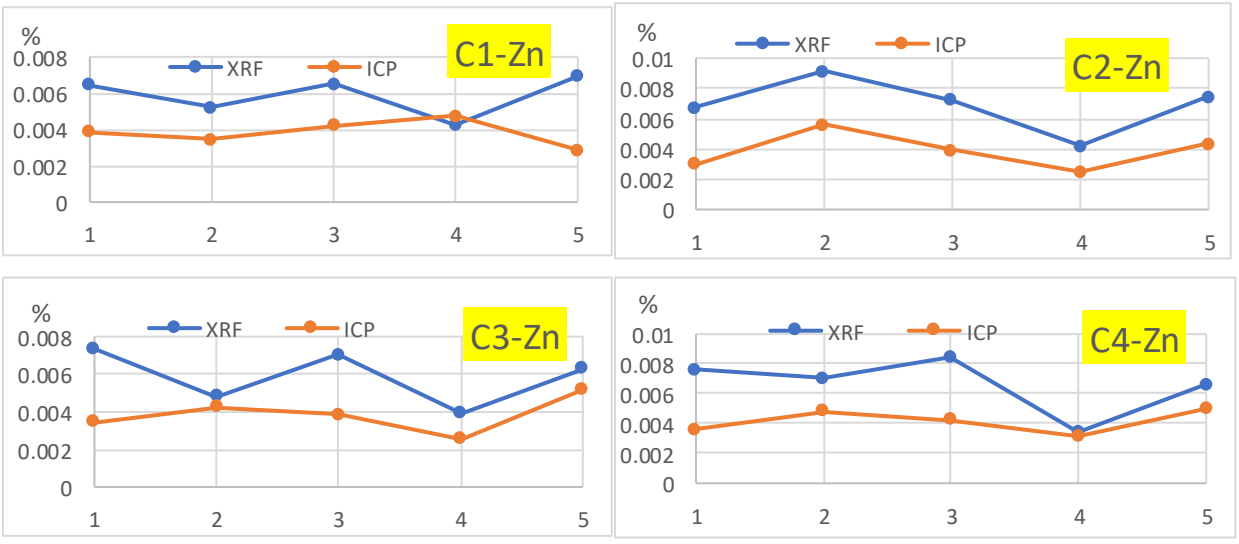


**Figure 32**: Zn concentrations of samples collected at the cemetery measured by XRF and ICP-MS

The concentration of Zn in all the samples is higher in XRF than in ICP-MS. The highest concentration of Zn measured by XRF is 0.00916% and the lowest concentration is 0.00429%. The limit of detection of Zn is 0.004 % (Table 11). The concentrations of Zn in the samples are generally at or above the detection limit of Zn using XRF. Zn has a good recovery in ICP-MS (80.4 ± 7.6%). Overall ICP-MS appears to be better suited to measuring the concentrations of Zn in the sediments.

# 4. Conclusions and future directions

This study suggests that X-ray Fluorescence spectroscopy has the capability to determine metal concentrations in soils and sediments, including Cu, Al, Ca, Zn, Pb, Cr and Fe. The results indicate that the choice of standard reference materials used for calibration is key for addressing possible matrix effects. When possible, the reference materials used for calibration should have a matrix that is closely similar to the sediment samples to prevent variations in the XRF response. Using background corrected peak heights of the XRF responses of the SRMs to the background corrected peak height of the Compton peak appeared to provide the best calibration results and suggest that corrections using Compton scattering may be able to counter some matrix effects.

A sequential extraction approach has been investigated and the results suggest that the approach can be used to explore the availability of different elements from the sediments. Elements such as Mn and Ca appear to be easily extracted in weakly acidic conditions. Measurements of the Poland sediment samples indicate that the concentrations of Cu, Al, Fe, Zn, Pb and Cr were not significantly high suggesting that the sediments are not highly polluted. It was also observed that changes in the metal concentrations over time didn't vary significantly or follow a consistent pattern. It is recommended that further studies be performed using a larger number of samples from the Poland site to further explore metal distributions and possible sources of pollution to Yellow Creek.

# REFERENCES:


Ahmed, Amel Yousif, et al. "Determination of Some Trace Elements in Marine Sediment Using ICP-MS and XRF (A Comparative Study)." *Oriental Journal of Chemistry*, vol. 29, no. 2, 2013, pp. 645–653

Atlanta, Ga "Toxicological Profile for Chromium. U.S. Department of Health and Human Services." *Agency for Toxic Substances and Disease Registry*, Atlanta, Ga. Sept 2000.

Carvalho, Patrícia M. S., et al. "Energy Dispersive X-Ray Fluorescence Quantitative Analysis of Biological Samples with the External Standard Method." *Spectrochimica Acta. Part B: Atomic Spectroscopy, vol*. 174, no. 105991, 2020, p. 105991.

Chen, Z. W., et al. "High-Definition X-Ray Fluorescence: Principles and Techniques." *X-Ray Optics and Instrumentation,* vol. 2008, 2008, pp. 1–10.

Congiu, A., et al. "Trace Metal Contaminants in Sediments and Soils: Comparison between ICP and XRF Quantitative Determination." *E3S Web of Conferences*, vol. 1, 2013, p. 09004.

Conly, A. K., et al. "Tolerance and Efficacy of Tribasic Manganese Chloride in Growing Broiler Chickens." *Poultry Science,* vol. 91, no. 7, 2012, pp. 1633–1640.

Dong, Cheng-Di, et al. "Contamination of Zinc in Sediments at River Mouths and Channel in Northern Kaohsiung Harbor, Taiwan." *International Journal of Environmental Science and Development,* 2012, pp. 517–521.

Firdiyono, F., et al. "The Degree of Lithium (Li) Stability Compared to Calcium (Ca) and Magnesium (Mg) from Low Lithium Grade Brine Water with Addition of Limestone and Oxalic Acid." *IOP Conference Series. Materials Science and Engineering*, vol. 858, no. 1, 2020, p. 012044.

Furukawa, Hiroaki, et al. "The Comparative Verification of Calibration Curve and Background Fundamental Parameter Methods for Impurity Analysis in Drug Materials: Impurity Analysis in Drug Materials." *X-Ray Spectrometry: XRS*, vol. 46, no. 5, 2017, pp. 382–387

https: www//xrf-spectroscopy.com

https://www.chem.purdue.edu/xray/docs/Theory of XRF.pdf

Kumar, S. Sanjay, and Sangita Dhara. "Energy Dispersive X-Ray Fluorescence Determination of Uranium in Different Uranates Using Rh Kα Scattered Peaks for Matrix Correction." *Spectrochimica Acta. Part B: Atomic Spectroscopy*, vol. 193, no. 106427, 2022, p. 106427.

Lin, Qingwei, et al. “Aluminum Distribution Heterogeneity and Relationship with Nitrogen, Phosphorus and Humic Acid Content in the Eutrophic Lake Sediment.” *Environmental Pollution (Barking, Essex: 1987),* vol. 253, 2019, pp. 516–524.

Rauret, G., et al. “Improvement of the BCR Three Step Sequential Extraction Procedure Prior to the Certification of New Sediment and Soil Reference Materials.” *Journal of Environmental Monitoring: JEM,* vol. 1, no. 1, 1999, pp. 57–61.

Rodgers, Kiri J., et al. “The Potential of Sequential Extraction in the Characterization and Management of Wastes from Steel Processing: A Prospective Review.” *International Journal of Environmental Research and Public Health*, vol. 12, no. 9, 2015, pp. 11724–11755.

Rouillon, Marek, and Mark P. Taylor. “Can Field Portable X-Ray Fluorescence (PXRF) Produce High Quality Data for Application in Environmental Contamination Research?” *Environmental Pollution (Barking, Essex: 1987),* vol. 214, 2016, pp. 255–264.

Sarah, G., & Amal Raj, S. (2023). Heavy metal bioaccumulation in sediment and benthic biota. *Heavy Metals - Recent Advances*, 2023, pp 210-215.

Schlesinger, William H. “Biogeochemistry in Freshwater Wetlands and Lakes.” *Biogeochemistry, Elsevier*, 1991, pp. 195–225.

Sinem Atgin, R., et al. “Investigation of the Sediment Pollution in Izmir Bay: Trace Elements.” *Spectrochimica Acta. Part B: Atomic Spectroscopy*, vol. 55, no. 7, 2000, pp. 1151–1164.

Stosnach, Hagen. “On-Site Analysis of Heavy Metal Contaminated Areas by Means of Total Reflection X-Ray Fluorescence Analysis (TXRF).” *Spectrochimica Acta. Part B: Atomic Spectroscopy,* vol. 61, no. 10–11, 2006, pp. 1141–1145,

Towett, Erick K., et al. “Quantification of Total Element Concentrations in Soils Using Total X-Ray Fluorescence Spectroscopy (TXRF).” *The Science of the Total Environment*, vol. 463–464, 2013, pp. 374–388,

Tubiana, M. “Wilhelm Conrad Rontgen and the discovery of X-rays.” *Bulletin de l’Academie nationale de medecine,* vol. 180, no. 1, 1996, pp. 97–108.

www.atsdr. cdc.gov/toxprofiles/tp7.html

# APPENDICES

Appendix 1: Calibration curves using calcium carbonate.

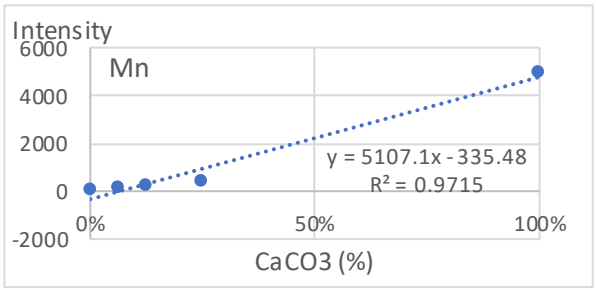


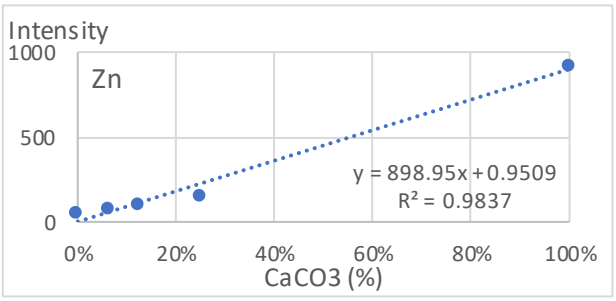


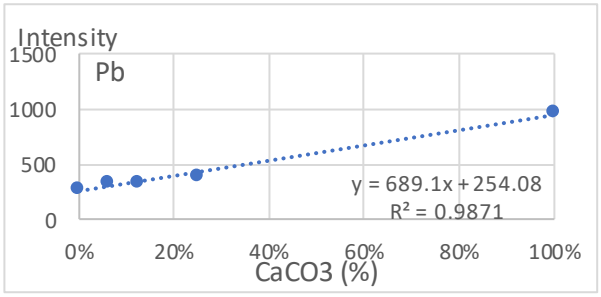


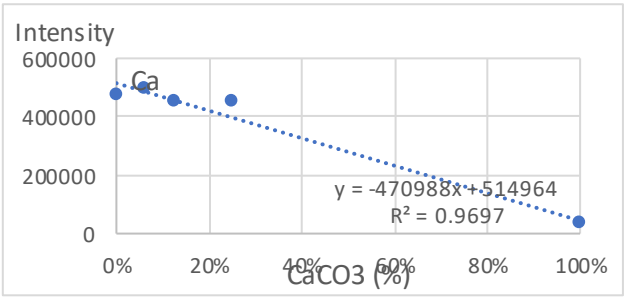


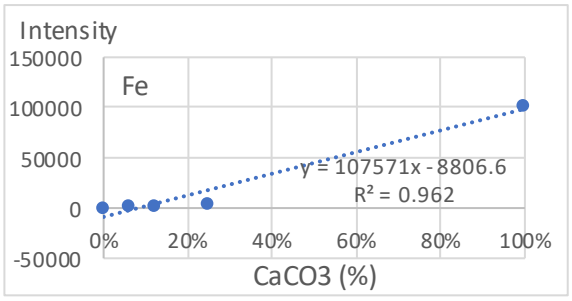


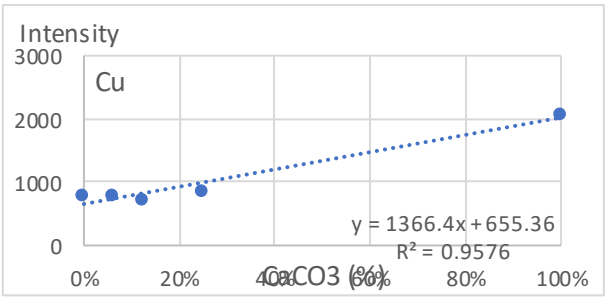


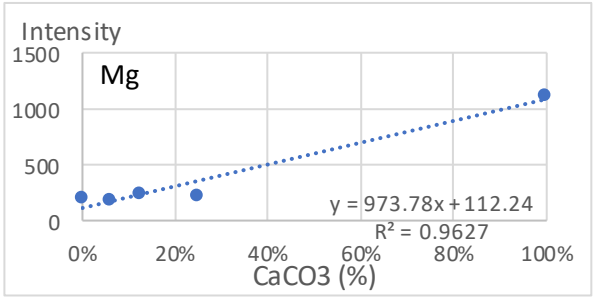


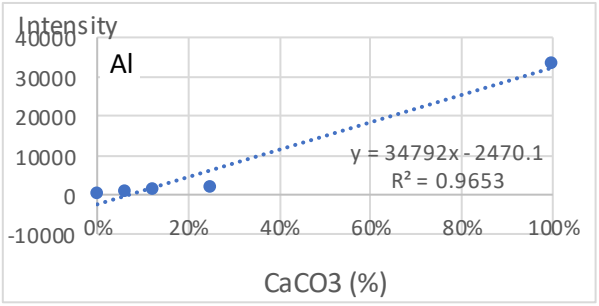


a

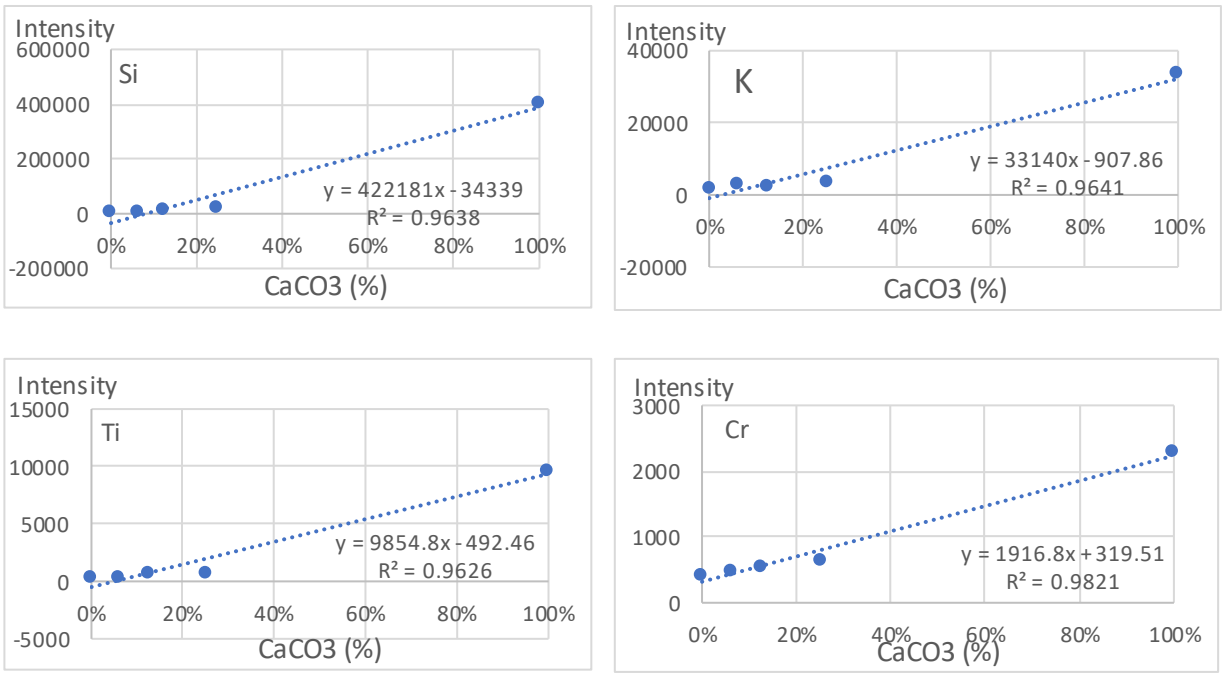


Appendix 2: Calibration curves using corrected peak height for different elements using multielement solution.

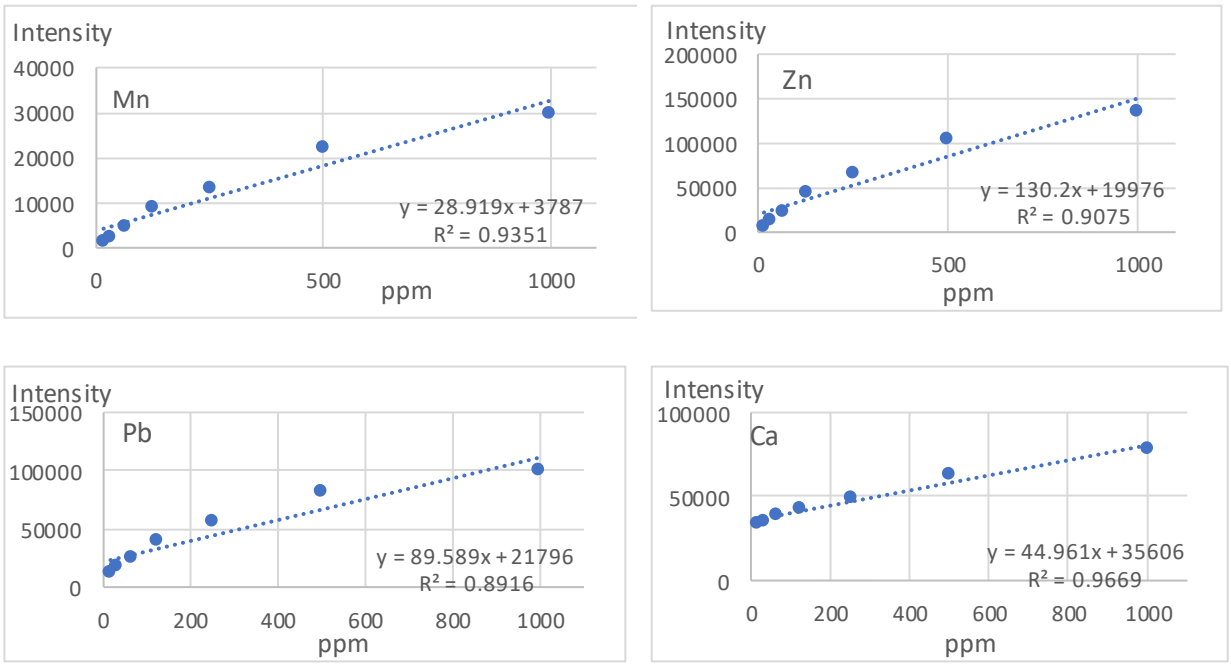


b

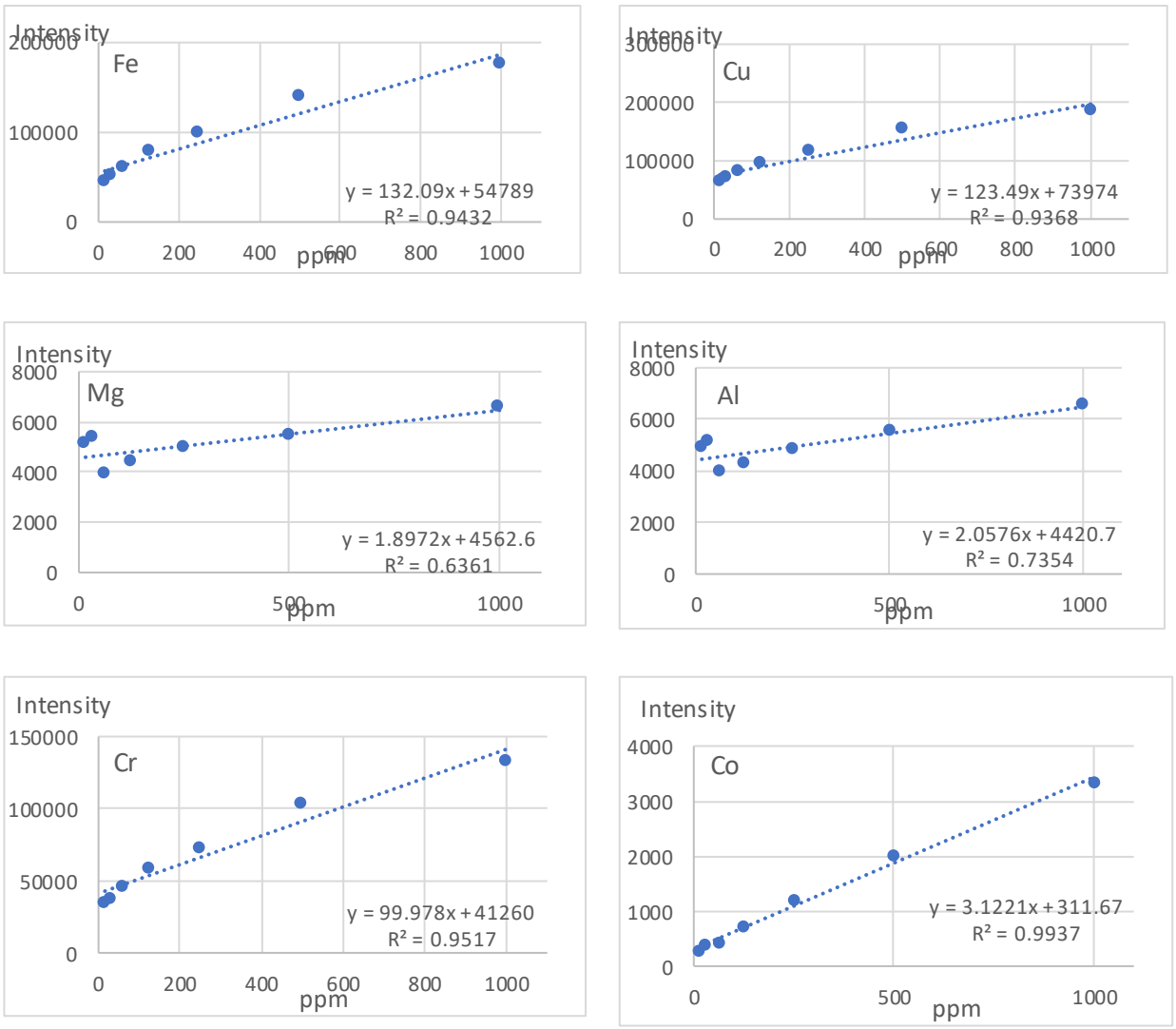


Appendix 3: Calibration curves calculated by peak height corrected by Compton.

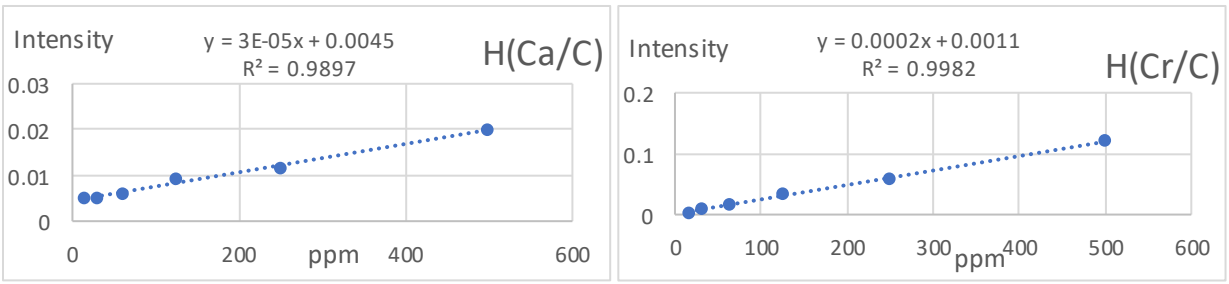


c

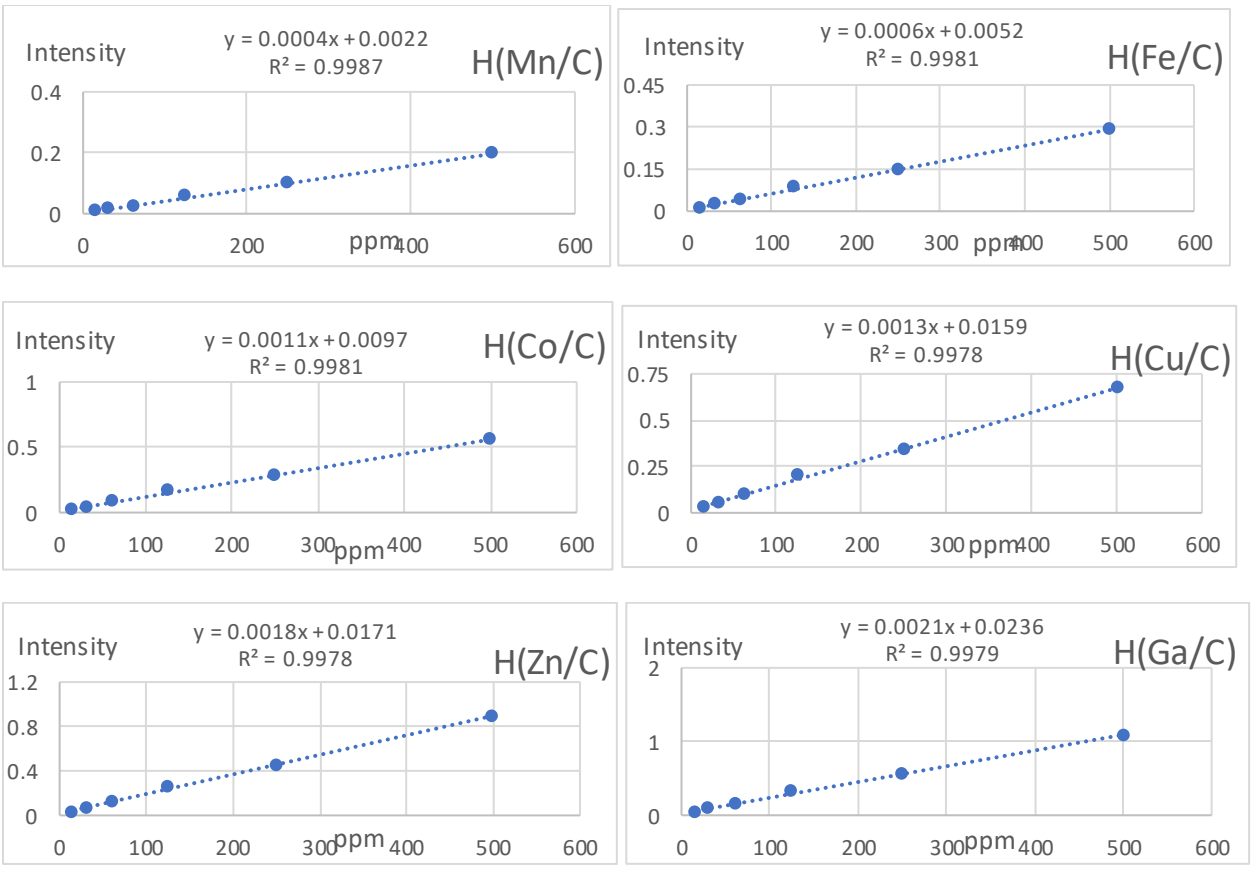


Appendix 4: Calibration curves for corrected vs uncorrected peak heights

**Uncorrected peak height** **Background corrected peak height**

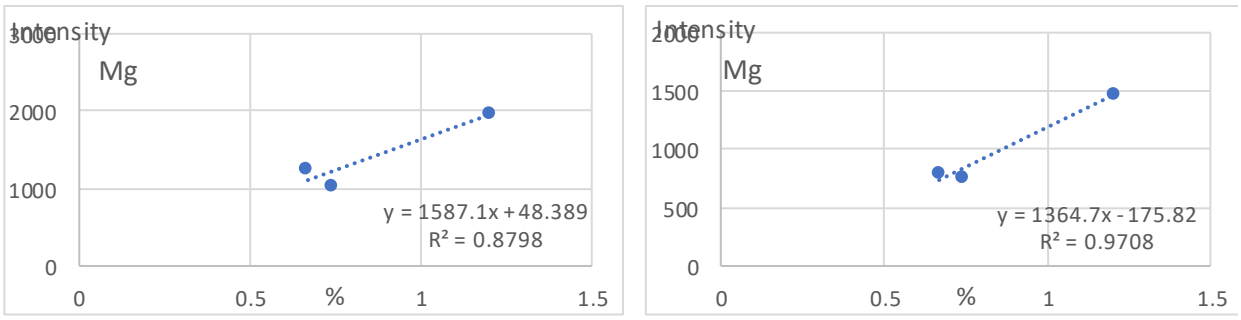


d

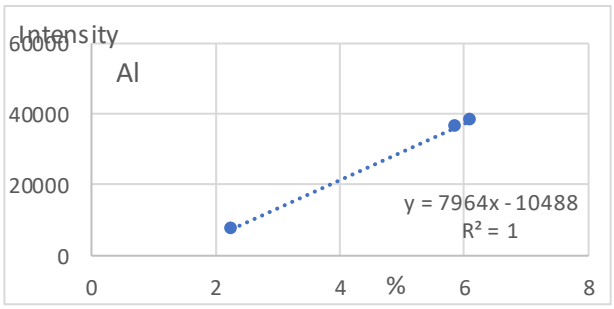
Intensity
Al
y = 7964x - 10488
R² = 1
%

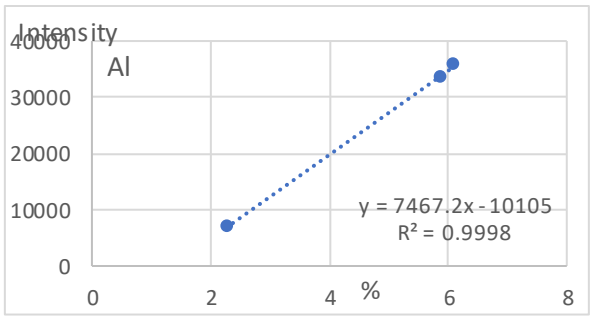
Intensity
Al
y = 7467.2x - 10105
R² = 0.9998
%

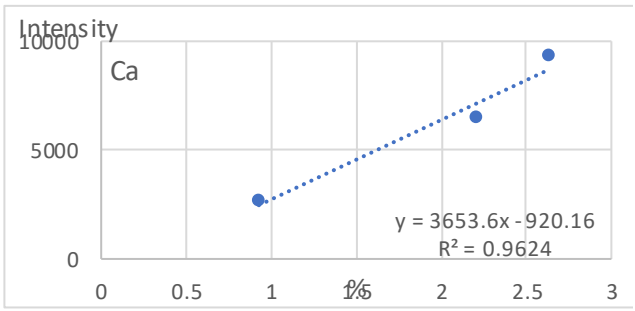
Intensity
Ca
y = 3653.6x - 920.16
R² = 0.9624
%

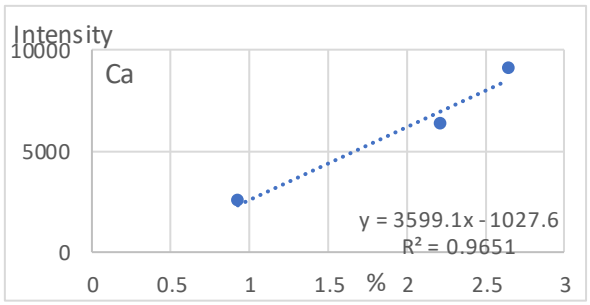
Intensity
Ca
y = 3599.1x - 1027.6
R² = 0.9651
%

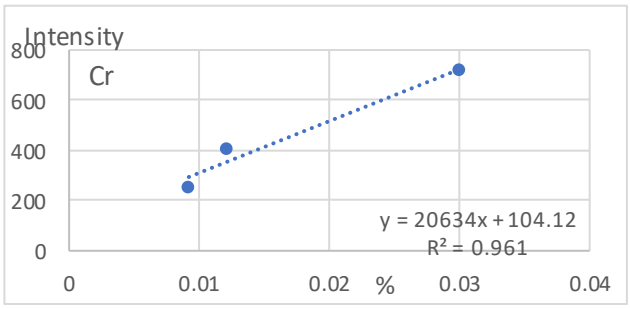
Intensity
Cr
y = 20634x + 104.12
R² = 0.961
%

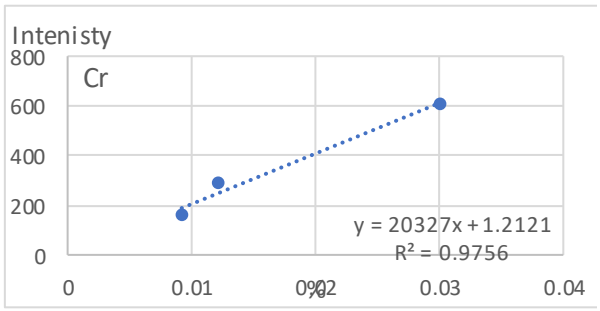
Intenisty
Cr
y = 20327x + 1.2121
R² = 0.9756
%

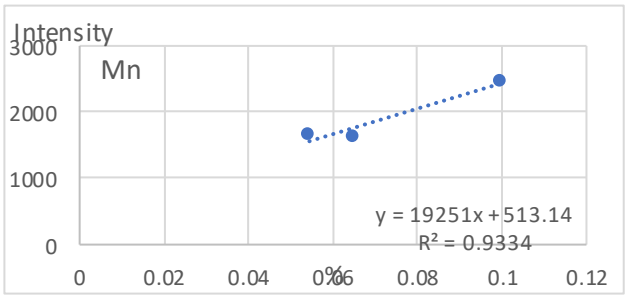
Intensity
Mn
y = 19251x + 513.14
R² = 0.9334
%

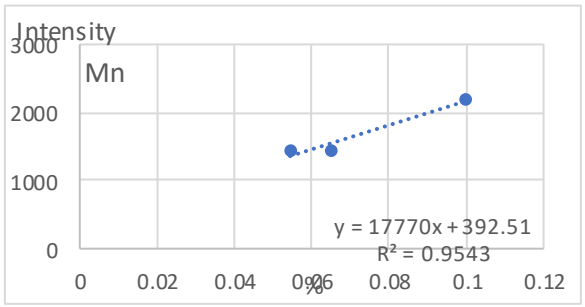
Intensity
Mn
y = 17770x + 392.51
R² = 0.9543
%

e

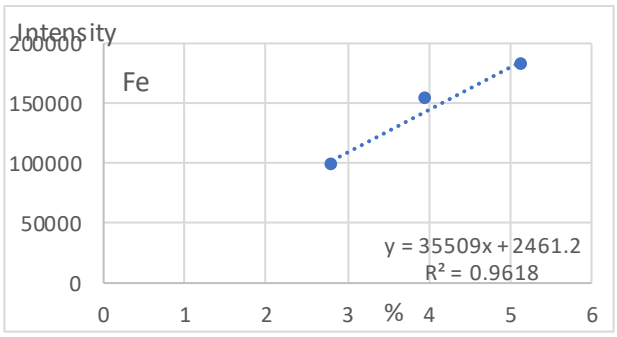
Intensity
Fe
y = 35509x + 2461.2
R² = 0.9618
%

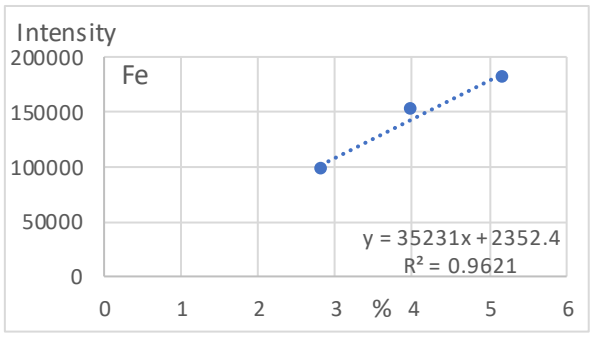
Intensity
Fe
y = 35231x + 2352.4
R² = 0.9621
%

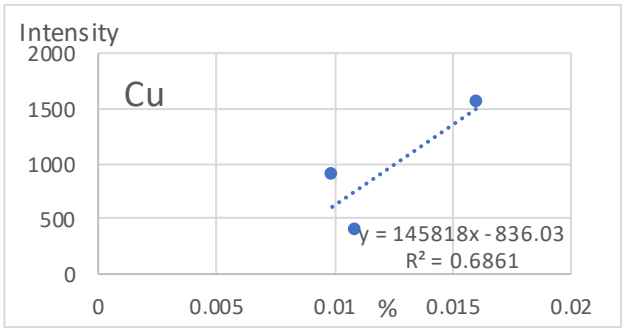
Intensity
Cu
y = 145818x - 836.03
R² = 0.6861
%

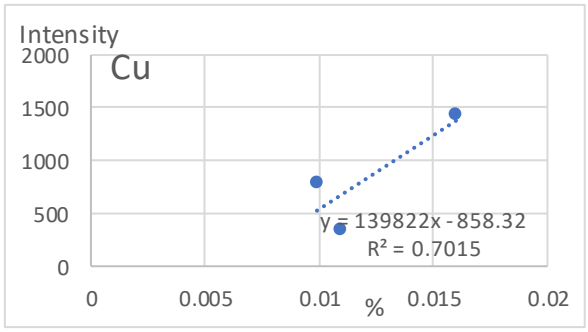
Intensity
Cu
y = 139822x - 858.32
R² = 0.7015
%

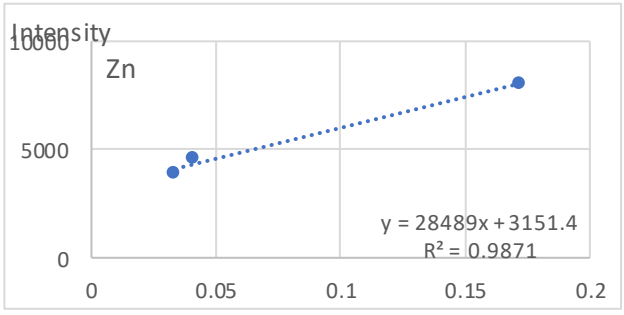
Intensity
Zn
y = 28489x + 3151.4
R² = 0.9871

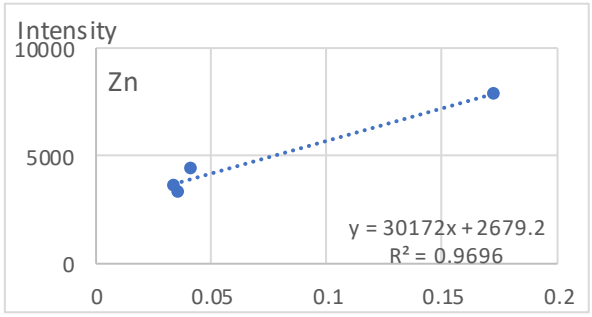
Intensity
Zn
y = 30172x + 2679.2
R² = 0.9696

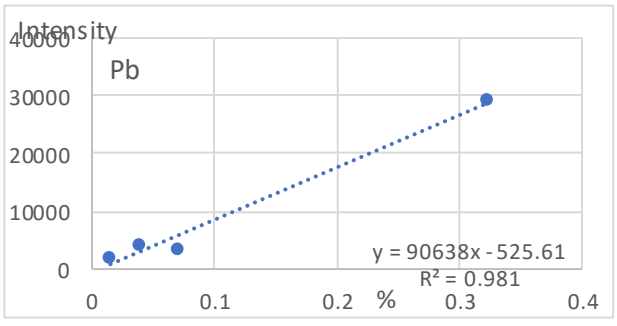
Intensity
Pb
y = 90638x - 525.61
R² = 0.981
%

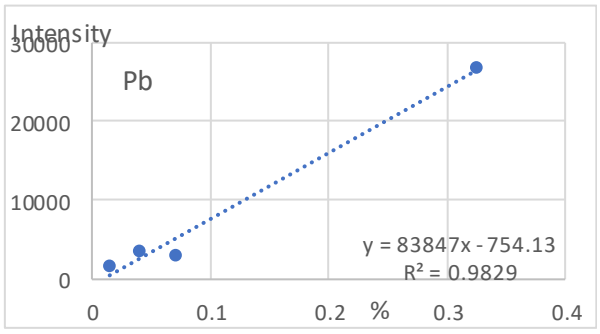
Intensity
Pb
y = 83847x - 754.13
R² = 0.9829
%

f

Appendix 5: Calibration curves using Peak height and peak area.

**Background corrected peak height** | **Background corrected peak area**

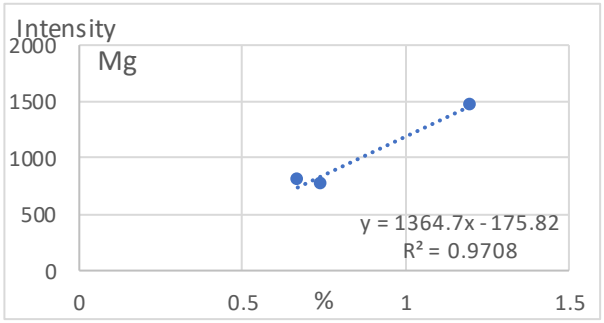


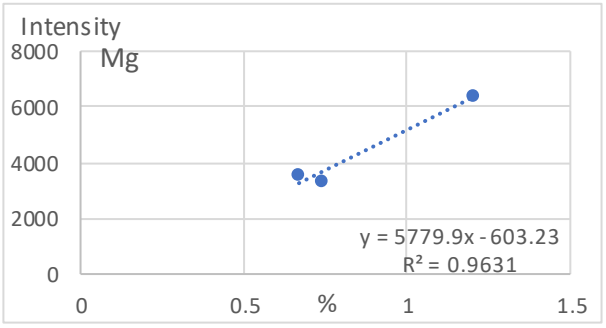


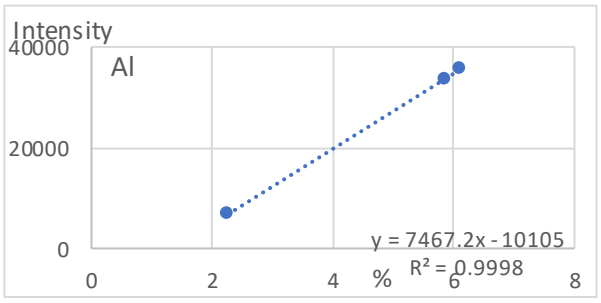


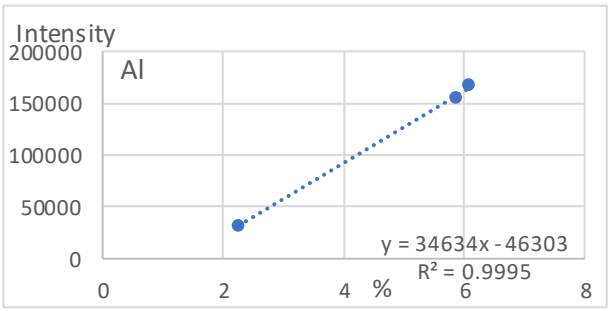


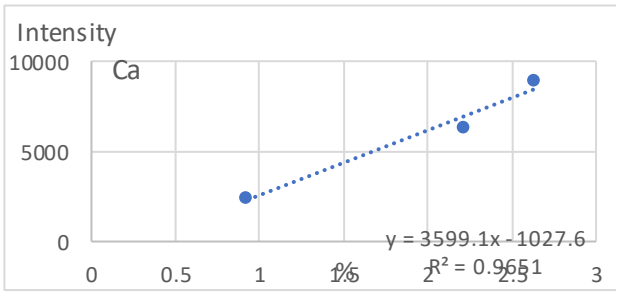


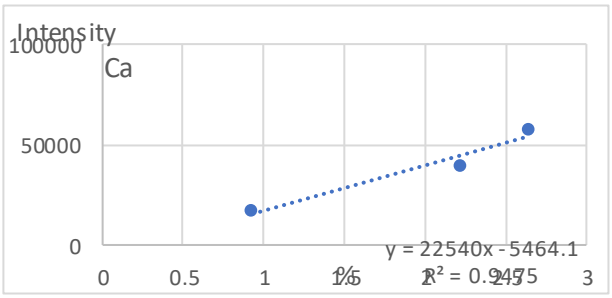


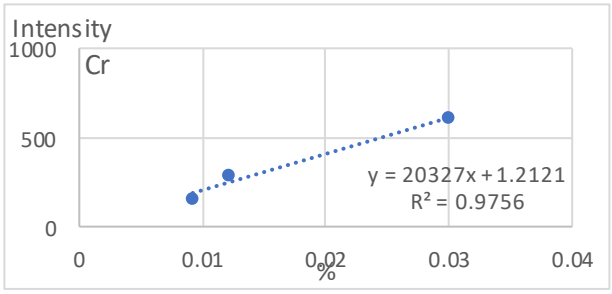


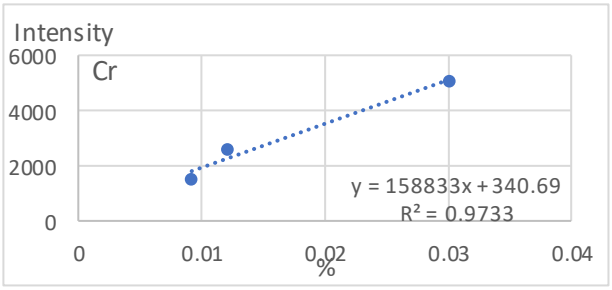

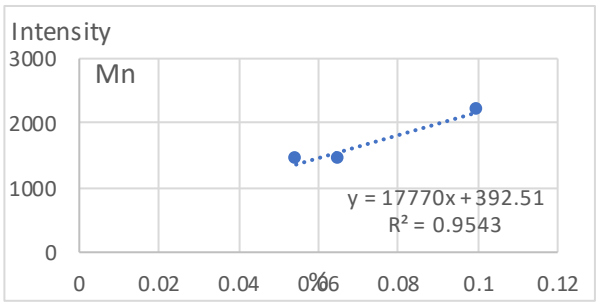
Intensity
Mn
y = 17770x + 392.51
R² = 0.9543
%

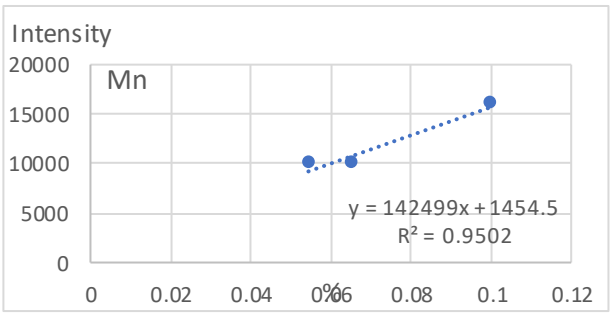
Intensity
Mn
y = 142499x + 1454.5
R² = 0.9502
%

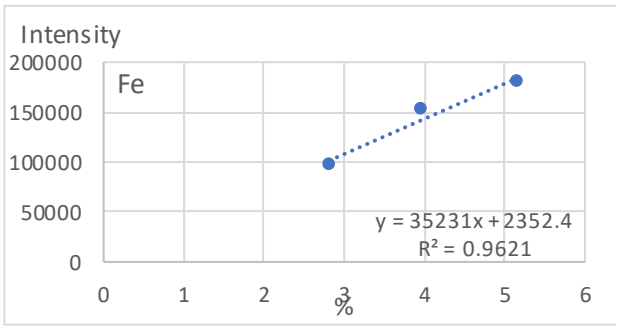
Intensity
Fe
y = 35231x + 2352.4
R² = 0.9621
%

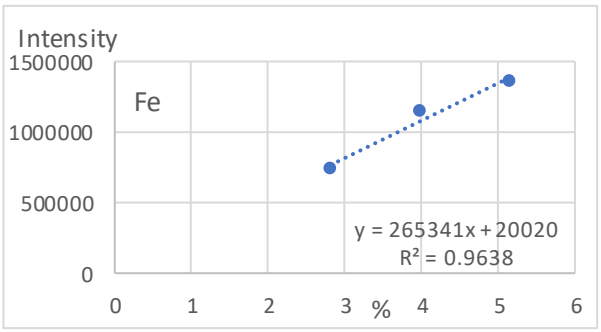
Intensity
Fe
y = 265341x + 20020
R² = 0.9638
%

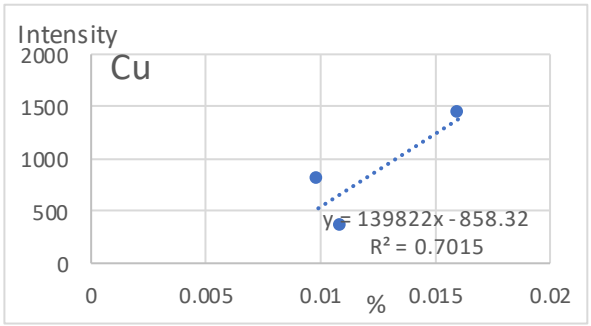
Intensity
Cu
y = 139822x - 858.32
R² = 0.7015
%

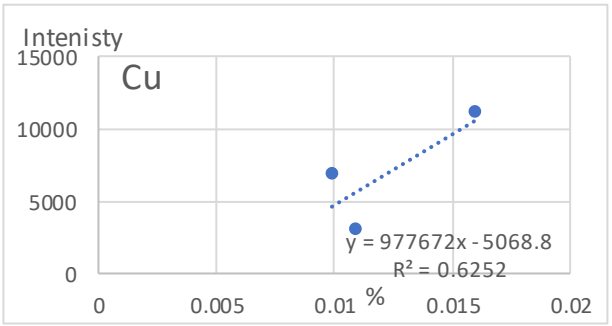
Intenisty
Cu
y = 977672x - 5068.8
R² = 0.6252
%

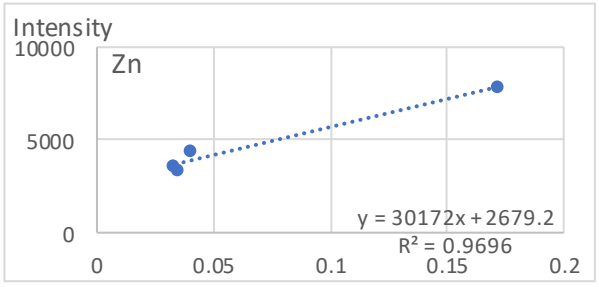
Intensity
Zn
y = 30172x + 2679.2
R² = 0.9696

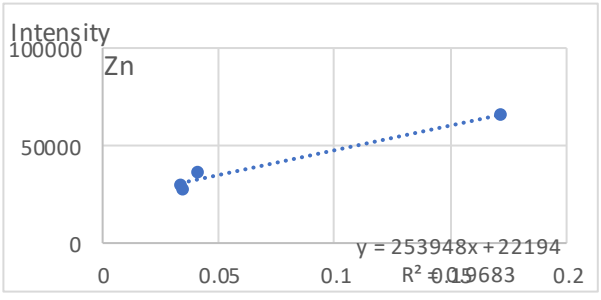
Intensity
Zn
y = 253948x + 22194
R² = 0.9683

h

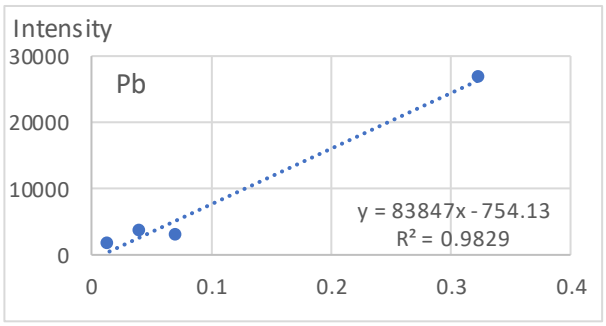


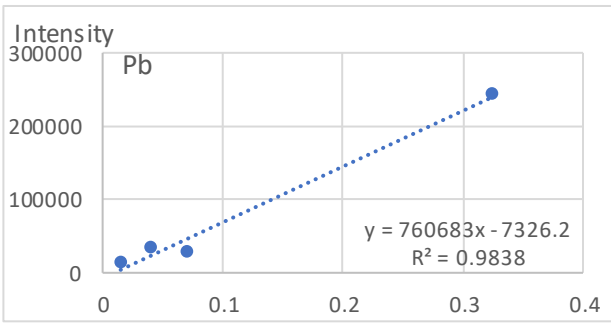


Appendix 6: Calibration curves using background corrected peak height to Compton peak height ratio.

**Background corrected peak height**

**Compton corrected peak height**

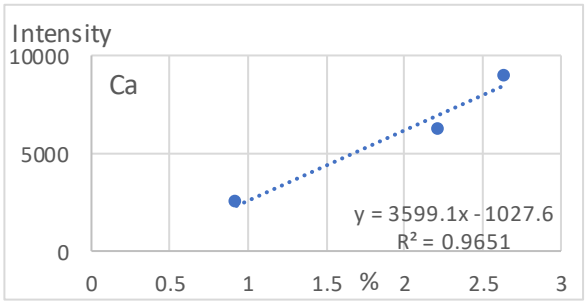


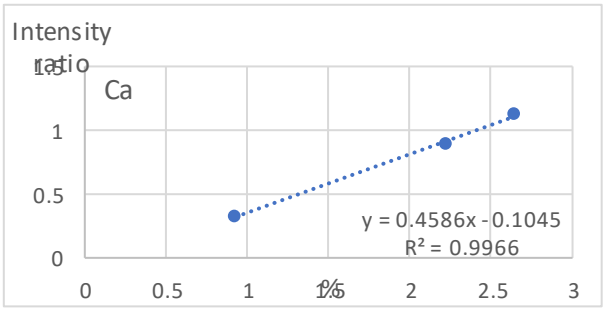


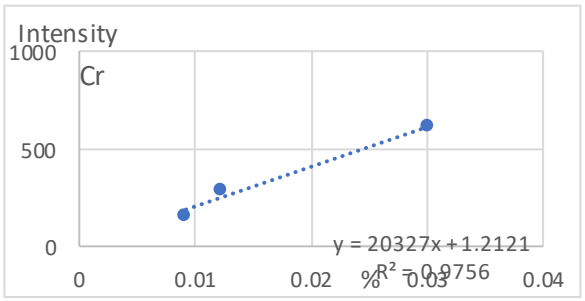


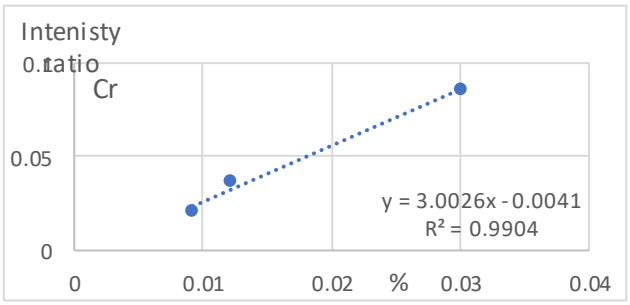


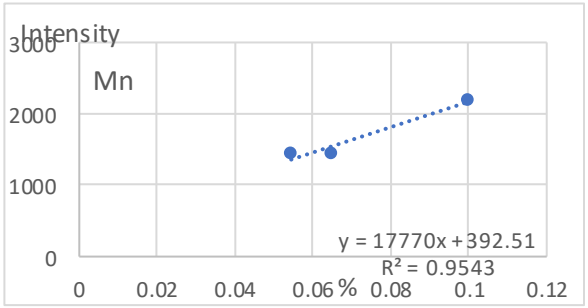


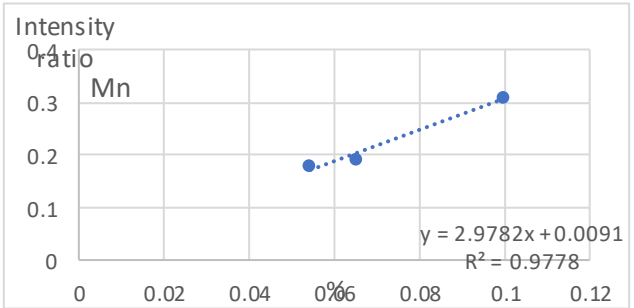

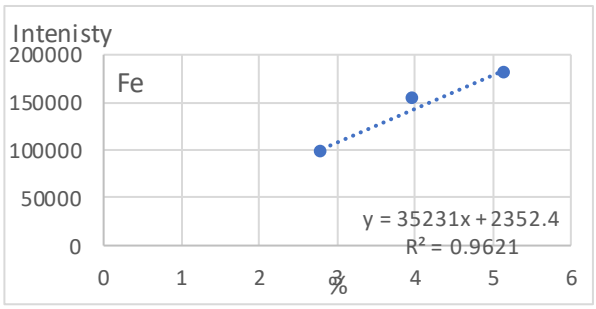
Intenisty
Fe
y = 35231x + 2352.4
R² = 0.9621
%

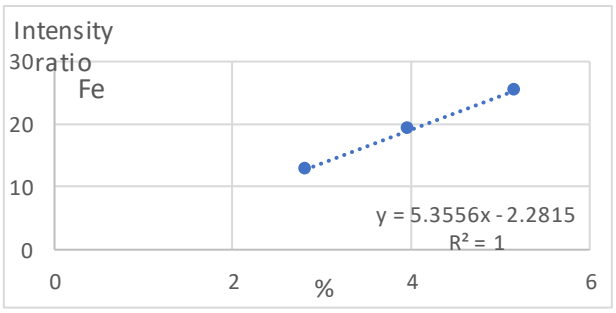
Intensity ratio
Fe
y = 5.3556x - 2.2815
R² = 1
%

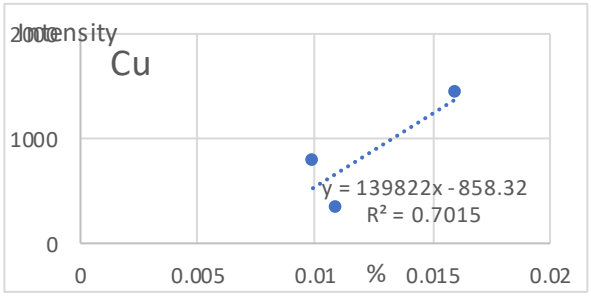
Intensity
Cu
y = 139822x - 858.32
R² = 0.7015
%

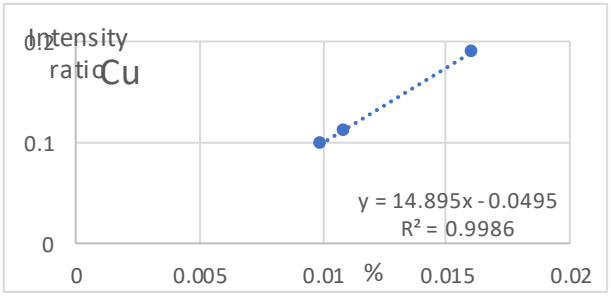
Intensity ratio
Cu
y = 14.895x - 0.0495
R² = 0.9986
%

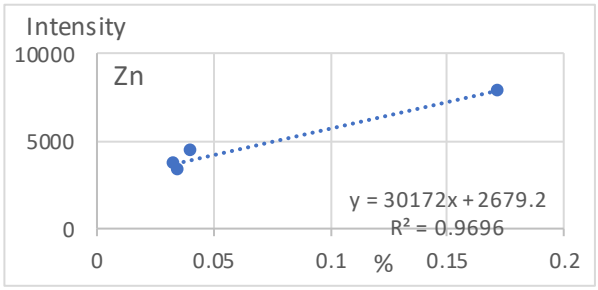
Intensity
Zn
y = 30172x + 2679.2
R² = 0.9696
%

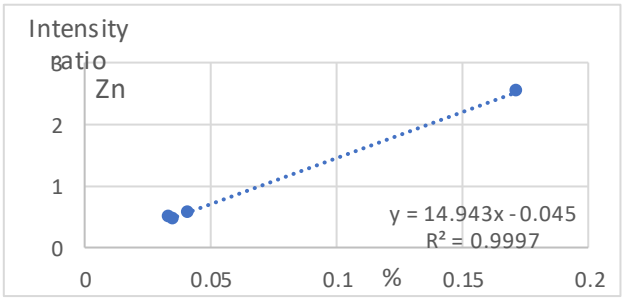
Intensity ratio
Zn
y = 14.943x - 0.045
R² = 0.9997
%

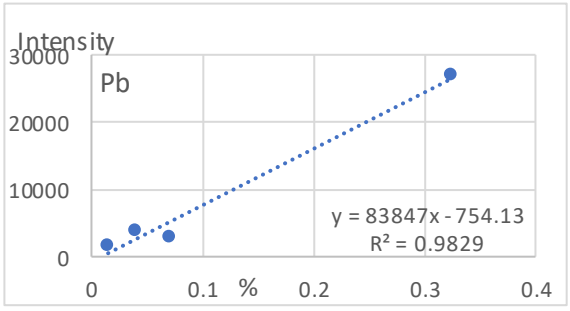
Intensity
Pb
y = 83847x - 754.13
R² = 0.9829
%

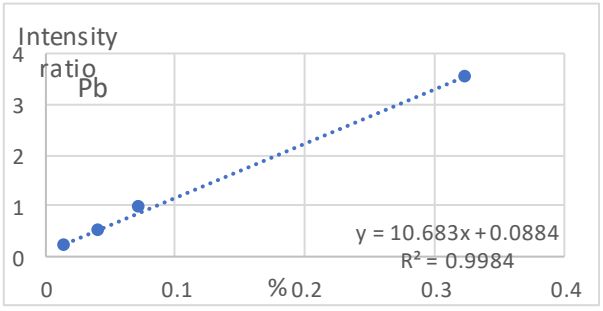
Intensity ratio
Pb
y = 10.683x + 0.0884
R² = 0.9984
%

Appendix 7: Element concentration before acetic extraction (SEQ 0).

| | SEQ0 | | | | | | | | | | | |
|---|---|---|---|---|---|---|---|---|---|---|---|---|
| | W1 (%) | W2 (%) | W3 (%) | W4 (%) | C1 (%) | C2 (%) | C3 (%) | C4 (%) | L1 (%) | L2 (%) | L3( %) | L4 (%) |
| Mg | 0.58 | 0.59 | 0.55 | 0.63 | 0.48 | 0.59 | 0.46 | 0.50 | 0.54 | 0.53 | 0.61 | 0.62 |
| Al | 5.52 | 5.30 | 5.18 | 5.37 | 4.50 | 4.74 | 4.45 | 4.61 | 4.51 | 4.28 | 4.36 | 4.76 |
| Ca | 0.64 | 0.59 | 0.67 | 0.59 | 1.18 | 1.13 | 0.96 | 1.04 | 1.48 10 | 1.37 53 | 1.42 71 | 1.19 79 |
| Cr | 0.00 37 | 0.00 21 | 0.00 17 | 0.00 25 | 0.00 22 | 0.00 29 | 0.00 16 | 0.00 26 | 0.00 40 | 0.00 34 | 0.00 44 | 0.00 27 |
| Mn | 0.13 95 | 0.06 67 | 0.09 42 | 0.09 28 | 0.08 52 | 0.17 32 | 0.14 00 | 0.11 53 | 0.12 26 | 0.12 57 | 0.19 57 | 0.11 19 |
| Fe | 1.62 | 1.39 | 1.24 | 1.39 | 1.48 | 1.59 | 1.28 | 1.43 | 1.75 | 1.49 | 2.37 | 1.59 |
| Cu | 0.00 32 | 0.00 34 | 0.00 31 | 0.00 34 | 0.00 34 | 0.00 34 | 0.00 35 | 0.00 30 | 0.00 35 | 0.00 35 | 0.00 37 | 0.00 35 |
| Zn | 0.00 82 | 0.00 69 | 0.00 72 | 0.00 74 | 0.00 78 | 0.00 84 | 0.00 75 | 0.00 78 | 0.00 81 | 0.00 80 | 0.00 81 | 0.00 79 |
| Pb | - 0.00 31 | - 0.00 33 | - 0.00 35 | - 0.00 29 | - 0.00 09 | - 0.00 13 | - 0.00 16 | - 0.00 06 | 0.00 87 | 0.00 52 | 0.00 65 | 0.00 59 |

Appendix 8: Element concentration in SEQ 1.

| | SEQ1 | | | | | | | | | | | |
|---|---|---|---|---|---|---|---|---|---|---|---|---|
| | W1 (%) | W2 (%) | W3 (%) | W4 (%) | C1 (%) | C2 (%) | C3 (%) | C4 (%) | L1 (%) | L2 (%) | L3( %) | L4 (%) |
| Mg | 0.47 | 0.38 | 0.44 | 0.55 | 0.32 | 0.38 | 0.44 | 0.37 | 0.38 | 0.41 | 0.44 | 0.37 |
| Al | 4.81 | 4.09 | 4.29 | 4.83 | 3.63 | 3.92 | 3.85 | 4.05 | 3.87 | 3.67 | 3.85 | 4.05 |
| Ca | 0.41 | 0.43 | 0.41 | 0.42 | 0.48 | 0.43 | 0.70 | 0.50 | 0.53 | 0.61 | 0.70 | 0.50 |

| | | | | | | | | | | | | |
|---|---|---|---|---|---|---|---|---|---|---|---|---|
| Cr | 0.0034 | 0.0026 | 0.0026 | 0.0045 | 0.0023 | 0.0028 | 0.0062 | 0.0020 | 0.0064 | 0.0033 | 0.0062 | 0.0020 |
| Mn | 0.0022 | 0.0010 | 0.0010 | 0.0004 | 0.0068 | 0.0006 | 0.0341 | 0.0046 | 0.0094 | 0.0118 | 0.0341 | 0.0046 |
| Fe | 1.28 | 1.06 | 0.98 | 1.21 | 1.21 | 1.02 | 2.60 | 1.31 | 1.42 | 1.48 | 2.60 | 1.31 |
| Cu | 0.0036 | 0.0035 | 0.0033 | 0.0034 | 0.0034 | 0.0033 | 0.0032 | 0.0033 | 0.0033 | 0.0033 | 0.0032 | 0.0033 |
| Zn | 0.0042 | 0.0040 | 0.0041 | 0.0045 | 0.0042 | 0.0041 | 0.0064 | 0.0044 | 0.0041 | 0.0040 | 0.0064 | 0.0044 |
| Pb | -0.0029 | -0.0028 | -0.0034 | -0.0026 | -0.0012 | -0.0016 | -0.0021 | -0.0020 | -0.0003 | -0.0025 | -0.0021 | -0.0020 |

Appendix 9: Element concentration in SEQ 2.

| | SEQ2 | | | | | | | | | | | |
|---|---|---|---|---|---|---|---|---|---|---|---|---|
| | W1 (%) | W2 (%) | W3 (%) | W4 (%) | C1 (%) | C2 (%) | C3 (%) | C4 (%) | L1 (%) | L2 (%) | L3( %) | L4 (%) |
| Mg | 0.38 | 0.32 | 0.36 | 0.35 | 0.32 | 0.33 | 0.39 | 0.37 | 0.45 | 0.39 | 0.42 | 0.37 |
| Al | 3.91 | 3.52 | 3.74 | 4.09 | 3.48 | 3.39 | 3.80 | 3.60 | 3.89 | 3.36 | 3.70 | 3.80 |
| Ca | 0.38 | 0.35 | 0.38 | 0.34 | 0.44 | 0.38 | 0.40 | 0.40 | 0.49 | 0.48 | 0.64 | 0.44 |
| Cr | 0.0023 | 0.0008 | 0.0033 | 0.0020 | 0.0038 | 0.0013 | 0.0001 | 0.0016 | 0.0023 | 0.0023 | 0.0098 | 0.0012 |
| Mn | 0.0114 | 0.0084 | 0.0124 | 0.0098 | 0.0186 | 0.0104 | 0.0104 | 0.0126 | 0.0148 | 0.0178 | 0.0454 | 0.0100 |
| Fe | 1.17 | 0.87 | 1.01 | 1.13 | 1.14 | 0.96 | 0.93 | 1.39 | 1.33 | 1.15 | 2.76 | 1.05 |
| Cu | 0.0015 | 0.0017 | 0.0015 | 0.0019 | 0.0015 | 0.0013 | 0.0016 | 0.0016 | 0.0016 | 0.0016 | 0.0017 | 0.0016 |
| Zn | 0.0036 | 0.0028 | 0.0033 | 0.0033 | 0.0033 | 0.0030 | 0.0030 | 0.0045 | 0.0034 | 0.0035 | 0.0047 | 0.0036 |

| | | | | | | | | | | | | |
|---|---|---|---|---|---|---|---|---|---|---|---|---|
| Pb | -0.0068 | -0.0070 | -0.0070 | -0.0061 | -0.0046 | -0.0057 | -0.0057 | -0.0035 | -0.0044 | -0.0064 | -0.0052 | -0.0061 |

Appendix 10: Element concentration in SEQ 3.

| | SEQ3 | | | | | | | | | | | |
|---|---|---|---|---|---|---|---|---|---|---|---|---|
| | W1 (%) | W2 (%) | W3 (%) | W4 (%) | C1 (%) | C2 (%) | C3 (%) | C4 (%) | L1 (%) | L2 (%) | L3(%) | L4 (%) |
| Mg | | 0.36 | 0.29 | 0.36 | 0.35 | 0.33 | 0.33 | 0.28 | 0.38 | 0.30 | 0.36 | |
| Al | | 4.24 | 4.04 | 4.17 | 3.76 | 4.04 | 3.88 | 3.76 | 3.70 | 3.45 | 3.60 | |
| Ca | | 0.20 | 0.19 | 0.21 | 0.23 | 0.18 | 0.23 | 0.22 | 0.30 | 0.27 | 0.41 | |
| Cr | | 0.0009 | 0.0021 | 0.0017 | 0.0020 | 0.0017 | 0.0015 | 0.0015 | 0.0036 | 0.0042 | 0.0062 | |
| Mn | | 0.0016 | 0.0044 | 0.0038 | 0.0075 | 0.0021 | 0.0066 | 0.0043 | 0.0091 | 0.0070 | 0.0326 | |
| Fe | | 0.64 | 0.73 | 0.70 | 0.76 | 0.64 | 0.72 | 0.65 | 0.94 | 0.80 | 2.10 | |
| Cu | | 0.0029 | 0.0028 | 0.0029 | 0.0030 | 0.0029 | 0.0031 | 0.0029 | 0.0030 | 0.0029 | 0.0030 | |
| Zn | | 0.0045 | 0.0047 | 0.0047 | 0.0048 | 0.0047 | 0.0047 | 0.0051 | 0.0054 | 0.0049 | 0.0056 | |
| Pb | | -0.0067 | -0.0065 | -0.0047 | -0.0049 | -0.0065 | -0.0057 | -0.0053 | -0.0046 | -0.0060 | -0.0047 | |

Appendix 11: Element concentration in SEQ 4.

| | SEQ4 | | | | | | | | | | | |
|---|---|---|---|---|---|---|---|---|---|---|---|---|
| | SEQ4-W1 | SEQ 4-W2 | SEQ 4-W3 | SEQ 4-W4 | SEQ 4-C1 | SEQ 4-C2 | SEQ 4-C3 | SEQ 4-C4 | SEQ 4-L1 | SEQ 4-L2 | SEQ 4-L3 | SEQ 4-L4 |
| Mg | | 0.29 | 0.25 | 0.29 | 0.28 | 0.32 | | 0.28 | 0.26 | 0.30 | 0.33 | |
| Al | | 4.40 | 4.13 | 4.03 | 3.96 | 4.75 | | 3.91 | 3.74 | 3.74 | 3.84 | |
| Ca | | 0.38 | 0.37 | 0.37 | 0.41 | 0.36 | | 0.41 | 0.49 | 0.50 | 0.50 | |
| Cr | | 0.0004 | 0.0004 | 0.0003 | 0.0018 | 0.0005 | | -0.0005 | 0.0026 | 0.0022 | 0.0021 | |
| Mn | | 0.0001 | -0.0006 | -0.0001 | 0.0028 | 0.0002 | | 0.0016 | 0.0093 | 0.0067 | 0.0103 | |
| Fe | | 0.42 | 0.41 | 0.36 | 0.49 | 0.46 | | 0.41 | 0.65 | 0.58 | 0.88 | |
| Cu | | 0.0020 | 0.0018 | 0.0019 | 0.0020 | 0.0020 | | 0.0019 | 0.0020 | 0.0019 | 0.0020 | |
| Zn | | 0.0022 | 0.0020 | 0.0019 | 0.0023 | 0.0021 | | 0.0021 | 0.0024 | 0.0022 | 0.0033 | |
| Pb | | -0.0053 | -0.0056 | -0.0048 | -0.0042 | -0.0053 | | -0.0040 | -0.0028 | -0.0052 | -0.0051 | |

Appendix 12: Mg concentrations (%) of samples collected 10 sampling days.

| **Mg (%)** | 1 | 2 | 3 | 4 | 5 | 6 | 7 | 8 | 9 | 10 |
|---|---|---|---|---|---|---|---|---|---|---|
| W1 | 0.7 | 0.8 | 1.0 | 0.8 | 0.7 | 1.4 | 0.7 | 0.7 | 1.5 | 0.8 |
| W2 | 0.7 | 0.8 | 1.1 | 0.7 | 0.7 | 1.3 | 0.7 | 0.8 | 1.0 | 0.9 |
| W3 | 0.8 | 0.8 | 1.1 | 0.8 | 0.7 | 1.3 | 0.7 | 0.7 | 1.4 | 0.9 |
| W4 | 0.8 | 0.8 | 1.1 | 0.7 | 0.7 | 1.2 | 0.7 | 0.7 | 1.3 | 0.9 |
| Average | 0.7 | 0.8 | 1.1 | 0.8 | 0.7 | 1.3 | 0.7 | 0.7 | 1.3 | 0.9 |
| RSD% | 3.8 | 1.1 | 3.6 | 2.9 | 2.0 | 6.7 | 3.4 | 9.0 | 14.5 | 3.3 |
| C1 | 0.8 | 0.8 | 1.3 | 0.8 | 0.7 | 1.3 | 0.7 | 0.8 | 1.3 | 0.9 |
| C2 | 0.7 | 0.8 | 1.3 | 0.8 | 0.7 | 1.2 | 0.7 | 0.7 | 1.4 | 0.9 |
| C3 | 0.7 | 0.8 | 1.4 | 0.8 | 0.7 | 1.4 | 0.7 | 0.7 | 1.4 | 0.9 |
| C4 | 0.8 | 0.8 | 1.0 | 0.8 | 0.7 | 1.2 | 0.7 | 0.8 | 1.4 | 0.8 |
| Average | 0.8 | 0.8 | 1.3 | 0.8 | 0.7 | 1.3 | 0.7 | 0.7 | 1.4 | 0.9 |
| RSD% | 2.4 | 2.8 | 13.0 | 1.4 | 3.6 | 6.1 | 2.5 | 6.1 | 1.7 | 1.7 |
| L1 | 0.7 | 0.8 | 1.2 | 0.8 | 0.7 | 1.6 | 0.7 | 0.6 | 1.3 | 0.9 |
| L2 | 0.8 | 0.8 | 1.2 | 0.8 | 0.7 | 1.2 | 0.8 | 0.6 | 1.4 | 0.8 |
| L3 | 0.8 | 0.8 | 1.1 | 0.8 | 0.7 | 1.3 | 0.8 | 0.7 | 1.2 | 0.9 |
| L4 | 0.8 | 0.8 | 1.1 | 0.8 | 0.7 | 1.5 | 0.7 | 0.7 | 1.4 | 0.8 |
| Average | 0.8 | 0.8 | 1.1 | 0.8 | 0.7 | 1.4 | 0.8 | 0.7 | 1.3 | 0.9 |
| RSD% | 4.6 | 3.9 | 5.5 | 1.6 | 3.6 | 11.5 | 7.3 | 8.7 | 6.2 | 2.2 |

Appendix 13: Al concentrations (%) of samples collected 10 sampling days.

| | 1 | 2 | 3 | 4 | 5 | 6 | 7 | 8 | 9 | 10 |
|---|---|---|---|---|---|---|---|---|---|---|
| W1 | 5.6 | 7.4 | 7.0 | 6.2 | 5.1 | 7.7 | 5.5 | 5.9 | 8.5 | 6.8 |
| W2 | 6.0 | 7.1 | 7.2 | 6.0 | 5.1 | 7.2 | 5.4 | 5.7 | 7.2 | 7.6 |
| W3 | 6.0 | 7.0 | 7.9 | 6.4 | 4.8 | 7.8 | 5.1 | 5.9 | 8.1 | 7.8 |
| W4 | 6.0 | 7.4 | 7.1 | 6.1 | 5.1 | 7.5 | 4.7 | 5.6 | 8.2 | 7.6 |
| Average | 5.9 | 7.2 | 7.3 | 6.2 | 5.0 | 7.6 | 5.2 | 5.7 | 8.0 | 7.5 |
| RSD% | 3.6 | 2.9 | 6.0 | 2.2 | 3.2 | 3.3 | 6.9 | 2.7 | 6.9 | 5.8 |
| C1 | 5.6 | 5.9 | 7.2 | 5.2 | 4.3 | 7.4 | 5.4 | 5.3 | 7.7 | 7.7 |
| C2 | 6.0 | 4.9 | 6.9 | 5.6 | 4.9 | 7.5 | 5.1 | 5.5 | 7.8 | 7.5 |
| C3 | 5.8 | 6.7 | 7.4 | 5.4 | 4.7 | 7.0 | 5.7 | 5.1 | 8.1 | 7.7 |
| C4 | 5.5 | 6.2 | 6.4 | 5.7 | 4.4 | 7.3 | 5.1 | 5.1 | 7.5 | 7.2 |
| Average | 5.7 | 6.0 | 7.0 | 5.5 | 4.6 | 7.3 | 5.3 | 5.3 | 7.8 | 7.5 |
| RSD% | 3.7 | 12.6 | 6.5 | 4.3 | 5.6 | 3.2 | 5.9 | 3.7 | 3.5 | 3.1 |
| L1 | 5.6 | 6.6 | 5.7 | 5.4 | 4.3 | 7.9 | 4.5 | 4.9 | 6.1 | 8.3 |
| L2 | 5.8 | 6.2 | 6.9 | 5.5 | 4.9 | 7.2 | 6.3 | 5.1 | 6.9 | 8.3 |
| L3 | 5.4 | 6.8 | 6.2 | 5.7 | 4.7 | 7.2 | 6.4 | 5.7 | 6.8 | 8.2 |
| L4 | 5.5 | 6.5 | 6.7 | 5.5 | 4.4 | 7.6 | 5.3 | 5.1 | 6.8 | 8.5 |
| Average | 5.6 | 6.5 | 6.4 | 5.5 | 4.6 | 7.5 | 5.6 | 5.2 | 6.6 | 8.3 |
| RSD% | 2.7 | 4.1 | 8.7 | 2.6 | 5.6 | 4.1 | 16.3 | 7.2 | 5.8 | 1.3 |

Appendix 14: Ca concentrations (%) of samples collected 10 sampling days.

| | 1 | 2 | 3 | 4 | 5 | 6 | 7 | 8 | 9 | 10 |
|---|---|---|---|---|---|---|---|---|---|---|
| W1 | 0.8 | 0.6 | 0.7 | 0.7 | 0.6 | 1.2 | 0.7 | 0.8 | 0.8 | 1.7 |
| W2 | 0.8 | 0.6 | 0.7 | 0.8 | 0.6 | 1.1 | 0.7 | 0.8 | 0.8 | 1.5 |
| W3 | 1.0 | 0.6 | 0.7 | 0.7 | 0.6 | 1.0 | 0.7 | 0.8 | 0.8 | 1.9 |

| | | | | | | | | | | |
|---|---|---|---|---|---|---|---|---|---|---|
| W4 | 0.8 | 0.7 | 0.7 | 0.7 | 0.8 | 1.2 | 0.6 | 0.7 | 0.8 | 1.9 |
| Average | 0.9 | 0.6 | 0.7 | 0.7 | 0.7 | 1.1 | 0.7 | 0.8 | 0.8 | 1.8 |
| RSD% | 10.1 | 3.5 | 3.2 | 9.1 | 12.3 | 8.1 | 6.7 | 4.2 | 2.5 | 8.7 |
| C1 | 1.1 | 1.2 | 1.4 | 1.2 | 1.2 | 1.3 | 1.7 | 1.7 | 1.4 | 1.4 |
| C2 | 1.0 | 1.2 | 1.4 | 1.1 | 1.4 | 1.4 | 1.4 | 1.5 | 1.5 | 1.3 |
| C3 | 1.1 | 1.0 | 1.2 | 1.2 | 1.3 | 1.5 | 1.6 | 1.1 | 1.2 | 1.3 |
| C4 | 1.2 | 1.3 | 1.1 | 1.3 | 1.2 | 1.2 | 0.8 | 1.3 | 1.3 | 1.3 |
| Average | 1.1 | 1.2 | 1.3 | 1.2 | 1.3 | 1.4 | 1.4 | 1.4 | 1.3 | 1.3 |
| RSD% | 6.3 | 8.4 | 9.9 | 8.0 | 5.4 | 8.8 | 27.4 | 17.8 | 9.9 | 5.0 |
| L1 | 1.0 | 1.4 | 1.1 | 1.3 | 1.2 | 0.9 | 0.9 | 1.4 | 1.8 | 0.8 |
| L2 | 1.4 | 1.0 | 1.3 | 1.5 | 1.4 | 0.9 | 1.3 | 1.3 | 1.4 | 0.8 |
| L3 | 1.6 | 1.1 | 1.2 | 1.2 | 1.3 | 0.8 | 1.4 | 1.2 | 1.5 | 0.7 |
| L4 | 1.7 | 1.0 | 1.2 | 1.3 | 1.2 | 0.9 | 1.1 | 1.4 | 1.4 | 0.9 |
| Average | 1.4 | 1.1 | 1.2 | 1.3 | 1.3 | 0.9 | 1.2 | 1.3 | 1.5 | 0.8 |
| RSD% | 22.5 | 14.1 | 7.2 | 7.7 | 5.4 | 9.2 | 17.0 | 7.5 | 12.3 | 8.6 |

Appendix 15: Cr concentrations (%) of samples collected 10 sampling days.

| | 1 | 2 | 3 | 4 | 5 | 6 | 7 | 8 | 9 | 10 |
|---|---|---|---|---|---|---|---|---|---|---|
| W1 | 0.0009 | 0.0022 | 0.0030 | 0.0054 | 0.0008 | 0.0023 | 0.0028 | 0.0010 | 0.0004 | 0.0134 |
| W2 | 0.0028 | 0.0045 | 0.0030 | 0.0042 | 0.0008 | 0.0021 | 0.0039 | 0.0013 | 0.0034 | 0.0035 |

| | | | | | | | | | | |
|---|---|---|---|---|---|---|---|---|---|---|
| W3 | 0.0018 | 0.0016 | 0.0025 | 0.0046 | 0.0012 | 0.0025 | 0.0022 | -0.0001 | 0.0011 | 0.0064 |
| W4 | 0.0021 | 0.0025 | 0.0047 | 0.0049 | 0.0012 | 0.0027 | 0.0020 | 0.0013 | 0.0000 | 0.0044 |
| Average | 0.0019 | 0.0027 | 0.0033 | 0.0048 | **0.0010** | 0.0024 | 0.0027 | 0.0009 | 0.0012 | 0.0069 |
| RSD% | 40.2 | 45.0 | 28.9 | 10.7 | 22.6 | 12.1 | 30.7 | 76.9 | 127.1 | 64.4 |
| C1 | 0.0033 | 0.0030 | 0.0048 | 0.0056 | 0.0087 | 0.0041 | 0.0050 | 0.0039 | 0.0066 | 0.0046 |
| C2 | 0.0031 | 0.0039 | 0.0055 | 0.0134 | 0.0024 | 0.0016 | 0.0045 | 0.0015 | 0.0021 | 0.0037 |
| C3 | 0.0032 | 0.0024 | 0.0038 | 0.0056 | 0.0019 | 0.0031 | 0.0052 | 0.0005 | 0.0029 | 0.0038 |
| C4 | 0.0111 | 0.0106 | 0.0064 | 0.0085 | 0.0015 | 0.0010 | 0.0033 | 0.0033 | 0.0037 | 0.0052 |
| Average | 0.0052 | 0.0050 | 0.0051 | 0.0083 | **0.0036** | 0.0025 | 0.0045 | 0.0023 | 0.0038 | 0.0043 |
| RSD% | 77.1 | 76.4 | 20.9 | 44.3 | 92.2 | 56.4 | 19.6 | 68.0 | 51.5 | 15.9 |
| L1 | 0.0038 | 0.0058 | 0.0047 | 0.0052 | 0.0087 | 0.0028 | 0.0041 | 0.0021 | 0.0404 | 0.0031 |
| L2 | 0.0038 | 0.0026 | 0.0041 | 0.0046 | 0.0024 | 0.0006 | 0.0046 | 0.0024 | 0.0095 | 0.0038 |
| L3 | 0.0060 | 0.0070 | 0.0094 | 0.0070 | 0.0019 | 0.0023 | 0.0035 | 0.0018 | 0.0009 | 0.0024 |
| L4 | 0.0042 | 0.0152 | 0.0043 | 0.0054 | 0.0015 | 0.0050 | 0.0040 | 0.0018 | 0.0040 | 0.0024 |
| Average | 0.0044 | 0.0077 | 0.0056 | 0.0056 | **0.0036** | 0.0027 | 0.0041 | 0.0020 | 0.0137 | 0.0029 |
| RSD% | 23.5 | 70.4 | 45.0 | 18.3 | 92.2 | 68.6 | 11.0 | 12.7 | 132.3 | 23.1 |

Appendix 16: Mn concentrations (%) of samples collected 10 sampling days.

| | 1 | 2 | 3 | 4 | 5 | 6 | 7 | 8 | 9 | 10 |
|---|---|---|---|---|---|---|---|---|---|---|
| W1 | 0.1 | 0.1 | 0.1 | 0.0 | 0.0 | 0.1 | 0.1 | 0.1 | 0.1 | 0.1 |
| W2 | 0.1 | 0.0 | 0.0 | 0.1 | 0.1 | 0.1 | 0.1 | 0.1 | 0.1 | 0.1 |
| W3 | 0.2 | 0.0 | 0.1 | 0.1 | 0.0 | 0.1 | 0.1 | 0.1 | 0.1 | 0.1 |
| W4 | 0.1 | 0.1 | 0.1 | 0.1 | 0.1 | 0.1 | 0.0 | 0.1 | 0.1 | 0.1 |
| Average | 0.2 | 0.0 | 0.1 | 0.1 | **0.1** | 0.1 | 0.1 | 0.1 | 0.1 | 0.1 |
| RSD% | 39.9 | 15.8 | 16.0 | 18.3 | 42.3 | 20.9 | 13.4 | 15.5 | 28.1 | 6.3 |
| C1 | 0.1 | 0.1 | 0.1 | 0.1 | 0.1 | 0.1 | 0.1 | 0.1 | 0.1 | 0.1 |
| C2 | 0.1 | 0.1 | 0.1 | 0.1 | 0.1 | 0.1 | 0.1 | 0.2 | 0.2 | 0.1 |

| | | | | | | | | | | |
|---|---|---|---|---|---|---|---|---|---|---|
| C3 | 0.1 | 0.1 | 0.1 | 0.1 | 0.1 | 0.1 | 0.1 | 0.1 | 0.1 | 0.2 |
| C4 | 0.1 | 0.1 | 0.1 | 0.1 | 0.1 | 0.1 | 0.1 | 0.1 | 0.1 | 0.2 |
| Average | 0.1 | 0.1 | 0.1 | 0.1 | **0.1** | 0.1 | 0.1 | 0.1 | 0.1 | 0.1 |
| RSD% | 8.1 | 19.5 | 19.8 | 20.3 | 20.4 | 11.2 | 20.2 | 21.5 | 32.6 | 36.9 |
| L1 | 0.1 | 0.1 | 0.1 | 0.1 | 0.1 | 0.2 | 0.1 | 0.2 | 0.2 | 0.1 |
| L2 | 0.1 | 0.1 | 0.1 | 0.1 | 0.1 | 0.2 | 0.1 | 0.1 | 0.1 | 0.1 |
| L3 | 0.1 | 0.1 | 0.1 | 0.1 | 0.1 | 0.1 | 0.0 | 0.1 | 0.1 | 0.1 |
| L4 | 0.1 | 0.1 | 0.1 | 0.1 | 0.1 | 0.1 | 0.1 | 0.1 | 0.1 | 0.1 |
| Average | 0.1 | 0.1 | 0.1 | 0.1 | **0.1** | 0.1 | 0.0 | 0.1 | 0.1 | 0.1 |
| RSD% | 12.7 | 21.9 | 4.5 | 12.5 | 20.4 | 24.1 | 24.5 | 14.1 | 41.8 | 24.8 |

Appendix 17: Fe concentrations (%) of samples collected 10 sampling days.

| | 1 | 2 | 3 | 4 | 5 | 6 | 7 | 8 | 9 | 10 |
|---|---|---|---|---|---|---|---|---|---|---|
| W1 | 1.6 | 1.5 | 1.2 | 1.7 | 1.3 | 1.9 | 1.5 | 1.7 | 1.7 | 2.9 |
| W2 | 1.7 | 1.6 | 1.3 | 1.8 | 1.3 | 1.6 | 1.7 | 1.5 | 1.7 | 2.1 |
| W3 | 1.6 | 1.3 | 1.8 | 1.7 | 1.3 | 1.7 | 1.4 | 1.6 | 1.5 | 2.1 |
| W4 | 1.8 | 1.6 | 1.5 | 1.7 | 1.5 | 1.7 | 1.2 | 1.4 | 1.6 | 2.1 |
| Average | 1.7 | 1.5 | 1.5 | 1.8 | **1.4** | 1.7 | 1.4 | 1.5 | 1.6 | 2.3 |
| RSD% | 5.5 | 11.6 | 18.9 | 3.1 | 8.1 | 6.5 | 13.6 | 7.1 | 6.2 | 17.2 |
| C1 | 1.5 | 1.6 | 1.7 | 1.9 | 1.8 | 2.0 | 1.8 | 1.7 | 2.4 | 1.9 |
| C2 | 1.7 | 2.3 | 2.2 | 1.9 | 1.4 | 2.1 | 1.6 | 1.6 | 2.4 | 1.8 |
| C3 | 1.5 | 1.9 | 1.6 | 1.6 | 1.6 | 1.7 | 1.9 | 1.6 | 1.9 | 1.9 |
| C4 | 2.1 | 2.5 | 1.8 | 1.9 | 1.3 | 1.7 | 1.3 | 1.4 | 2.1 | 1.9 |
| Average | 1.7 | 2.1 | 1.8 | 1.8 | **1.5** | 1.9 | 1.7 | 1.6 | 2.2 | 1.9 |
| RSD% | 18.3 | 19.8 | 15.0 | 8.4 | 14.6 | 10.4 | 14.6 | 6.3 | 10.6 | 2.5 |
| L1 | 1.4 | 2.0 | 1.9 | 2.4 | 1.8 | 2.0 | 1.2 | 1.8 | 5.5 | 2.0 |
| L2 | 2.3 | 1.5 | 1.8 | 1.9 | 1.4 | 1.9 | 1.7 | 1.6 | 2.7 | 1.8 |
| L3 | 2.3 | 2.5 | 1.5 | 1.8 | 1.6 | 1.7 | 1.2 | 1.9 | 2.4 | 1.7 |
| L4 | 1.9 | 1.5 | 1.8 | 2.0 | 1.3 | 1.9 | 1.6 | 1.8 | 3.4 | 1.7 |
| Average | 2.0 | 1.9 | 1.7 | 2.0 | **1.5** | 1.9 | 1.4 | 1.8 | 3.5 | 1.8 |
| RSD% | 22.6 | 24.0 | 9.5 | 13.8 | 14.6 | 8.3 | 18.6 | 8.3 | 40.2 | 7.3 |

Appendix 18: Cu concentrations (%) of samples collected 10 sampling days.

| | 1 | 2 | 3 | 4 | 5 | 6 | 7 | 8 | 9 | 10 |
|---|---|---|---|---|---|---|---|---|---|---|
| W1 | 0.0024 | 0.0022 | 0.0024 | 0.0021 | 0.0037 | 0.0029 | 0.0042 | 0.0030 | 0.0035 | 0.0039 |
| W2 | 0.0029 | 0.0023 | 0.0024 | 0.0023 | 0.0035 | 0.0028 | 0.0041 | 0.0033 | 0.0033 | 0.0042 |
| W3 | 0.0024 | 0.0022 | 0.0027 | 0.0020 | 0.0035 | 0.0028 | 0.0041 | 0.0032 | 0.0034 | 0.0041 |
| W4 | 0.0024 | 0.0019 | 0.0026 | 0.0022 | 0.0036 | 0.0030 | 0.0039 | 0.0029 | 0.0032 | 0.0040 |
| Average | 0.0025 | 0.0021 | 0.0025 | 0.0021 | **0.0036** | 0.0029 | 0.0041 | 0.0031 | 0.0033 | 0.0041 |
| RSD% | 9.5 | 7.0 | 6.2 | 6.9 | 2.6 | 3.2 | 2.9 | 5.6 | 4.0 | 3.4 |
| C1 | 0.0023 | 0.0022 | 0.0028 | 0.0022 | 0.0037 | 0.0029 | 0.0041 | 0.0031 | 0.0033 | 0.0041 |
| C2 | 0.0023 | 0.0024 | 0.0025 | 0.0021 | 0.0037 | 0.0030 | 0.0041 | 0.0029 | 0.0035 | 0.0039 |
| C3 | 0.0025 | 0.0021 | 0.0028 | 0.0021 | 0.0036 | 0.0027 | 0.0042 | 0.0031 | 0.0031 | 0.0040 |
| C4 | 0.0024 | 0.0025 | 0.0031 | 0.0026 | 0.0036 | 0.0029 | 0.0040 | 0.0031 | 0.0032 | 0.0041 |
| Average | 0.0024 | 0.0023 | 0.0028 | 0.0022 | **0.0036** | 0.0029 | 0.0041 | 0.0030 | 0.0033 | 0.0041 |
| RSD% | 2.8 | 7.1 | 7.7 | 10.4 | 2.0 | 4.0 | 2.0 | 2.6 | 5.0 | 2.1 |
| L1 | 0.0024 | 0.0026 | 0.0025 | 0.0022 | 0.0037 | 0.0030 | 0.0039 | 0.0028 | 0.0041 | 0.0043 |
| L2 | 0.0024 | 0.0021 | 0.0025 | 0.0019 | 0.0037 | 0.0028 | 0.0039 | 0.0031 | 0.0034 | 0.0042 |
| L3 | 0.0025 | 0.0022 | 0.0026 | 0.0022 | 0.0036 | 0.0029 | 0.0040 | 0.0029 | 0.0034 | 0.0041 |
| L4 | 0.0023 | 0.0020 | 0.0026 | 0.0022 | 0.0036 | 0.0031 | 0.0041 | 0.0031 | 0.0036 | 0.0039 |
| Average | 0.0024 | 0.0022 | 0.0025 | 0.0021 | **0.0036** | 0.0030 | 0.0040 | 0.0030 | 0.0036 | 0.0041 |
| RSD% | 2.6 | 10.3 | 2.2 | 6.5 | 2.0 | 3.3 | 2.1 | 5.2 | 9.7 | 4.3 |

Appendix 19: Zn concentrations (%) of samples collected 10 sampling days.

| | 1 | 2 | 3 | 4 | 5 | 6 | 7 | 8 | 9 | 10 |
|---|---|---|---|---|---|---|---|---|---|---|
| W1 | 0.0068 | 0.0061 | 0.0041 | 0.0072 | 0.0031 | 0.0065 | 0.0028 | 0.0065 | 0.0081 | 0.0102 |
| W2 | 0.0081 | 0.0062 | 0.0041 | 0.0075 | 0.0033 | 0.0060 | 0.0032 | 0.0062 | 0.0079 | 0.0096 |
| W3 | 0.0074 | 0.0059 | 0.0048 | 0.0069 | 0.0033 | 0.0067 | 0.0026 | 0.0059 | 0.0070 | 0.0104 |
| W4 | 0.0067 | 0.0062 | 0.0043 | 0.0071 | 0.0037 | 0.0063 | 0.0020 | 0.0058 | 0.0072 | 0.0098 |
| Average | 0.0073 | 0.0061 | 0.0043 | 0.0072 | **0.0034** | 0.0064 | 0.0026 | 0.0061 | 0.0075 | 0.0100 |
| RSD% | 9.1 | 2.0 | 7.8 | 3.5 | 7.1 | 4.9 | 19.8 | 4.7 | 7.3 | 3.7 |
| C1 | 0.0067 | 0.0065 | 0.0052 | 0.0065 | 0.0042 | 0.0069 | 0.0041 | 0.0068 | 0.0083 | 0.0091 |
| C2 | 0.0076 | 0.0067 | 0.0092 | 0.0072 | 0.0042 | 0.0075 | 0.0039 | 0.0069 | 0.0094 | 0.0081 |
| C3 | 0.0075 | 0.0073 | 0.0048 | 0.0070 | 0.0039 | 0.0063 | 0.0046 | 0.0077 | 0.0090 | 0.0096 |

| | | | | | | | | | | |
|---|---|---|---|---|---|---|---|---|---|---|
| C4 | 0.0070 | 0.0076 | 0.0070 | 0.0084 | 0.0034 | 0.0066 | 0.0034 | 0.0057 | 0.0084 | 0.0084 |
| Average | 0.0072 | 0.0070 | 0.0065 | 0.0073 | **0.0040** | 0.0068 | 0.0040 | 0.0068 | 0.0088 | 0.0088 |
| RSD% | 5.8 | 7.7 | 30.5 | 11.4 | 9.7 | 7.6 | 13.0 | 11.9 | 5.8 | 7.8 |
| L1 | 0.0066 | 0.0074 | 0.0039 | 0.0076 | 0.0042 | 0.0054 | 0.0025 | 0.0066 | 0.0142 | 0.0085 |
| L2 | 0.0079 | 0.0064 | 0.0056 | 0.0076 | 0.0042 | 0.0054 | 0.0032 | 0.0064 | 0.0082 | 0.0074 |
| L3 | 0.0091 | 0.0072 | 0.0053 | 0.0079 | 0.0039 | 0.0050 | 0.0031 | 0.0096 | 0.0084 | 0.0075 |
| L4 | 0.0078 | 0.0062 | 0.0051 | 0.0085 | 0.0034 | 0.0055 | 0.0032 | 0.0075 | 0.0093 | 0.0075 |
| Average | 0.0079 | 0.0068 | 0.0050 | 0.0079 | **0.0040** | 0.0053 | 0.0030 | 0.0075 | 0.0101 | 0.0077 |
| RSD% | 13.0 | 9.3 | 15.3 | 5.2 | 9.7 | 3.5 | 11.2 | 19.2 | 28.0 | 7.1 |

Appendix 20: Metals' concentrations of samples C1 collected at the cemetery measured by XRF and ICP-MS

| C1 | **Al** | **Mn** | **Fe** | **Cr** | **Cu** | **Zn** | **Pb** |
|---|---|---|---|---|---|---|---|
| 11.1.21-XRF | 5.9 | 0.057 | 1.6 | 0.003 | 0.002 | 0.006 | -0.003 |
| 11.1.21-ICP-MS | 1.6 | 0.055 | 1.3 | 0.002 | 0.001 | 0.004 | 0.002 |
| 11.13.21-XRF | 7.2 | 0.088 | 1.7 | 0.005 | 0.003 | 0.005 | -0.004 |
| 11.13.21-ICP-MS | 0.2 | 0.073 | 1.0 | 0.002 | 0.001 | 0.003 | 0.001 |
| 12.20.21-XRF | 5.2 | 0.068 | 1.9 | 0.006 | 0.002 | 0.006 | -0.007 |
| 12.20.21-ICP-MS | 0.2 | 0.070 | 1.4 | 0.001 | 0.002 | 0.004 | 0.001 |
| 1.21.22-XRF | 4.3 | 0.101 | 1.8 | 0.009 | 0.004 | 0.004 | -0.006 |
| 1.21.22-ICP-MS | 0.3 | 0.099 | 2.1 | 0.002 | 0.001 | 0.005 | 0.001 |
| 2.6.22-XRF | 7.4 | 0.087 | 2.0 | 0.004 | 0.003 | 0.007 | -0.004 |
| 2.6.22-ICP-MS | 0.2 | 0.050 | 0.7 | 0.001 | 0.001 | 0.003 | 0.001 |

Appendix 21: Metals' concentrations of samples C2 collected at the cemetery measured by XRF and ICP-MS

| C2 | **Al** | **Mn** | **Fe** | **Cr** | **Cu** | **Zn** | **Pb** |
|---|---|---|---|---|---|---|---|
| 11.1.21-XRF | 4.9 | 0.087 | 2.3 | 0.004 | 0.002 | 0.007 | -0.003 |
| 11.1.21-ICP-MS | 0.2 | 0.039 | 1.5 | 0.002 | 0.003 | 0.003 | 0.001 |
| 11.13.21-XRF | 6.9 | 0.103 | 2.2 | 0.005 | 0.003 | 0.009 | -0.004 |

| | | | | | | | |
|---|---|---|---|---|---|---|---|
| 11.13.21-ICP-MS | 0.3 | 0.088 | 1.5 | 0.001 | 0.001 | 0.006 | 0.001 |
| 12.20.21-XRF | 5.6 | 0.095 | 1.9 | 0.013 | 0.002 | 0.007 | -0.006 |
| 12.20.21-ICP-MS | 0.2 | 0.052 | 0.9 | 0.001 | 0.001 | 0.004 | 0.001 |
| 1.21.22-XRF | 4.9 | 0.081 | 1.4 | 0.002 | 0.004 | 0.004 | -0.007 |
| 1.21.22-ICP-MS | 0.2 | 0.062 | 0.9 | 0.001 | 0.001 | 0.002 | 0.001 |
| 2.6.22-XRF | 7.5 | 0.090 | 2.1 | 0.002 | 0.003 | 0.007 | -0.004 |
| 2.6.22-ICP-MS | 0.3 | 0.069 | 1.0 | 0.002 | 0.001 | 0.004 | 0.001 |

Appendix 22: Metals' concentrations of samples C3 collected at the cemetery measured by XRF and ICP-MS

| C3 | **Al** | **Mn** | **Fe** | **Cr** | **Cu** | **Zn** | **Pb** |
|---|---|---|---|---|---|---|---|
| 11.1.21-XRF | 6.7 | 0.088 | 1.9 | 0.002 | 0.002 | 0.007 | -0.004 |
| 11.1.21-ICP-MS | 0.2 | 0.052 | 1.1 | 0.001 | 0.001 | 0.003 | 0.001 |
| 11.13.21-XRF | 7.4 | 0.092 | 1.6 | 0.004 | 0.003 | 0.005 | -0.005 |
| 11.13.21-ICP-MS | 0.3 | 0.096 | 1.3 | 0.002 | 0.001 | 0.004 | 0.002 |
| 12.20.21-XRF | 5.4 | 0.104 | 1.6 | 0.006 | 0.002 | 0.007 | -0.007 |
| 12.20.21-ICP-MS | 0.2 | 0.071 | 0.9 | 0.001 | 0.001 | 0.004 | 0.009 |
| 1.21.22-XRF | 4.7 | 0.078 | 1.6 | 0.002 | 0.004 | 0.004 | -0.006 |
| 1.21.22-ICP-MS | 0.2 | 0.050 | 1.1 | 0.001 | 0.001 | 0.003 | 0.001 |
| 2.6.22-XRF | 7.0 | 0.071 | 1.7 | 0.003 | 0.003 | 0.006 | -0.004 |
| 2.6.22-ICP-MS | 0.4 | 0.092 | 1.5 | 0.002 | 0.001 | 0.005 | 0.001 |

Appendix 23: Metals' concentrations of samples C4 collected at the cemetery measured by XRF and ICP-MS

| C4 | **Al** | **Mn** | **Fe** | **Cr** | **Cu** | **Zn** | **Pb** |
|---|---|---|---|---|---|---|---|
| 11.1.21-XRF | 6.2 | 0.072 | 2.5 | 0.011 | 0.002 | 0.008 | -0.004 |
| 11.1.21-ICP-MS | 0.2 | 0.042 | 1.8 | 0.002 | 0.002 | 0.004 | 0.004 |
| 11.13.21-XRF | 6.4 | 0.062 | 1.8 | 0.006 | 0.003 | 0.007 | -0.005 |
| 11.13.21-ICP-MS | 0.2 | 0.066 | 2.9 | 0.007 | 0.008 | 0.005 | 0.001 |
| 12.20.21-XRF | 5.7 | 0.072 | 1.9 | 0.009 | 0.003 | 0.008 | -0.006 |

| | | | | | | | |
|---|---|---|---|---|---|---|---|
| 12.20.21-ICP-MS | 0.3 | 0.040 | 1.1 | 0.001 | 0.001 | 0.004 | 0.001 |
| 1.21.22-XRF | 4.4 | 0.061 | 1.3 | 0.002 | 0.004 | 0.003 | -0.007 |
| 1.21.22-ICP-MS | 0.2 | 0.057 | 0.9 | 0.001 | 0.001 | 0.003 | 0.001 |
| 2.6.22-XRF | 7.3 | 0.076 | 1.7 | 0.001 | 0.003 | 0.007 | -0.004 |
| 2.6.22-ICP-MS | 0.3 | 0.071 | 1.0 | 0.002 | 0.001 | 0.005 | 0.002 |